Analysis of Kinase Signaling Pathways Regulating Filamentous Growth and mRNP Granules in Filamentous Yeast

by

Nebibe Mutlu

A dissertation submitted in partial fulfillment
of the requirements for the degree of
Doctor of Philosophy
(Molecular, Cellular and Developmental Biology)
in the University of Michigan
2019

Doctoral Committee:

Professor Anuj Kumar, Chair
Assistant Professor Mara Duncan
Professor Daniel Klionsky
Professor Laura Olsen

Nebibe Mutlu

nmutlu@umich.edu

ORCID iD: 0000-0001-8978-2720

ACKNOWLEDGMENTS

I would like to start by thanking my PhD advisor Dr. Anuj Kumar for his patience, guidance and allowing me to discover my other interests besides research during graduate school. I am grateful to my committee members, Dr. Daniel Klionsky for his support when I was a precandidate and guidance after I became a candidate, Dr. Laura Olsen for all the journal clubs she attended to help me prepare for my prelim and Dr. Mara Duncan for her ideas and enthusiasm for my research and helping me with techniques. I also want to thank Dr. Amy Chang and Dr. Ming Li who has been our lab neighbors in the last year and helped me with techniques as well as shared their equipment.

I am also grateful to all my professors and mentors I had before and during my PhD. I am especially thankful to Dr. Mahinur Akkaya of METU for once telling me I can still do excellent things when I was ready to give up and my master's advisor Dr. Cory Dunn for teaching me how to do science and continuing being a mentor to me.

I also want to extend my thanks to all Kumar lab members of last 5 years. I enjoyed working with all of them. I want to especially thank to the undergraduate researchers Angela and Han for all their help. It was a privilege to mentor them in the lab. I also would like to thank the lab

neighbors of the last year. They have provided me with help, conversation and friendship.

I am very lucky to have a great cohort in the graduate school. I am particularly happy to share this journey with my good friends Po Ju, Damian, Wenjia, Lulu, Yi and Jiyuan.

I found an unexpected joy for teaching during graduate school. I am thankful to all the professors and fellow GSIs I have taught with who sparked this joy. I am particularly thankful to Angy and Kathryn for sharing their experiences with me when I was a first time GSI and Anne, Michelle and Kushal for their friendship and for all the fun we had together when I was GSI for the last time.

I was very lucky to make friends outside of the department in Ann Arbor. Among those, I want to thank Cintia for her friendship, for our weekly eating outs and for once telling me to stop to enjoy the sunset. I also want to thank Liz for her friendship and support throughout the years. Ann Arbor became a lot more fun after I met her. I am very happy to be a part of "Average Joes", the legendary bar trivia team.

I cannot thank enough to the people of "Her sey mi canim sayns". My college friends Ilke, Alperen, Seyda and Ezgi provided daily fun and support from the other side of world that kept me going.

I am grateful to my family for always putting education first and encouraging me to go as far as I can in terms of education.

Last but not the least, I want to thank my fiancé Mark for his love and support. For the last 3 years, he has been a main source of my daily power that made completing this thesis possible.

PREFACE

This dissertation summarizes research that I have conducted in Dr. Anuj Kumar's laboratory. Sections of this thesis have been previously published and are presented here with some modifications as outlined below.

Chapter two is currently under revision as an article with equal contributions from Daniel Sheidy and me. The mass spectrometry data was created at Phil Andrews' laboratory at the University of Michigan. Daniel Sheidy generated the strains and the data related to the pseudohyphal growth phenotypes, I did the cell morphology analysis and RNA-sequencing experiment. The sequencing was performed by University of Michigan Sequencing Core and bioinformatics analysis was performed by Christopher Sifuentes from the Bioinformatics Core, I did the related gene ontology analysis. Daniel Sheidy and I both contributed to stress granule phenotype analysis.

Chapter three contains portions of the work that has been previously published as follows: Norman KL, Shively CA, De La Rocha AJ, **Mutlu N,** Basu S, et al. (2018) Inositol polyphosphates regulate and predict yeast pseudohyphal growth phenotypes. *PLOS Genetics* 14(6): e1007493. https://doi.org/10.1371/journal.pgen.1007493. Kaitlyn Norman, Amberlene De La Rocha and I generated all the inositol polyphosphate species profiles for this paper. I did all the gene expression analysis. This chapter also contains unpublished characterization of inositol polyphosphate species in *Candida albicans* which is done solely by me. The introduction of this

chapter contains a portion of a review I have written with my PhD advisor, Anuj Kumar. The review is published in full as: Mutlu, N., and Kumar, A. (2019). Messengers for morphogenesis: inositol polyphosphate signaling and yeast pseudohyphal growth. Current Genetics, 65: 119. https://doi.org/10.1007/s00294-018-0874-0.

Appendix A contains information about an overexpression library in filamentous yeast I generated as a part of my PhD work. All the screen analysis and data collection were performed at Damian Krysan's laboratory in University of Rochester and University of Iowa. The library has been to generate foundational data for the study published as follows: Koselny, K., **Mutlu, N.,** Minard, A. Y., Kumar, A., Krysan, D. J., & Wellington, M. (2018). A Genome-Wide Screen of Deletion Mutants in the Filamentous Saccharomyces cerevisiae Background Identifies Ergosterol as a Direct Trigger of Macrophage Pyroptosis. *MBio*, *9*(4), e01204-18. https://doi.org/10.1128/mBio.01204-18.

TABLE OF CONTENTS

LIST OF FIGURES

LIST OF TABLES

ABSTRACT

Pseudoyphal growth is a stress response in which *S. cerevisiae* cells form elongated multicellular filaments, similar to processes of filamentous development required for virulence in pathogenic yeast such as *C. albicans*. The signaling pathways that regulate pseudohyphal growth in *S. cerevisiae* include TORC1, MAPK, PKA and AMPK; however, the exact mechanisms by which these pathways integrate and regulate pseudohyphal growth is largely unknown. To fill this gap in knowledge, our lab previously identified targets of kinases that regulate this process via SILAC-based quantitative phosphoproteomics. This thesis builds upon these studies by focusing on a kinase that is required for pseudohyphal growth as evidenced by genome-wide studies of regulators of pseudohyphal growth. Ksp1 is a kinase that regulates pseudohyphal growth, however the mechanism was unknown. Here, we show that Ksp1 regulates pseudohyphal growth both at the transcriptional and post-translational levels. Transcriptional profiling revealed Ksp1 kinase activity is required for wild type transcript abundance of genes related to a variety of stress responses, including pseudohyphal growth, sporulation, cell morphology, DNA damage, and autophagy, as well as amino acid metabolism. Mass spectrometry-based analysis of the Ksp1-dependent phosphoproteome identified Ksp1 regulation of a statistically overrepresented set of stress granule-localized proteins, including the p21-activated kinase Ste20 which localizes to stress granules. Deletion of *KSP1* resulted in elevated abundance of stress granule marker protein Pbp1-containing foci, suggesting a function for Ksp1 in modulating stress granule abundance. In total, we identify Ksp1 as an effector of different stress responses and as one of a handful of kinases

identified as a regulator of stress granules via the phosphorylation-based control of stress granule components.

In addition to Ksp1, our lab performed quantitative phosphoproteomic analysis of additional kinases required for pseudohyphal growth. These analyses identified target proteins that regulate inositol polyphosphate metabolism. Through metabolite analysis by HPLC, we observe a correlation between the ratio of different inositol polyphosphate species in the cell and pseudohyphal growth phenotypes, as well as expression levels of Flo11, the master transcriptional regulator of pseudohyphal growth. Similar metabolite analysis in *Candida albicans* suggests inositol polyphosphate metabolism might play a role in filamentation in other fungi as well.

To further understand the genes important for pseudohyphal growth in *S. cerevisiae*, I constructed an overexpression library which then used to screen for effects on filament formation. Using a collection of approximately 1500 plasmids from an existing yeast genomic tiling library, I created a corresponding collection of filamentous *Saccharomyces cerevisiae* strains that overexpresses 95% of the genome in large fragments. The resulting library library has been used by Damien Krysan's laboratory at University of Iowa to screen for regulators of yeast-triggered macrophage pyroptosis, indicating its utility as a tool in dissecting signaling pathways mediating filamentation.

Collectively, the work included in this thesis sheds light on the control of two different stress responses, namely pseudohyphal growth and translational regulation in stress granules, and suggests a link between the signaling pathways that regulate these processes.

CHAPTER 1

Introduction

1.1 Yeast stress response

All living organisms must adapt to their environments to survive under different circumstances. For the unicellular simple eukaryote budding yeast *Saccharomyces cerevisiae* these circumstances include both extrinsic stress-creating situations such as starvation, heat shock, osmotic stress, and drug treatment, as well as intrinsic stress factors such as aging and disruption of proteoastasis.

When encountering stress, cells must sense the stress and signal to make sure that the necessary changes, including modified transcription and translation, occur. The general response to stress in yeast is called the environmental stress response (ESR) [1]. The ESR induces changes that include suppressing most of the genes/proteins that have housekeeping roles while increasing expression of stress specific factors. Microarray studies in the early 2000's showed that there are common a set of ~300 genes upregulated and ~600 genes downregulated in response to a variety of stresses in *Saccharomyces cerevisiae.* The upregulated transcripts belong to genes that take part in carbohydrate metabolism, metabolite transport, fatty acid metabolism, autophagy and DNA damage repair, while transcripts of genes that regulate cell wall biosynthesis, amino acid and

pyruvate metabolism, nucleotide biosynthesis, non-sense mediated mRNA decay, DNA replication and ribosome biosynthesis are downregulated during environmental stress [2,3].

Regulating transcription is not the only response against stress. Translation is also regulated when stress is sensed [4,5]. This is achieved by translating selective mRNAs under stress. Different mechanisms are proposed to explain how the mRNAs to be translated are selected. These include intrinsic properties and secondary structures of mRNAs such as the presence of internal ribosome entry sites at the 5'UTR of mRNAs of genes regulating invasive growth [6]; binding of non-coding mRNAs such as microRNAs to regulate expression of a transcript [7,8], as well as the specialized ribosome hypothesis which posits that heterogenous ribosomes regulate translation of different transcripts [9]. Most likely, a combination of all those mechanisms ensure translation of stress specific transcripts, while allowing downregulation of general translation at the same time.

1.2 Filamentous growth

One of the specific responses to stress employed by many fungi is filamentous growth. Filamentous growth is triggered by a variety of stresses and other environmental signals in different fungi. For example, the presence of serum in media and/or high temperature triggers hyphal growth in the human opportunistic pathogen *Candida albicans* [10]. A mating signal is required for hyphal growth of the plant pathogen *Ustilago maydis* [11], and nitrogen or glucose depletion cause hyphal-like growth in the budding yeast *Saccharomyces cerevisiae* [12,13]. Upon perception of stress or these inducing signals, yeast cells can switch to a filamentous form. This morphology may allow cells to scavange more effectively. Yeast cells are not motile. However, by extending their length via filamentation, they make themselves able to reach areas they would not able to reach otherwise. Reaching new areas may be beneficial for yeast to find new nutrients or to avoid toxicity.

1.2.1 Filamentous growth and fungal pathogenicity

Some fungi that cause human disease are only able to adopt one morphology. They are found either in predominantly yeast-like or predominantly filamentous forms. However, many pathogenic fungi including the leading cause of fungal infections in humans, *Candida albicans*, are capable of growth in a yeast-like or in a filamentation mode. Therefore, a possible link between virulence of fungi and filamentous growth were sought out since the early days of filamentous growth research. In 1997, work from Gerald Fink's laboratory showed that mutants in the human opportunistic pathogen *Candida albicans* that cannot form filaments are avirulent in a mouse model [14]. However, since then it has become clear that the relationship between filamentation and virulence is far more complex. Employing a deletion library, Noble *et al*. showed that infectivity of *Candida albicans* and its morphological form is not strictly correlated [15]. Moreover, *Candida albicans* is found in both filamentous and yeast form in the human gut and its versatility in changing its form between hyphae, pseudohypahe and yeast contributes to its success as a pathogen [16,17]. Hence, studying regulation of those processes is important for understanding how fungal pathogenicity arises.

As the climate change is making the majority of earth a more favorable environment for fungi, fungal disease is expected to rise as global warming accelerates [18]. Hence, there is an urgent need to study fungal processes that leads to infectivity. These include the mechanistic details of filamentous growth.

1.2.2 Filamentous growth in Saccharomyces cerevisiae

The budding yeast *Saccharomyces cerevisiae* is a great model organism to study filamentation in fungi. Most of the signaling pathways that regulate filamentation are conserved among fungi. The availability of genetic tools in *Saccharomyces cerevisiae*, its genetic tractability,

the ease of growth and maintenance, as well as the short doubling time makes *S. cerevisiae* a great fit for any studies of cellular signaling.

Although a lot of natural isolates of *S. cerevisiae* are capable of filamentous growth, most lab strains of *S. cerevisiae* are not. This is possibly due to the laboratory-based selection of spores that did not result in clumped cells when grown in liquid culture. This clumping which is called flocculation strongly correlates with filamentous growth. However, there are some cultivars of S. cerevisiae that filament under lab conditions. The background we use in our lab Σ1278b, is the one that is the most widely used. In recent years, through the effort of our lab and others, this background now has the genetic tools, such as a deletion library [19] and overexpression library [20], that have been available for non-filamentous backgrounds and revolutionized the yeast genetics and systems biology fields in the early 2000s. The availability of those tools let us study mechanisms regulating filamentous growth in detail.

Filamentation in *S. cerevisiae* does not create true hyphae, as it does in some other yeasts including *Candida albicans*. Instead of forming true hyphae, *S. cerevisiae* cells become elongated and form a chain by remaining connected after cytokinesis. These elongated cells are called pseudohyphae and are easily observable under the microscope. The observation of pseudohyphal growth in *S. cerevisiae* is done in two ways. Both methods require spotting culture onto a plate that is suitable for inducing pseudohyphal growth. After letting the spotted culture grow on media that can induce pseudohyphal growth, filamentation can be monitored by observing the colony formed. The non-filamentous cells would create a smooth and near perfectly round colony, while the filamentous colony will have extrusions and would look wavy around the edge. Another way of observing pseudohyphal growth is by scraping the edge of those colonies and observing the individual cells under the microscope [21]. Usually, the cells with a height/width ratio>2 are

designated as psuedohyphae (Figure 1.1). Only diploid cells are capable of pseudohyphal formation.

Another way filamentous growth can be monitored in *S. cerevisiae* is invasive growth. Although this mostly occurs in haploid cells, both haploid and diploid filamentous budding yeast cells can undergo invasive growth. When encountering stress such as nitrogen deprivation, filamentous *S. cerevisiae* cells become capable of penetrating into semi-soft surfaces such as agar plates. The extent of invasive growth is measured by a wash assay. In this assay, colonies of filamentous yeast are spotted on a plate and let grow. After growth, the plate is gently washed with water which causes the non-filamentous cells to wash off while the filamentous cells remain in the agar. [22]

1.2.2.1 Regulation of filamentous growth by cellular signaling pathways

Nutrient limitation such as lack of nitrogen or a fermentable carbon source has been shown to induce filamentous growth. As expected, nutrient-sensing pathways such as the 5' **AMP**-activated protein **k**inase (AMPK)**, P**rotein **K**inase **A** (PKA) and **t**arget **o**f **r**apamycin (TOR) pathways are important for the regulation of filamentous growth. In addition, **m**itogen-**a**ctivated **p**rotein **k**inase (MAPK) pathways have been shown to be major regulators of filamentous growth in yeast. In the following subsections I will discuss the details of how these pathways regulate filamentous growth.

1.2.2.1.1 MAPK signaling pathways regulating filamentous growth

MAPKs are kinases that are regulated by extracellular signals. MAPK signaling cascades are activated by a variety of signals and stresses such as pheromone exposure, partial nutrient deprivation, hyperosmolarity, cell wall stress and nutrient starvation. For each of those signals,

there are different receptors in the cell membrane. The MAPK pathway contains a three-protein component which is composed of the MAPK kinase kinase (MAPKKK), which activates a MAPK kinase (MAPKK), which activates a MAPK. While the receptors for different signals are distinct, three of the MAPKKK-MAPKK-MAPK cascades are activated by the p21-activated kinase Ste20 [23,2425]. The MAPK cascades that are activated by Ste20 are parts of the pheromone, partial nutrient deprivation and hyperosmolarity-related MAPK pathways. Among those pathways, the hyperosmolarity three-protein MAPK cascade is mostly different than the others. However, the pheromone and partial nutrient deprivation MAPK cascades are composed of the same three proteins- namely Ste11 as the MAPKKK, Ste7 as the MAPKK and Kss1 as the MAPK. Despite this similarity, while the pheromone signal activates the pheromone response pathway downstream of the MAPK cascade, a partial nutrient deprivation signal activates the filamentous growth pathway. So, when it was revealed that the same MAPK cascade from the pheromone response pathway also regulates filamentous growth[26] and that Kss1 activates the same transcription factor Ste12 for both pathways [27], the big question was "How the same MAPKs can initiate different responses to different signals?". Over the years it became clear that the difference occurs upstream of Ste20 as well as the proteins interacting with the MAPK cascade under these different conditions as detailed below [28,29].

For the initiation of filamentous growth in *Saccharomyces cerevisiae*, four transmembrane receptors are necessary. Those are the **s**ynthetic, **h**igh **o**smolarity-sensitive protein Sho1, the ammonium permease Mep2, the mucin family protein Msb2 and the **G** **p**rotein coupled **r**eceptor Gpr1. While the mechanism by which these receptors transmit signals is unclear, two cyclin dependent kinases, Cdc24 and Cdc25 localize to the plasma membrane upon nitrogen depletion. In the filamentous pathway, Cdc25 activates Ras2, exchanging its GDP-bound form to a GTP-

bound form [30,31]. Subsequently, the GEF Cdc24 is activated by Ras2 [32,33] and activates Cdc42 by releasing GDP from Cdc42 to allow binding of GTP [34–36]. One difference between the pheromone response (mating) and the filamentous MAPK pathways is that Cdc24 is activated by its association with Far1 in the pheromone response pathway instead of its Ras2-dependent activation in the filamentous pathway [37].

The MAPK of the filamentous growth pathway, Kss1, is also a MAPK for the pheromone response pathway. However, in the pheromone pathway Kss1 works with another MAPK, Fus3, redundantly [38,39]. A complete abolition of mating is achieved only in double knockout mutant *fus3Δkss1Δ*. On the other hand, in the filamentous growth pathway Fus3 and Kss1 have opposite roles. Deletion of Fus3 causes hyperfilamentation and reverses the lack of invasive growth of *kss1Δ* mutants. Ste7, the MAPKK of both pathways is required for filamentous growth [40]. The triple knockout *fus3Δkss1Δste7Δ* is able to invade agar as much as the wild type. All this implies that Fus3 might also be involved in the filamentous growth pathway, and more work needs to be done to understand how the filamentous growth and mating MAPK pathways relate to each other.

Downstream of Kss1, transcriptional factors in the nucleus are activated during filamentous growth. I will discuss these downstream effectors in Section 1.2.2.2 Transcriptional control of filamentous growth.

In an important genome-wide study that made use of the recently constructed deletion library in the filamentous *S. cerevisiae* background, 97 proteins were identified as regulators of MAPK pathway-dependent filamentation [41]. These included a subset of Ras2 pathway regulators, some components of the chromatin remodeling complex, and some proteins that are important for mitochondrial function. Hence, the MAPK pathway is extensively regulated and important for the signal integration between pathways during filamentous growth.

1.2.2.1.2 AMPK signaling pathways regulating filamentous growth

Snf1 is the yeast homolog of AMPK of higher eukaryotes. AMPK is the main sensor for the availability of glucose. The involvement of Snf1 in filamentous growth became obvious when it was shown that glucose availability regulates filamentous growth [42]. Subsequent studies showed that Snf1 regulates both pseudohyphal and invasive growth [43]. Moreover, Snf1 activity in the filamentous yeast cells is regulated by other main nutrient sensing pathways in filamentous cells, such as TOR and PKA [44].

1.2.2.1.3 PKA dependent regulation of filamentous growth

As discussed in a previous section, Ras2 is needed to activate Cdc24 which in turn activates the MAPK pathway via Cdc42. Ras2, together with its ortholog Ras1, is a homolog of the mammalian RAS (rat sarcoma) proto-oncogene [45]. When activated by Cdc25, Ras2 stimulates the production of cAMP by adenylate cyclase. The receptor on the membrane that triggers the Cdc25-Ras2-cAMP module is the G protein coupled receptor Gpr1[46]. The level of cAMP in the cells has been shown to regulate filamentous growth[47]. cAMP, as it does in higher eukaryotes, activates PKA when it binds to its regulatory subunit Bcy1. In addition to Bcy1, PKA has three catalytic subunits, namely Tpk1, Tpk2 and Tpk3[48]. Interestingly, those subunits do not have the same effect on filamentous growth when deleted. Tpk1 deletion does not affect filamentation. Tpk2 deletion inhibits filamentous growth, while Tpk3 deletion causes hyperfilamentation [49]. Moreover, only Bcy1 and Tpk2 were shown to localize to the nucleus during pseudohyphal growth [50]. Although Tpk1 deletion does not cause a change in filamentous growth, Tpk1 phosphorylates Yak1, rendering it inactive. Yak1 is a positive regulator of filamentous growth when it is

unphosphorylated [51]. These data imply that all subunits of PKA are important for filamentous growth despite all of them having different roles and effects.

1.2.2.1.4 TOR dependent regulation of filamentous growth

Another pathway that is at the center of nutrient sensing in the cell is the Target of Rapamycin (TOR) pathway. TOR pathway is the main pathway that coordinates cell growth and nutrient sensing [52]. Rapamycin targets two protein complexes in the cell. These complexes, TORC1 and TORC2, are conserved from yeast to humans [53].

Rapamycin has been shown to inhibit pseudohyphal growth in 2001 [54]. However, the role of the TOR pathway in the regulation of pseudohyphal growth has come to be appreciated only within the last decade. In 2011, Bruckner *et al*., showed that the TOR and MAPK pathways are linked through the transcription factor Tec1 in filamentous yeast [55]. Laxman & Tu showed that TORC1-associated proteins regulate pseudohyphal growth but not invasive growth in both the common filamentous lab background Σ1278b and the otherwise non-filamentous background CEN.PK [56].

Moreover, TOR pathway seems to be an important regulator of filamentous growth and virulence in pathogenic fungi. TOR regulates adhesins in *Candida albicans*[57]. This regulation is important for *Candida* to form biofilms, which are an important feature for *Candida* pathogenesis. Furthermore, the TOR pathway regulates virulence and vegetative development in *Fusarium graminearum*[58].

1.2.2.1.5 Other pathways that regulate filamentous growth

In addition to the main nutrient sensing pathways, some other more accessory pathways have been found to regulate filamentous growth. These include the pH sensing Rim101p pathway[59], mitochondrial dysfunction[60] , tRNA modification complex Elongator[61], and the

chromatin remodeling complex[62].

1.2.2.2 Transcriptional control of filamentous growth

The pathways described above act through transcription factors to change gene expression when regulating filamentous growth. Filamentous growth can even be induced independent of external induction via synthetic regulation of transcription factors, such as Flo8 and Phd1[63].

The MAPK of the filamentous growth pathway, Kss1, works through the transcription factor Ste12 both during mating and filamentous growth [27]. When it was first discovered that the same transcription factor is activated by both the mating and filamentous growth pathways, it was thought that the mating pathway becomes activated in haploid cells, while the filamentous growth pathway gets activated in diploid cells [64]. Subsequent research showed that this was an oversimplification, and the filamentous growth pathway is activated not only in diploid cells but also in haploid cells [65]. Later, it was understood that the transcription factor Tec1, which is required for pseudohyphal growth, associates with Ste12. Tec1 and Ste12 binds to the filamentous response elements (FREs) and cooperatively work to activate transcription of filamentous response genes [66]. On the other hand, Tec1 is ubiquitylated and degraded when it encounters pheromone [67].

Another level of specification of the MAPK filamentous pathway comes from its ability to respond to different signals. Snf1 is the main pathway that responds to glucose stress in the budding yeast. When glucose starvation triggers filamentous growth, Snf1 regulates filamentous growth via transcriptional repressors Nrg1 and Nrg2 [68]. Other transcriptional repressor targets of Snf1 are Mig1 and Mig2. Mig1, which is an active repressor when it is unphosphorylated, is phosphorylated by Snf1. When phosphorylated, it can no longer repress transcription [69]. Mig1 also interacts with Opy2, a membrane receptor for hyperosmolarity pathway, and this interaction is important filamentous growth [70].

Another transcription factor that is important for filamentous growth is Flo8. The most common lab background of *S. cerevisiae*, S288C, is actually non-filamentous due to a mutation in *FLO8* [71]. Flo8 is a substrate for the PKA subunit Tpk2. Tpk2 phosphorylates Flo8. This phosphorylation is required for the interaction of Flo8 with the *FLO11* promoter [72].

The promoter targeted most prominently by transcription factors during filamentous growth is the unusually long promoter of the flocculation gene, *FLO11* [47]. *FLO11* codes for an adhesin and is required for pseudohyphal growth [73]. Both Ste12 and Flo8 binds to the *FLO11* promoter. While not perfectly correlated, Flo11 is usually expressed more strongly in pseudohyphal growth, and it is the gene that was studied the most as part of the transcriptional control of filamentous growth.

In 2014, in an effort to identify transcription factor regulation of pseudohyphal growth, Mayhew & Mitra identified 14 transcription factors that regulate pseudohyphal growth as a complex[74]. The proteins of this complex included Flo8, the cell wall protein Mss11 and Mfg1. *FLO11* is one of the targets of this complex. This complex binds to *FLO11* both at the promoter and terminator regions essentially forming a loop. Formation of this loop is important for the efficient transcription of *FLO11*. *FLO11* is a telomere-adjacent gene, and in addition to transcription factors, it is also regulated by epigenetic modifications[75,76].

In total, filamentous growth is very tightly regulated at the transcriptional level, and this regulation has been studied very broadly. Another aspect of the regulation of filamentous growth comes from translational regulation of target genes.

1.2.2.3 Translational control of filamentous growth

When cells sense stress, they shut down translation. For example, glucose stress represses translation initiaton very rapidly [77]. Hence, during the switch from the yeast form to pseudohyphal

form, translation of many genes' changes. Although there are comprehensive studies of regulation of pseudohyphal growth at the cellular signaling and transcriptional levels, the field lacks a comprehensive understanding of how translational regulation of specific transcripts regulate filamentous growth (refs).

Polyribosome analysis and RT-PCR analysis of a small number of potential targets of pseudohyphal growth transcription factors revealed Ste12, Gpa2 and Cln1 as three genes whose translation is regulated during pseudohyphal growth. This regulation is dependent on eIF4E binding protein Caf20 and the decapping protein Dhh1 [78]. The cap-binding translation initiation factor eIF4E has been shown to regulate pseudohyphal growth as temperature sensitive eIF4E mutants are unable to switch to a filamentous form, and this regulation is dependent on its interaction with Caf20 [79,80]. It is also known that filamentous *S. cerevisiae* uses non-canonical translation for translation of stress specific transcripts. 5'UTRs of pseudohyphal growth related genes contain internal ribosome entry sites (IRES). IRES mediated cap-independent translation is required for filamentous growth. This translation is dependent on the scaffolding translation initiation factor eIF4G [6].

All in all, these data imply translation initiation regulates filamentous growth. However, the exact mechanism of this regulation is still largely unknown.

1.2.2.4 Small molecule/metabolite control of filamentous growth

Nutritional starvation is not the only signal that induces filamentous growth. Small metabolites have also been found to induce the yeast to filamentous switch. For example, 1-butanol is a short-chain alcohol that induces pseudohyphal growth through mitochondrial retrograde signaling and quorum sensing [81]. Vitamin B9 is another metabolite that induces pseudohyphal growth through *FLO11* [82]. Moreover, phytohormone indole-3-acetic acid is a yeast metabolite that can induce

invasive growth [83]. Recently, farnesol, an acyclic sesquiterpene alcohol, has been found to inhibit translation and pseudohyphal growth both in *C. albicans* and *S. cerevisiae* [84].

Our lab, through the study that is also discussed in Chapter 3 of this thesis identified inositol polyphosphates as regulators of pseudohyphal growth [85].

1.3 mRNP granules

One of the changes in the cells that occurs as a response to different stresses is mRNP granule formation. mRNPs are RNA-protein complexes. mRNAs usually form complexes with proteins upon being generated, forming mRNPs, and they spend their lifetime being bound to different proteins that dictate their fate in the cell. Naturally, not all mRNAs are translated in the cell constitutively. Under conditions of nutritional/environmental stress, some mRNA transcripts are repressed, and this repression usually occurs through the formation of nonfunctional mRNPs. These mRNPs with untranslated and/or stored mRNAs often assemble into cytoplasmic non-membranous organelle-like structures called mRNP granules [86–88].

mRNP granule formation is observed in a variety of eukaryotic organisms including yeast, trypanosomes, worms, flies and humans. The conservation of mRNP granule formation implies an important biological function which is yet to be determined clearly. Two of the possible functions that are proposed by others so far are that the aggregation of specific proteins together with RNAs in a specific location might facilitate the reactions that these proteins and RNAs can have together; or the sequestration of certain signaling molecules to mRNP granules might regulate the stoichiometry of those molecules that might be important for activation/deactivation of the signaling pathways of those molecules[89,90].

mRNP granules are dynamic structures whose protein composition, size and number might change during the course of stress[91]. On the other hand, the RNA composition of mRNP granules

was found to be more static[92]. The current model of mRNP granules is that they form through the interactions of RNAs with a core set of proteins. Outside of that core, there is a dynamic shell of proteins[93].

1.3.1 Stress granules and P bodies

Although the literature regarding the dynamic nature of mRNP granules is growing, historically, mRNP granules are classified depending on which proteins they are harboring. Among the previously classified mRNP granules, the two most well characterized are P bodies and stress granules. P bodies have been seen as sites for decay of translationally repressed mRNAs. However, it should also be noted that some of the mRNAs localizing to P bodies might traffic back to ribosomes for translation. P bodies harbor translationally repressed mRNA, decapping factors such as Dcp1, Dcp2, Pat1, Edc3, the Lsm1-7 complex, and the 5' to 3' exonuclease Xrn1; P-bodies are free of ribosomes. Stress granules, on the other hand, harbor mostly translation initiation factors such as eIF4A, eIF4G, the Poly A binding protein Pab1p and the small subunit of ribosomes. Some proteins, such as Xrn1, can be found in both stress granules and P-bodies [9488,95,96].

1.3.2 Regulation of mRNP granule formation

mRNP granules form through the interactions of RNAs of with RNA-binding proteins, the interaction between different RNA binding proteins and the interactions between RNAs[97]. It is also thought that mRNP granules form through liquid-liquid phase separation of RNA and proteins[90]. The intrinsically disordered regions of RNA binding proteins are thought to be positive regulators of this process [98,99].

The protein composition of mRNP granules both in yeast and mammalian has been proteomically identified recently[93]. However, those lists of proteins that are found in mRNP granules even using proteomic methods give only a snapshot of the state of mRNP granules. mRNP

granule protein composition is dynamic and dependent on the stress [91]. Moreover, one protein that promotes mRNP granule formation in one condition might inhibit it in another condition.

Several posttranslational modifications that regulate mRNP granules have been identified. More than 20 kinases localize to mRNP granules[93]. In humans G3BP1 is a core stress granule protein whose ability to form stress granules is regulated by phosphorylation by Casein Kinase 2[100]. Dual specificity kinase DYRK3 regulates dissolution of stress granules via TORC1[101]. Grb7 is another kinase that regulates stress granule disassembly[102]. PKA dependent phosphorylation of Pat1 regulates P body formation in yeast[103]. Arginine methylation of many RNA binding proteins regulate their recruitment to stress granules[104] and stress granule clearance by autophagy[105]. Stress granule formation is positively regulated by O-Glyc-NAc glycosylation[106]. It is highly likely that these posttranslational modifications regulating mRNP granules that are identified so far are only a small subset of the ones that are waiting to be discovered.

1.4 mRNP granules and filamentous growth

Most of the stresses that induce filamentous growth, do not induce mRNP granule formation. However, recently, two studies suggested that mRNP granule formation and filamentous growth might be related. Our lab has shown that the filamentous growth kinases Kss1, Fus3, Tpk2 and Ste20 colocalize with the mRNP granule protein Igo1, and the filamentous growth pathway MAPK Kss1 is required for wild type numbers of RNA granules[107]. More recently, Pizzinga *et al*. showed that mRNA granules that carry the mRNAs of translation initiation factors localize to the tips of growth in daughter cells during filamentous growth [108]. These studies suggest an intriguing relationship between mRNP granules and filamentous growth.

1.5 Figures

Figure 1.1 Morphological changes in *S. cerevisiae* pseudohyphal growth.
Images of yeast cells and colonies grown in media with limited ammonium sulfate as a nitrogen source (low nitrogen media) or in media with normal nutrient availability. Quantification of cell elongation is indicated as the percentage of cells exhibiting a cell length:width ratio of greater than two. Arrowheads indicate elongated cells typical of pseudohyphal growth. Colony images are shown from a culture spread on an agar plate after 3 days growth. Scale bar for cells, 3 µm; scale bars for colony images are each 2 mm (Reprinted from Mutlu and Kumar, 2019)

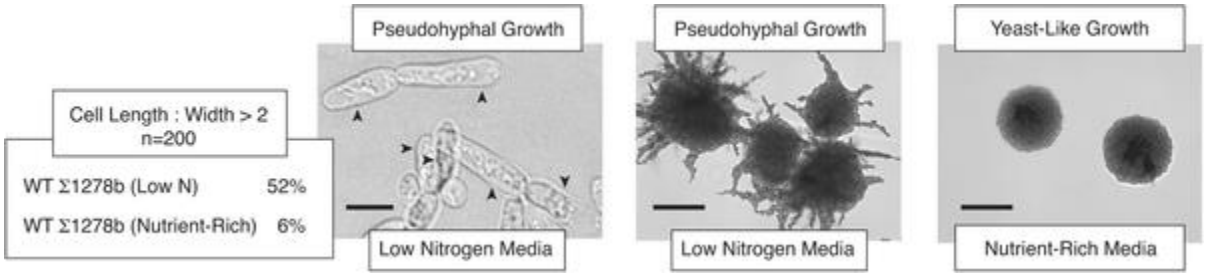

1.6 References

1. Gasch, A. P. The environmental stress response: a common yeast response to diverse environmental stresses. in *Yeast Stress Responses* 11–70 (Springer Berlin Heidelberg, 2003). doi:10.1007/3-540-45611-2_2
2. Gasch, A. P. *et al.* Genomic Expression Programs in the Response of Yeast Cells to Environmental Changes. *Mol. Biol. Cell* **11**, 4241–4257 (2000).
3. Causton, H. C. *et al.* Remodeling of Yeast Genome Expression in Response to Environmental Changes. *Mol. Biol. Cell* **12**, 323–337 (2001).
4. Crawford, R. A. & Pavitt, G. D. Translational regulation in response to stress in *Saccharomyces cerevisiae*. *Yeast* **36**, 5–21 (2019).
5. Ashe, M. P., De Long, S. K. & Sachs, A. B. Glucose Depletion Rapidly Inhibits Translation Initiation in Yeast. *Mol. Biol. Cell* **11**, 833–848 (2000).
6. Gilbert, W. V., Zhou, K., Butler, T. K. & Doudna, J. A. Cap-Independent Translation Is Required for Starvation-Induced Differentiation in Yeast. *Science (80-.).* **317**, 1224–1227 (2007).
7. Leung, A. K. L. & Sharp, P. A. MicroRNA Functions in Stress Responses. *Mol. Cell* **40**, 205 (2010).
8. Kucherenko, M. M. & Shcherbata, H. R. miRNA targeting and alternative splicing in the stress response - events hosted by membrane-less compartments. *J. Cell Sci.* **131**, jcs202002 (2018).
9. Guo, H. Specialized ribosomes and the control of translation. *Biochem. Soc. Trans.* **46**, 855–869 (2018).
10. TASCHDJIAN, C. L., BURCHALL, J. J. & KOZINN, P. J. Rapid Identification of

Candida Albicans by Filamentation on Serum and Serum Substitutes. *Arch. Pediatr. Adolesc. Med.* **99**, 212 (1960).

11. Banuett, F. Genetics of *Ustilago maydis* , a Fungal Pathogen that Induces Tumors in Maize. *Annu. Rev. Genet.* **29**, 179–208 (1995).
12. Liu, H., Styles, C. & Fink, G. Elements of the yeast pheromone response pathway required for filamentous growth of diploids. *Science (80-.).* **262**, 1741–1744 (1993).
13. Cullen, P. J. & Sprague, G. F. Glucose depletion causes haploid invasive growth in yeast. *Proc. Natl. Acad. Sci. U. S. A.* **97**, 13619–24 (2000).
14. Lo, H.-J. *et al.* Nonfilamentous C. albicans Mutants Are Avirulent. *Cell* **90**, 939–949 (1997).
15. Noble, S. M., French, S., Kohn, L. A., Chen, V. & Johnson, A. D. Systematic screens of a Candida albicans homozygous deletion library decouple morphogenetic switching and pathogenicity. *Nat. Genet.* **42**, 590–598 (2010).
16. Kornitzer, D., Kornitzer & Daniel. Regulation of Candida albicans Hyphal Morphogenesis by Endogenous Signals. *J. Fungi* **5**, 21 (2019).
17. Cleary, I. A. *et al.* Examination of the pathogenic potential of Candida albicans filamentous cells in an animal model of haematogenously disseminated candidiasis. *FEMS Yeast Res.* **16**, fow011 (2016).
18. Garcia-Solache, M. A. & Casadevall, A. Global Warming Will Bring New Fungal Diseases for Mammals. *MBio* **1**, e00061-10 (2010).
19. Ryan, O. *et al.* Global Gene Deletion Analysis Exploring Yeast Filamentous Growth. *Science (80-.).* **337**, 1353–1356 (2012).
20. Jin, R., Dobry, C. J., McCown, P. J. & Kumar, A. Large-Scale Analysis of Yeast

Filamentous Growth by Systematic Gene Disruption and Overexpression. *Mol. Biol. Cell* **19**, 284–296 (2008).

21. Cullen, P. J. Evaluating yeast filamentous growth at the single-cell level. *Cold Spring Harb. Protoc.* **2015**, 272–5 (2015).

22. Cullen, P. J. The plate-washing assay: a simple test for filamentous growth in budding yeast. *Cold Spring Harb. Protoc.* **2015**, 168–71 (2015).

23. Leberer, E., Dignard, D., Harcus, D., Thomas, D. Y. & Whiteway, M. The protein kinase homologue Ste20p is required to link the yeast pheromone response G-protein beta gamma subunits to downstream signalling components. *EMBO J.* **11**, 4815–24 (1992).

24. Leberer, E. *et al.* Signal transduction through homologs of the Ste20p and Ste7p protein kinases can trigger hyphal formation in the pathogenic fungus Candida albicans. *Proc. Natl. Acad. Sci.* **93**, 13217–13222 (1996).

25. Martin, H., Rodriguez-Pachon, J. M., Ruiz, C., Nombela, C. & Molina, M. Regulatory Mechanisms for Modulation of Signaling through the Cell Integrity Slt2-mediated Pathway in Saccharomyces cerevisiae. *J. Biol. Chem.* **275**, 1511–1519 (2000).

26. Liu, H., Styles, C. & Fink, G. Elements of the yeast pheromone response pathway required for filamentous growth of diploids. *Science (80-.).* **262**, 1741–1744

27. Bardwell, L. *et al.* Repression of yeast Ste12 transcription factor by direct binding of unphosphorylated Kss1 MAPK and its regulation by the Ste7 MEK. *Genes Dev.* **12**, 2887–2898 (1998).

28. Madhani, H. D., Styles, C. A. & Fink, G. R. MAP kinases with distinct inhibitory functions impart signaling specificity during yeast differentiation. *Cell* **91**, 673–84 (1997).

29. Lamson, R. E., Winters, M. J. & Pryciak, P. M. Cdc42 regulation of kinase activity and

signaling by the yeast p21-activated kinase Ste20. *Mol. Cell. Biol.* **22**, 2939–51 (2002).

30. Broek, D. *et al.* The S. cerevisiae CDC25 gene product regulates the RAS/adenylate cyclase pathway. *Cell* **48**, 789–99 (1987).

31. Toda, T. *et al.* In yeast, RAS proteins are controlling elements of adenylate cyclase. *Cell* **40**, 27–36 (1985).

32. Sloat, B. F. & Pringle, J. R. A mutant of yeast defective in cellular morphogenesis. *Science* **200**, 1171–3 (1978).

33. Mösch, H. U., Roberts, R. L. & Fink, G. R. Ras2 signals via the Cdc42/Ste20/mitogen-activated protein kinase module to induce filamentous growth in Saccharomyces cerevisiae. *Proc. Natl. Acad. Sci. U. S. A.* **93**, 5352–6 (1996).

34. Gancedo, J. M. *Control of pseudohyphae formation in Saccharomyces cerevisiae*. doi:10.1111/j.1574-6976.2001.tb00573.x

35. Peter1', M., Neiman3, A. M., Park, H.-O., Van Lohuizen4, M. & Herskowitz, I. *Functional analysis of the interaction between the small GTP binding protein Cdc42 and the Ste2O protein kinase in yeast*. *The EMBO Journal* **15**, (1996).

36. Bassilana, M., Blyth, J. & Arkowitz, R. A. Cdc24, the GDP-GTP exchange factor for Cdc42, is required for invasive hyphal growth of Candida albicans. *Eukaryot. Cell* **2**, 9–18 (2003).

37. Shimada, Y., Gulli, M.-P. & Peter, M. Nuclear sequestration of the exchange factor Cdc24 by Far1 regulates cell polarity during yeast mating. *Nat. Cell Biol.* **2**, 117–124 (2000).

38. Elion, E. A., Brill, J. A. & Fink, G. R. FUS3 represses CLN1 and CLN2 and in concert with KSS1 promotes signal transduction. *Proc. Natl. Acad. Sci. U. S. A.* **88**, 9392–6 (1991).

39. Elion, E. A., Grisafi, P. L. & Fink, G. R. FUS3 encodes a cdc2+/CDC28-related kinase required for the transition from mitosis into conjugation. *Cell* **60**, 649–64 (1990).

40. Cook, J. G., Bardwell, L. & Thorner, J. Inhibitory and activating functions for MAPK Kss1 in the S. cerevisiae filamentous- growth signalling pathway. *Nature* **390**, 85–88 (1997).

41. Chavel, C. A., Caccamise, L. M., Li, B. & Cullen, P. J. Global regulation of a differentiation MAPK pathway in yeast. *Genetics* **198**, 1309–28 (2014).

42. Cullen, P. & Sprague, G. Glucose depletion causes haploid invasive growth in yeast. *Proc Natl Acad Sci U S A* **97**,

43. Orlova, M., Ozcetin, H., Barrett, L. & Kuchin, S. Roles of the Snf1-activating kinases during nitrogen limitation and pseudohyphal differentiation in Saccharomyces cerevisiae. *Eukaryot. Cell* **9**, 208–14 (2010).

44. Shashkova, S., Welkenhuysen, N. & Hohmann, S. Molecular communication: crosstalk between the Snf1 and other signaling pathways. *FEMS Yeast Res.* **15**, 26 (2015).

45. Kataoka, T. *et al.* Genetic analysis of yeast RAS1 and RAS2 genes. *Cell* **37**, 437–45 (1984).

46. Lorenz, M. C. *et al.* The G Protein-Coupled Receptor Gpr1 Is a Nutrient Sensor That Regulates Pseudohyphal Differentiation in Saccharomyces cerevisiae. *Genetics* **154**, (2000).

47. Rupp, S., Summers, E., Lo, H. J., Madhani, H. & Fink, G. MAP kinase and cAMP filamentation signaling pathways converge on the unusually large promoter of the yeast FLO11 gene. *EMBO J.* **18**, 1257–69 (1999).

48. Toda, T., Cameron, S., Sass, P., Zoller, M. & Wigler, M. Three different genes in S.

cerevisiae encode the catalytic subunits of the cAMP-dependent protein kinase. *Cell* **50**, 277–87 (1987).

49. Robertson, L. S. & Fink, G. R. The three yeast A kinases have specific signaling functions in pseudohyphal growth. *Proc. Natl. Acad. Sci.* **95**, 13783–13787 (1998).

50. Bharucha, N. *et al.* Analysis of the Yeast Kinome Reveals a Network of Regulated Protein Localization during Filamentous Growth. *Mol. Biol. Cell* **19**, 2708–2717 (2008).

51. Malcher, M., Schladebeck, S. & Mösch, H.-U. The Yak1 Protein Kinase Lies at the Center of a Regulatory Cascade Affecting Adhesive Growth and Stress Resistance in *Saccharomyces cerevisiae*. *Genetics* **187**, 717–730 (2011).

52. Sabatini, D. M. Twenty-five years of mTOR: Uncovering the link from nutrients to growth. *Proc. Natl. Acad. Sci. U. S. A.* **114**, 11818–11825 (2017).

53. De Virgilio, C. & Loewith, R. The TOR signalling network from yeast to man. *Int. J. Biochem. Cell Biol.* **38**, 1476–1481 (2006).

54. Cutler, N. S., Pan, X., Heitman, J. & Cardenas, M. E. The TOR signal transduction cascade controls cellular differentiation in response to nutrients. *Mol. Biol. Cell* **12**, 4103–13 (2001).

55. Brückner, S. *et al.* The TEA Transcription Factor Tec1 Links TOR and MAPK Pathways to Coordinate Yeast Development. *Genetics* **189**, 479–494 (2011).

56. Laxman, S. & Tu, B. P. Multiple TORC1-Associated Proteins Regulate Nitrogen Starvation-Dependent Cellular Differentiation in Saccharomyces cerevisiae. *PLoS One* **6**, e26081 (2011).

57. Bastidas, R. J., Heitman, J. & Cardenas, M. E. The Protein Kinase Tor1 Regulates Adhesin Gene Expression in Candida albicans. *PLoS Pathog.* **5**, e1000294 (2009).

58. Yu, F. *et al.* The TOR signaling pathway regulates vegetative development and virulence in *Fusarium graminearum*. *New Phytol.* **203**, 219–232 (2014).

59. Lamb, T. M. & Mitchell, A. P. The transcription factor Rim101p governs ion tolerance and cell differentiation by direct repression of the regulatory genes NRG1 and SMP1 in Saccharomyces cerevisiae. *Mol. Cell. Biol.* **23**, 677–86 (2003).

60. Aun, A., Tamm, T. & Sedman, J. Dysfunctional mitochondria modulate cAMP-PKA signaling and filamentous and invasive growth of Saccharomyces cerevisiae. *Genetics* **193**, 467–81 (2013).

61. Abdullah, U. & Cullen, P. J. The tRNA modification complex elongator regulates the Cdc42-dependent mitogen-activated protein kinase pathway that controls filamentous growth in yeast. *Eukaryot. Cell* **8**, 1362–72 (2009).

62. Brosch, G., Loidl, P. & Graessle, S. Histone modifications and chromatin dynamics: a focus on filamentous fungi. *Fems Microbiol. Rev.* **32**, 409 (2008).

63. Pothoulakis, G. & Ellis, T. Synthetic gene regulation for independent external induction of the Saccharomyces cerevisiae pseudohyphal growth phenotype. *Commun. Biol.* **1**, 7 (2018).

64. Bardwell, L., Cook, J. G., Zhu-Shimoni, J. X., Voora, D. & Thorner, J. Differential regulation of transcription: Repression by unactivated mitogen-activated protein kinase Kss1 requires the Dig1 and Dig2 proteins. *Proc. Natl. Acad. Sci.* **95**, 15400–15405 (1998).

65. Lo, W. S., Raitses, E. I. & Dranginis, A. M. Development of pseudohyphae by embedded haploid and diploid yeast. *Curr. Genet.* **32**, 197–202 (1997).

66. Madhani, H. D. & Fink, G. R. The control of filamentous differentiation and virulence in fungi. *Trends Cell Biol.* **8**, 348–53 (1998).

67. Bao, M. Z., Schwartz, M. A., Cantin, G. T., Yates, J. R. & Madhani, H. D. Pheromone-dependent destruction of the Tec1 transcription factor is required for MAP kinase signaling specificity in yeast. *Cell* **119**, 991–1000 (2004).

68. Kuchin, S., Vyas, V. K. & Carlson, M. Snf1 Protein Kinase and the Repressors Nrg1 and Nrg2 Regulate FLO11, Haploid Invasive Growth, and Diploid Pseudohyphal Differentiation. *Mol. Cell. Biol.* **22**, 3994 (2002).

69. Treitel, M. A., Kuchin, S. & Carlson, M. Snf1 protein kinase regulates phosphorylation of the Mig1 repressor in Saccharomyces cerevisiae. *Mol. Cell. Biol.* **18**, 6273–80 (1998).

70. Karunanithi, S. & Cullen, P. J. The Filamentous Growth MAPK Pathway Responds to Glucose Starvation Through the Mig1/2 Transcriptional Repressors in *Saccharomyces cerevisiae*. *Genetics* **192**, 869–887 (2012).

71. Liu, H., Styles, C. A. & Fink, G. R. Saccharomyces cerevisiae S288C has a mutation in FLO8, a gene required for filamentous growth. *Genetics* **144**, 967–78 (1996).

72. Pan, X. & Heitman, J. Protein kinase A operates a molecular switch that governs yeast pseudohyphal differentiation. *Mol. Cell. Biol.* **22**, 3981–93 (2002).

73. Lo, W. S. & Dranginis, A. M. The cell surface flocculin Flo11 is required for pseudohyphae formation and invasion by Saccharomyces cerevisiae. *Mol. Biol. Cell* **9**, 161–71 (1998).

74. Mayhew, D. & Mitra, R. D. Transcription factor regulation and chromosome dynamics during pseudohyphal growth. *Mol. Biol. Cell* **25**, 2669–76 (2014).

75. Barrales, R. R., Jimenez, J. & Ibeas, J. I. Identification of Novel Activation Mechanisms for FLO11 Regulation in Saccharomyces cerevisiae. *Genetics* **178**, 145 (2008).

76. Barrales, R. R., Korber, P., Jimenez, J. & Ibeas, J. I. Chromatin modulation at the FLO11

promoter of Saccharomyces cerevisiae by HDAC and Swi/Snf complexes. *Genetics* **191**, 791–803 (2012).

77. Ashe, M. P., De Long, S. K. & Sachs, A. B. Glucose Depletion Rapidly Inhibits Translation Initiation in Yeast. *Mol. Biol. Cell* **11**, 833–848 (2000).

78. Park, Y.-U., Hur, H., Ka, M. & Kim, J. Identification of translational regulation target genes during filamentous growth in Saccharomyces cerevisiae: regulatory role of Caf20 and Dhh1. *Eukaryot. Cell* **5**, 2120–7 (2006).

79. Ross, D., Saxena, M. & Altmann, M. eIF4E Is an Important Determinant of Adhesion and Pseudohyphal Growth of the Yeast S. cerevisiae. *PLoS One* **7**, e50773 (2012).

80. Ibrahimo, S., Holmes, L. E. A. & Ashe, M. P. Regulation of translation initiation by the yeast eIF4E binding proteins is required for the pseudohyphal response. *Yeast* **23**, 1075–1088 (2006).

81. Lorenz, M. C., Cutler, N. S. & Heitman, J. Characterization of Alcohol-induced Filamentous Growth in *Saccharomyces cerevisiae*. *Mol. Biol. Cell* **11**, 183–199 (2000).

82. Güldener, U. *et al.* Characterization of the Saccharomyces cerevisiae Fol1 protein: starvation for C1 carrier induces pseudohyphal growth. *Mol. Biol. Cell* **15**, 3811–28 (2004).

83. Prusty, R., Grisafi, P. & Fink, G. R. The plant hormone indoleacetic acid induces invasive growth in Saccharomyces cerevisiae. *Proc. Natl. Acad. Sci. U. S. A.* **101**, 4153–7 (2004).

84. Egbe, N. E., Dornelles, T. O., Paget, C. M., Castelli, L. M. & Ashe, M. P. Farnesol inhibits translation to limit growth and filamentation in C. albicans and S. cerevisiae. *Microb. Cell* **4**, 294–304 (2017).

85. Norman, K. L. *et al.* Inositol polyphosphates regulate and predict yeast pseudohyphal

growth phenotypes. *PLOS Genet.* **14**, e1007493 (2018).

86. Mitchell, S. F. & Parker, R. Principles and properties of eukaryotic mRNPs. *Mol. Cell* **54**, 547–58 (2014).

87. Decker, C. J. & Parker, R. P-bodies and stress granules: possible roles in the control of translation and mRNA degradation. *Cold Spring Harb. Perspect. Biol.* **4**, a012286 (2012).

88. Guzikowski, A. R., Chen, Y. S. & Zid, B. M. Stress-induced mRNP granules: Form and function of processing bodies and stress granules. *Wiley Interdiscip. Rev. RNA* **10**, e1524 (2019).

89. Buchan, J. R. mRNP granules. *RNA Biol.* e29034 (2014). doi:10.4161/rna.29034

90. Holehouse, A. S. & Pappu, R. V. Functional Implications of Intracellular Phase Transitions. *Biochemistry* **57**, 2415–2423 (2018).

91. Buchan, J. R., Yoon, J.-H. & Parker, R. Stress-specific composition, assembly and kinetics of stress granules in Saccharomyces cerevisiae. *J. Cell Sci.* **124**, 228–39 (2011).

92. Khong, A. *et al.* The Stress Granule Transcriptome Reveals Principles of mRNA Accumulation in Stress Granules. *Mol. Cell* **68**, 808-820.e5 (2017).

93. Jain, S. *et al.* ATPase-Modulated Stress Granules Contain a Diverse Proteome and Substructure. *Cell* **164**, 487–498 (2016).

94. Mitchell, S. F., Jain, S., She, M. & Parker, R. Global analysis of yeast mRNPs. *Nat. Struct. Mol. Biol.* **20**, 127–33 (2013).

95. Swisher, K. D. & Parker, R. Localization to, and effects of Pbp1, Pbp4, Lsm12, Dhh1, and Pab1 on stress granules in Saccharomyces cerevisiae. *PLoS One* **5**, e10006 (2010).

96. Shah, K. H., Zhang, B., Ramachandran, V. & Herman, P. K. Processing body and stress granule assembly occur by independent and differentially regulated pathways in

Saccharomyces cerevisiae. *Genetics* **193**, 109–23 (2013).

97. Treeck, B. Van *et al.* RNA self-assembly contributes to stress granule formation and defining the stress granule transcriptome. *Proc. Natl. Acad. Sci.* **115**, 2734–2739 (2018).

98. Wheeler, J. R., Matheny, T., Jain, S., Abrisch, R. & Parker, R. Distinct stages in stress granule assembly and disassembly. *Elife* **5**, (2016).

99. Protter, D. S. W. & Parker, R. Principles and Properties of Stress Granules. *Trends Cell Biol.* **26**, 668–679 (2016).

100. Reineke, L. C. *et al.* Casein Kinase 2 Is Linked to Stress Granule Dynamics through Phosphorylation of the Stress Granule Nucleating Protein G3BP1. *Mol. Cell. Biol.* **37**, (2017).

101. Wippich, F. *et al.* Dual specificity kinase DYRK3 couples stress granule condensation/dissolution to mTORC1 signaling. *Cell* **152**, 791–805 (2013).

102. Tsai, N.-P., Ho, P.-C. & Wei, L.-N. Regulation of stress granule dynamics by Grb7 and FAK signalling pathway. *EMBO J.* **27**, 715–26 (2008).

103. Ramachandran, V., Shah, K. H. & Herman, P. K. The cAMP-dependent protein kinase signaling pathway is a key regulator of P body foci formation. *Mol. Cell* **43**, 973–81 (2011).

104. Tsai, W.-C. *et al.* Arginine Demethylation of G3BP1 Promotes Stress Granule Assembly. *J. Biol. Chem.* **291**, 22671–22685 (2016).

105. Chitiprolu, M. *et al.* A complex of C9ORF72 and p62 uses arginine methylation to eliminate stress granules by autophagy. *Nat. Commun.* **9**, 2794 (2018).

106. Ohn, T., Kedersha, N., Hickman, T., Tisdale, S. & Anderson, P. A functional RNAi screen links O-GlcNAc modification of ribosomal proteins to stress granule and processing body

assembly. *Nat. Cell Biol.* **10**, 1224–31 (2008).

107. Shively, C. A. *et al.* Large-Scale Analysis of Kinase Signaling in Yeast Pseudohyphal Development Identifies Regulation of Ribonucleoprotein Granules. *PLOS Genet.* **11**, e1005564 (2015).

108. Pizzinga, M. *et al.* Translation factor mRNA granules direct protein synthetic capacity to regions of polarized growth. *J. Cell Biol.* jcb.201704019 (2019). doi:10.1083/jcb.201704019

CHAPTER 2

Proteomic and Transcriptomic Analysis Reveals Yeast Kinase Ksp1 as a Regulator for Filamentous Growth and Ribonucleoprotein Granule Formation

2.1 Abstract

Pseudoyphal growth is a cellular stress response where yeast cells form elongated multicellular filaments, similar to processes of filamentous development required for virulence in pathogenic yeast such as *C. albicans*. We have identified *KSP1* as a gene required for wild-type yeast pseudohyphal growth, likely through its association with the Target of Rapamycin Complex (TORC1). *KSP1* was first identified as a high-copy suppressor of a mutation in the nucleotide exchange factor *SRM1*. It negatively regulates autophagy via TORC1, and its localization changes during pseudohyphal growth. We have found that Ksp1 kinase activity is required for pseudohyphal growth in *S. cerevisiae*. The signaling network of Ksp1, however, has not been studied directly on a proteome-wide scale in a filamentous background. To address this, we undertook an analysis of Ksp1 signaling through quantitative phosphoproteomics. We identified proteins differentially phosphorylated in a catalytically inactive kinase-defective Ksp1 mutant under conditions of nitrogen and glucose stress. Analysis of the proteins differentiall

phosphorylated upon loss of Ksp1 kinase activity identified a statistically significant set of proteins associated with mRNA-protein (mRNP) granules. mRNPs, encompassing P-bodies and stress granules, present an additional form of stress response thought to regulate mRNA translation. We found that Ksp1 localizes to mRNP granules in a filamentous background, in agreement with recent studies of mRNPs in a non-filamentous yeast strain. Moreover, the kinase activity of Ksp1 was required for wild-type localization of several mRNP component proteins/regulators upon growth to a high cell density, including Pbp1 and the P21-activated kinase ortholog Ste20. A transcriptome analysis of genes differently expressed in kinase defective Ksp1 mutants under nitrogen stress showed that the kinase activity of Ksp1 regulates expression of a variety of stress response related genes. Collectively, these results suggest a function for Ksp1 in coordinating pseudohyphal growth, translation and the regulation of mRNP dynamics and various other stress responses, likely through phosphorylation of key effectors.

2.2 Introduction

Many species of fungi are capable of adopting two different morphological types. In the certain strains of budding yeast Saccharomyces cerevisiae, these two stages are a yeast form that is observed under rich nutrient conditions and a filamentous form that is induced upon induction of external stimuli such as nitrogen deprivation[1]. For many pathogenic fungi such as the human opportunistic pathogen *Candida albicans*, the ability to filament is important for virulence[2,3]. In the budding yeast the filamentation manifests itself either as invasive growth during which the cells gain ability to invade semi-soft surfaces such as agar or as pseudohyphal growth during which the cells elongate and remain attached to each other after cell division. Studying filamentation in the budding yeast, a traditional model organism with a vast array of genetic tools available, gives

insights about not only how the pathogenic fungi become virulent but also how developmental switches occur at eukaryotic cells.

One of the main questions about filamentation is how it is regulated by signaling pathways. Genetic and genomic approaches employed by our lab and others has shown a vast array of proteins regulate filamentous growth [4,5]. The main pathways that have been implicated to have a role in regulation of filamentation in the budding yeast are the evolutionary conserved nutrient stress responsive signaling pathways TOR, PKA and AMPK as well as the MAPK pathway. However, how these pathways integrate with each other to promote the diverse changes required for filamentous growth is still unknown. One of the proteins that is known to regulate pseudoyphal growth is the Kinase Suppressing Prp20-10, Ksp1. Independent from its role in pseudohyphal growth, *KSP1* was first identified as a high-copy suppressor of a mutation in the nucleotide exchange factor *SRM1*[6]. It negatively regulates autophagy via TORC1 [7], and its localization changes during pseudohyphal growth. It also regulates the localization of other kinases that are important for pseudohyphal growth including some subunits of PKA [8]. Conversely, a high-throughput study of rapamycin sensitive proteome showed that Ksp1 phosphorylation is rapamycin sensitive, indicating it is regulated by mTORC1. Moreover, this rapamycin sensitive phosphorylation is mediated by PKA , indicating a high level of interconnectedness between Ksp1, mTORC1 and PKA, that is potentially involved in filamentous growth. [9]. Although these studies suggest a role for Ksp1 in integrating main nutrient responsive pathways TORC1 and PKA, little is known about the proteins that are the direct or downstream targets of Ksp1.

In previous work, we have shown that Ksp1 is required for pseudohyphal growth [4]. Here, we show that the kinase activity of Ksp1 is important for filamentation. Transcriptomic and phosphoproteomic analysis of downstream targets of Ksp1 shows it regulates other stress

responses, most strikingly stress granules, besides pseudohyphal growth. Our results suggest that pseudohyphal growth and stress granule (dis)assembly are governed by signaling pathways that converge on Ksp1.

2.3 Results

2.3.1 The kinase activity of Ksp1 is required for pseudohyphal growth

Ksp1 is a kinase and its deletion impairs pseudohyphal growth in response to nutrient stress. The first question we asked was if Ksp1 kinase activity is required for pseudohyphal growth. We have generated a previously defined catalytically inactive mutant of Ksp1 ksp1K47D) in the filamentous Σ1278b background. We tested WT, *ksp1Δ* and ksp1K47D mutants for pseudoyphal growth after 7 days of growth on nitrogen limited Synthetic Low Ammonium Dextrose (SLAD) plates. Both *ksp1Δ* and ksp1K47D mutants showed filamentation defects when compared to wild type as evidenced by surface spread filamentation assay and cell morphology analysis (Figure 2.1 A,B, C and D) ($p<0.01$, n=151 for WT, 119 for *ksp1Δ/Δ,* 167 for ksp1K47D). We also tested for pseudohyphal growth in media that is limited both in nitrogen and dextrose (Synthetic Low Ammonium Low Dextrose (SLALD)). We observed a statistically significant decrease in filamentous growth in *ksp1Δ/Δ* mutants when compared to wild type ($p<0.01$, n=139 for WT, 169 for *ksp1Δ/Δ*). A nonsignificant decrease in elongated cells was also observed in ksp1K47D mutants. ($p>0.05$, n=228) (Figure 2.1 E)

2.3.2 RNA-sequencing reveals Ksp1 regulates transcription of metabolism, stress and cell wall related genes

Pseudohyphal growth is regulated by a number of transcription factors [10] and can be induced by inducing expression of those transcription factors including Flo11 and Tec1 [11–13] . In

order to understand how kinase activity of Ksp1 might contribute to pseudohyphal growth, we performed a transcriptome wide RNA sequencing analysis to compare the expression levels of genes in wild type and Ksp1 kinase inactive mutants under pseudohyphal growth inducing conditions (Figure 2.7 A). We analyzed the RNA sequencing data using two different methods: deseq2 [14] and the Tuxedo suite [15]. Deseq2 identified 972 differentially expressed transcripts among 6499 transcripts detected. Tuxedo identified 7036 transcripts 1142 of which were differentially expressed (Figure 2.7 B). For the enrichment analysis, we used the transcripts that were significantly differentially expressed in both datasets.

We performed Gene Ontology (GO) term enrichment analysis on genes that were preferentially down regulated in the Ksp1-K47D mutant compared to wild-type under nitrogen stress. We found that genes related to the morphogenesis checkpoint, DNA replication, and cell wall organization were highly represented in the group of transcripts that were expressed less in Ksp1-K47D mutants than in wild type under conditions of nitrogen stress (Figure 2.7 C). It is known that sudden starvation activates morphogenesis and DNA replication checkpoints in the cell cycle [16,17] . The decrease in the expression of related genes in the Ksp1-K47D mutant points to a defect in sensing or processing the starvation information in the kinase defective Ksp1 mutant.

Expression of flocculation genes, especially *FLO11*, correlate with pseduohyphal growth [18]. Since Ksp1 kinase activity is required for pseudohyphal growth, we expected a decrease in the expression of flocculation and pseudohyphal growth-related genes in ksp1-K47D mutants. Accordingly, GO term analysis showed that downregulated transcripts in the Ksp1 kinase defective mutants were enriched in flocculation and pseudohyphal growth-related genes, and *FLO11* was one of the genes downregulated in the ksp1-K47D mutants (Figure 2.7 D).

When we analyzed the transcripts that were significantly expressed at higher levels in ksp1-

K47D mutants compared to wild-type, we found out that our dataset was enriched in GO terms that are related to metabolism, such as cellular amino acid biosynthesis, sulfate assimilation, and transmembrane transport (Figure 2.7 E). Another cluster of genes that were significantly expressed at higher levels in Ksp1-K47D mutants were related to the cellular response to oxidative stress. Sporulation was another term that was enriched in the GO term analysis of genes expressed more strongly in the mutant (Figure 2.7H). Along with pseudohyphal growth, sporulation is a response to starvation in diploid yeast. This implies that Ksp1 might be involved in not only the yeast-pseudohypae switch but also in the yeast-pseudohyphae-sporulation switch.

Although autophagy as a GO term was not significantly enriched in our analysis, some autophagy related genes were significantly more expressed in Ksp1-K47D mutants. ATG41 was one of the genes whose expression increased in ksp1-K47D mutants the most. In total, we have observed an increase in the expression of autophagy-related genes, ATG41, YIL165C, RTG3, ATG1, ATG38, VPS30, ATG36, ATG16, ATG13, ATG34 in the Ksp1-K47D mutant (Figure 2.7G).

In total, these data show that Ksp1 kinase activity regulates transcription of genes related to a variety of processes, most of which are activated or repressed in response to starvation. This implies an important role for Ksp1 in coordinating different stress responses in the cell.

2.3.3 Analysis of the proteins differentially phosphorylated upon loss of Ksp1 kinase activity identifies a statistically significant set of proteins associated with mRNA-protein (mRNP) granules

In order to understand what downstream signaling events contribute to the regulation of pseudohyphal growth by the kinase activity of Ksp1, we performed a Stable Isotope Labeling by

Amino Acids in Cell Culture (SILAC) [19] analysis of differentially phosphorylated peptides in wild type and kinase deficient Ksp1 mutant under filamentous growth inducing conditions (Figure 2.2A) and identified 146 unique genes whose encoded peptides were differentially phosphorylated. 47 novel phosphorylation sites were also unveiled by our analysis. The list of proteins accounting for the hypo- or hyperphosphorylated peptides in the Ksp1-K47D background include translation initiation machinery components, such as the eIF4G homolog Tif4631 and the PolyA binding protein Pbp1; the exonuclease Xrn1; the mRNA binding kinase Ste20; other kinases such as calmodulin dependent kinases Cmk1 and Cmk2, mRNA deadenylation regulator Yak1, DNA damage response kinase Rad53 as well as proteins that regulate metabolism such as those involved in the trehalose metabolism pathway Nth2,Nth1,Ugp1,Tsl1 (Figure 2.2 B). In order to understand what type of genes are enriched in our data set, we performed a Gene Ontology (GO) term analysis. GO term analysis of the differentially phosphorylated peptides showed that our data set is enriched in mRNA binding proteins that take part in stress granule assembly (Figure 2.3 A & B).

Stress granules are a specific type of mRNA-protein complex (mRNP granules) that form under a variety of stresses [20]. They are membraneless organelles that form via phase separation of translationally stalled/inactive RNA and proteins. Our lab has previously shown a relationship between other kinases that regulate pseudohyphal growth and mRNP granule formation by the specific mRNP associated protein Igo1 [21]. This made us wonder whether there is a relationship between Ksp1 dependent phosphorylation of stress granule associated proteins and stress granule formation.

When we used Cytoscape [22] to visualize complex networks of proteins that are related to stress granule assembly and whose phosphorylation levels depend on Ksp1 during filamentous growth, we found that the networks consist of proteins with mRNA binding capabilities as well as

those associated with MAPK and TORC1 signaling- two pathways that are important for nutrient responses in cells. Moreover, many of the proteins that belonged to the network are known to be regulators of pseudohyphal growth (Figure 2.3C).

2.3.4 Ksp1 dependent phosphorylation of mRNP granule associated proteins regulate pseudohyphal growth

The phosphoproteome analysis suggested that Ksp1 dependent phosphorylation of stress granule assembly proteins may play a role in filamentous growth. To consider this possibility, we tested both pseudohyphal growth and invasive growth in deletion mutants of stress granule assembly proteins as well as in point mutants of Ksp1-dependent phosphorylation sites making them unphosphorylable. The deletion mutants of the yeast homolog of translation initiation factor eIF4G Tif4631, the PolyA binding protein binding protein Pbp1, and the pheromone response pathway kinase Ste20 resulted in a decrease in both pseudohyphal and invasive growth phenotypes. We identified two phosphorylation sites for Tif4631. Those were Serine 176 and Serine 180. The phosphorylation site mutants tif4631S176A and tif4631S176S180A showed decreased pseudohyphal growth. On the other hand, we identified Serine 436 of Pbp1 as a site that gets hyperphosphorylated in the ksp1-K47D mutant. Interestingly, colonies of the pbp1-S436A mutant grew to a wider area than wild type, and 99.9% of the colony persisted on the agar after washing for indications of invasive growth (Figure 2.4 A&B).

FLO11 is an adhesin whose expression levels usually correlate with pseudohyphal growth. Using a plasmid that carries the PKA responsive promoter of *FLO11* followed by the LacZ gene we showed that all the mutants that showed reduced pseudohyphal growth have a decrease in PKA responsive *FLO11* promoter activity as measured by a beta-galactosidase assay. The only mutant

that showed an increase in PKA responsive *FLO11* promoter activity was the pbp1-S436A mutant which is a mutant of the phosphosite that gets hyper-phosphorylated in ksp1-K47D mutants (Figure 2.4 C). These results indicate that Ksp1 dependent phosphorylation/dephosphorylation of stress granule proteins regulate filamentous growth in *S. cerevisiae*.

2.3.5 Ksp1 is required for wild type numbers of stress granules

Since phosphorylation of some stress-granule assembly proteins depend on Ksp1, we hypothesized that Ksp1 regulates stress granules. We used a core stress granule protein, Pbp1, as a marker for stress granules. After seven days of growth in minimal medium containing normal ammonium sulfate levels, we observed an increase in the number of cells containing Pbp1-GFP puncta in *ksp1Δ* mutants when compared to wild type (Figure 2.5A). We further verified the increase in stress granules by monitoring RNA localization. For that purpose, we used a slightly modified version of a commonly used system to observe RNA under the microscope. In this system, cells are transformed with two plasmids. One of the plasmids codes for PGK1 mRNA with 16 human U1A binding sites at the 3' end. The other plasmid codes for the U1A protein tagged with mCherry. This system allowed us to visualize RNA granules. Analysis of wild type and *ksp1Δ* cells showed that KSP1 deletion results in an increase in the number of cells with PGK1-mRNA puncta. (Figure 2.5B)

2.3.6 Ksp1-dependent phosphorylation of stress granule associated proteins regulates stress granule numbers

Next, we tested if Ksp1-dependent phosphorylation of stress granule assembly proteins is important for the regulation of stress granules. Not surprisingly, we saw an increase in the number

of cells with PGK1 mRNA foci in the kinase deficient Ksp1 strain when compared to wild type. This shows that Ksp1 kinase activity is important for wild type localization of stress granules. Moreover, we tested whether Ksp1 dependent phosphorylation of stress granule assembly proteins were important for stress granule assembly. The Ksp1 dependent phosphorylation mutant ste20T203A resulted in more cells with foci when fused with GFP when compared to wild type Ste20. This was true also for PGK1-mRNA foci and they partially colocalized with the Ste20 foci (Figure 2.6 B). On the other hand, the increase in cells with protein and RNA foci was observed in the phosphosite mutant of Pbp1 where the Serine 436 of Pbp1 that gets hyperhopshorylated when Ksp1 kinase activity is defective is mutated to aspartic acid mimicking hyperphosphorylation. (Figure 2.6 A). These data show that Ksp1 dependent phosphorylation of stress granule proteins regulate the number of cells with stress granules under stress.

2.4 Discussion

The budding yeast S. cerevisiae switches to a filamentous form from a yeast form under different stimuli such as nutritional stress. While some of the cellular signalling pathways that regulate this developmental switch are known, much remains to be known about how these pathways interact with each other and how filamentous growth is related to other stress responses [1]. Here we show that a kinase, Ksp1, that is important for filamentous growth also regulates other types of cellular stress responses such as oxidative stress response and autophagy in the transcriptional level and stress granule assembly in the posttranslational level.

Ksp1 was one of the many genes identified as required for pseudohyphal growth in genome wide studies by our lab or others [4,23]. Although, Ksp1 was suggested to function as a kinase hub for pseudohyphal growth, this was not formally tested. This study showed that kinase activity of

Ksp1 is required for pseudohyphal growth because the kinase inactive mutant of Ksp1 shows reduced pseudohyphal growth. Both the colony morphology assay and cell elongation microcopy showed less pseudohyphal growth in deletion and kinase inactive Ksp1 mutants when nitrogen is limited. Although we saw a significant decrease in pseudohyphal growth in Ksp1 deletion mutants when both nitrogen and oxygen is limited, the decrease was not seen in the Ksp1 kinase inactive mutants. This might be due to subtle differences between the nitrogen starvation response and glucose starvation response[24].

The developmental switch from yeast-form to filamentous growth requires extensive transcriptional reprogramming [10]. To understand why Ksp1 kinase inactive mutants were incapable of pseudohyphal growth, we performed an analysis of differentially expressed transcripts in wild type and Ksp1 kinase inactive mutant cells under low nitrogen stress. In the dataset of transcripts that were differentially expressed, the genes related to the morphogenesis checkpoint, cell wall organization, DNA replication, cellular amino acid biosynthesis, cell cycle, oxidative stress response, transmembrane transport as well as flocculation and pseudohyphal growth were overrepresented. Interestingly the first 3 of those gene ontology terms were found to be enriched in another large-scale analysis of yeast pseudohyphal growth by gene disruption and overexpression [4]. It is known that sudden starvation activates morphogenesis and DNA replication checkpoints in the cell cycle [16,17]. Interestingly, through proteomic analysis we found that in kinase inactive Ksp1 mutants, the DNA damage response kinase Rad53 is hypophosphorylated. The phosphorylation site we identified (S198) is known to be a direct target for Mec1 and Rad9 [25]. However, we do not see any difference in transcription or phosphorylation levels of those proteins in Ksp1 kinase inactive mutants under pseudohyphal growth-inducing conditions, which could suggest a novel Ksp1 dependent mechanism. One possibility is that Mec1 and Rad9 are activated

at the post-transcriptional level in kinase defective Ksp1 mutants. Interestingly, a recent phosphoproteomic study showed that Rad53 targets a significant amount of RNA metabolic proteins including Xrn1, Ded1, Pab1, Rpg1, Ecm32 and Dcp2 [26]. According to our results, 3 of those proteins (Xrn1, Ecm32 and Dcp2) are also differentially phosphorylated in the Ksp1 kinase inactive mutants under pseudohyphal growth-inducing conditions. It's possible that Ksp1 is upstream of Rad53 under pseudohyphal growth inducing conditions and regulates RNA metabolism via Rad53.

Cell wall reorganization-related transcripts are expected to be enriched when cells are defective in pseudohyphal growth, as filamentation requires cell elongation. It is possible that the activation of morphogenesis and DNA replication checkpoints, as well as cell wall reorganization, contribute to pseudohyphal growth and are regulated by Ksp1 under nitrogen stress.

Autophagy is another starvation response that involves degradation and recycling of proteins and organelles [27]. Interestingly, one of the most increased transcripts in Ksp1-K47D mutants under stress conditions belongs to an auotophagy-related gene, Atg41. Atg41 transcription level has been shown to increase under autophagy-inducing conditions, and this increase contributes to the induction of autophagy [28]. Although autophagy as a GO term was not significantly enriched in our analysis, some autophagy-related genes were significantly more expressed in Ksp1-K47D mutants. Ksp1 has been shown to negatively regulate autophagy [7], and recently several studies showed transcriptional control is an important regulator of autophagy (for a comprehensive review see Delorme-Axford & Klionsky, 2018) . We have observed an increase in the expression of autophagy-related genes, ATG41, YIL165C, RTG3, ATG1, ATG38, VPS30, ATG36, ATG16, ATG13, ATG34 in the ksp1-K47D mutant. It is worth noting that ATG1 and ATG13 are subunits of the Atg1 complex that forms at the induction step of autophagy at the

phagophore assembly site. VPS30 and Atg38 are subunits of the class III phosphatidylinositol 3-kinase complex that localizes to the phagophore assembly site. This raises the possibility that Ksp1 regulates autophagy at the induction step.

Furthermore, the enrichment for oxidative stress response, pseudohyphal growth, sporulation-related genes, as well as differential expression of genes related to autophagy, implies Ksp1 likely regulates integration of different kinds of stress responses.

Our lab has performed extensive phosphoproteomic analysis of other pseudohyphal growth-related kinases in order to better understand the signaling pathways that regulate pseudohyphal growth. Through phosphoproteomic analysis of differentially phosphorylated peptides in ksp1-K47D mutants under pseudohyphae inducing conditions, we have found more than 100 unique peptides that are hypo- or hyperphosphorylated. Interestingly, proteins that localize to stress granules and take part in stress granule assembly were enriched in the dataset of differentially phosphorylated mutants in ksp1-K47D mutants.

Stress granules form in response to different stresses in eukaryotic cells. They are dynamic membraneless structures composed of proteins and RNAs that are stalled for translation [20]. They are composed of a more stable core and a dynamic shell. The dynamics of stress granules are regulated by the protein-protein and protein-RNA interactions. It is thought that the prion like intrinsically disordered regions (IDRs) contribute to these interactions significantly [30]. Ksp1 is a component of the stress granule core [31] and contains an IDR at the N terminus [32]. It is thought that the stress granule core proteins are required for stress granule formation and have a positive effect in the formation of stress granules [33]. However, we have seen an increase in stress granule numbers after deleting Ksp1. Therefore, it is possible that Ksp1 is a noncanonical stress granule core protein whose presence in stress granules either inhibits excessive stress granule formation or facilitates

disassembly.

Ksp1 is one of two kinases that were found to bind mRNA in a large-scale study of mRNA binding proteins in yeast [34]. In a study that did not include Ksp1, our lab showed that a subset of main yeast protein kinases that regulate pseudohyphal growth colocalize with mRNP granules, and some of those kinases, such as the MAPK kinase Kss1, cause a decrease in mRNP numbers when deleted. Moreover, deleting some of the mRNP granule proteins caused defects in pseudohyphal growth [21]. However, a direct relationship between phosphorylation events by the pseudohyphal growth-regulating kinases and mRNP granules was not shown in this paper. Here, we show that not only the deletion mutants, but also Ksp1-dependent phosphorylation site mutants of stress granule proteins Tif4631 and Pbp1, show aberrant pseudohyphal and invasive growth phenotypes. Interestingly, mutating only one of the two possible phosphorylation residues in Tif4631 created a more severe phenotype than a mutant of both sites. This implies that the S176 site is enough to reduce pseudohyphal growth, and phosphorylation of S180 has an inhibitory effect on this reduction. Moreover, the nonphosphorylable mutant Pbp1S436A caused a dramatic increase in the invasive growth phenotype. The colony spread depicting pseudohyphal growth is not very informative since it spread more than wild type colonies, possibly hindering our ability to see the colony extrusions under the microscope. However, the significant increase in Flo11 reporter activity points to an increase in pseudohyphal growth.

Stress granules are regulated by different signalling events including phosphorylation [35–38]. We were able to show that Ksp1 kinase activity regulates stress granule numbers. A Ksp1-dependent phosphorylation mutant of the stress granule protein Ste20 caused an increase in the number of cells with Ste20-containing stress granules. On the other hand, the S436 residue of Pbp1 is hyperphosphorylated in Ksp1-K47D mutants. A phosphomimetic mutant of Pbp1 showed a

similar effect to the nonphosphorylable mutant of Ste20, an increase in the number of cells with stress granules that the mutant colocalizes with. We did not see any significant difference in stress granule numbers in nonphosphorylable mutants of Tif4631. In total, Ksp1 may regulate pseudohyphal growth by phosphorylating Tif4631 and indirectly dephosphorylating Pbp1. Dephosphophorylation of Pbp1 and phosphorylation of Ste20 directly or indirectly by Ksp1 regulates stress granules. On the other hand, Ste20 regulates pseudohyphal growth as evidenced by the lack of pseudohyphal and invasive growth of deletion mutants. Tif4631 is a core stress granule which is required for their formation. All these pieces of evidence suggest that the regulation of pseudohyphal growth and stress granule formation are intertwined and that Ksp1 is a kinase that regulates both. However, it is clear that there are other kinases and phosphatases that contribute to this regulation, and those kinases and phosphatases are most possibly different for each pathway.

Although different theories have been proposed regarding the function of stress granules and other membraneless mRNP granules, it is still not clear what their function in the cell is [39,40]. The translationally stalled RNAs are thought to go to stress granules. Limited nitrogen availability in yeast causes a striking decrease in the translation of many genes. This is usually achieved by targeting translation initiation [41]. The upregulation of aminoacid biosynthesis in Ksp1-K47D mutants under nitrogen stress and the differential phosphorylation of proteins that are either part of the translation initiation closed loop complex, such as Tif4631, or bind to proteins of this complex, such as Pbp1 (binds Pab1) and Caf20 (binds Cdc33), raises the question whether translation is upregulated in Ksp1K47D mutants. We did not see any significant difference in general translation between wild type and Ksp1 mutants under nutrient rich conditions. However, we cannot rule out a difference in translation under stress as we were not able to perform polysome

fractionation analysis under stress. Another possibility relies on the fact that while most translation in the cell shuts down during stress, stress related genes have to be translated. Interestingly, invasive growth genes have been shown to activate different modes of translation under stress. It is possible that Ksp1 regulates translation of a specific set of RNAs.

In sum, this study shows that Ksp1 is a kinase that regulates different stress responses. Both pseudohyphal growth and mRNP granule regulation depends on the kinase activity of Ksp1.

2. 5 Materials and Methods

2.5.1 Strains, plasmids, and media

The yeast strains used in this study can be found at Table 2.1. Standard protocols and techniques were used for the propagation of budding yeast, DNA was introduced by methods of yeast transformation using lithium acetate treatment and heat shock. Plasmids used in this study are listed in Table 2.2.

S. cerevisiae strains were cultured on YPD (1% yeast extract, 2% peptone, 2% glucose) or Synthetic Complete (SC) (0.67% yeast nitrogen base (YNB) without amino acids, 2% glucose, and 0.2% of the appropriate amino acid drop-out mix). Nitrogen deprivation and filamentous phenotypes were assayed using Synthetic Low Ammonium Dextrose (SLAD) medium (0.17% YNB without amino acids, 2% glucose, 50 μM ammonium sulfate and supplemented with appropriate amino acids) and Synthetic Low Ammonium Low Dextrose (SLALD) or by supplementing growth medium with 1% 1-butanol.

2.5.2 Pseudohyphal growth assays

Cultures of diploid wild type or mutant strains were grown overnight in YPD, back diluted

1:20 in fresh YPD, and grown for 4-6 h. Cells were washed 3 times with sterile deionized water and normalized to a final OD600 of 1.0 before being diluted and plated to SLAD plus uracil at a density of approximately 50 cells/plate. Plates were incubated at 30^{o}C until filamentation was observed in wild type strains (about 7-8 days) before colonies were visualized. For the cell-level analysis of filamentation, cells were scraped from the edge of the colonies and resuspended in a small amount of media before spotting onto a slide for microscopy. The pictures were taken with an upright Nikon Eclipse 80i microscope with CoolSnap ES2 CCD (Photometrics). Images were acquired using the MetaMorph software package (Molecular Devices). For the analysis of filamentation, the dimensions of the cells were measured and a height to width ratio was calculated. The cells with height to width ratio equal to or greater than 2 were designated as 'filamented'.

2.5.3 Fluorescent microscopy

The liquid cultures from single colonies were grown in synthetic complete (if bearing no plasmids) or uracil and leucin lacking synthetic medium (if carrying pDS7 and pRP1194) overnight. The overnight cultures were back diluted to OD_{600}=0.1 and were grown for times indicated. 1 ml of grown cultures were centrifuged at 1000 rpm for 1 min and the cells were resuspended in ~80-100 ul media and spotted onto a slide. The cells were observed with a DeltaVision™ Elite system (GE Healthcare Life Sciences), equipped with an Olympus IX-71 inverted microscope, a sCMOS camera, a 100X/ 1.4 Oil Super-Plan APO objective, and a DeltaVision Elite Standard Filter Set with the FITC filter (Excitation:475/28, Emission: 525/48) for GFP and the TRITC filter (Excitation:542/27, Emission: 594/45) for mCherry. Image acquisition and deconvolution were done with softWoRx. ImageJ software was used for image cropping and adjustment (National Institutes of Health).

2.5.4 Sample preparation for Mass Spectrometry

S. cerevisiae Y825 control and ksp1K47D mutant cells were isotopically labeled with heavy (Lys-8/Arg-10) amino acids during cell culture (SILAC). Cell cultures were lysed by bead beating in lysis buffer; the lysis buffer was composed of 50 mM tris buffer (pH 8.2), 8 M urea, and protease inhibitors (Roche) and phosphatase inhibitors (50 mM NaF, 50 mM beta-glycerophosphate, 1 mM sodium vanadate, 10 mM sodium pyrophosphate, 1 mM phenylmethylsulfonyl fluoride). Frozen cells were suspended in 400 µl lysis buffer and were lysed by applying three cycles of bead beating (for one minute each) with a 2-minute rest on ice between cycles. Supernatants containing protein extract were recovered by centrifugation at 14,000 g for 10 minutes, and protein concentrations were measured by Bradford assay. Equal amounts of protein from three SILAC-labeled cells were combined, treated for disulfide reduction and alkylation, and digested with TMPK-treated trypsin (Worthington Biochemical Corp., Lakewood, NJ) at a trypsin:protein ratio of 1:10 at 37 °C overnight. Peptide mixtures were desalted with C18 (Waters) and separated into 12 strong cation exchange (SCX) fractions on a PolySulfoethyl A column (PolyLC, 150 x 4 mm) over a 48 minute salt gradient with two mobile phases: 100% solvent A (5 mM KH2PO4, 30% acetonitrile, pH 2.7) for 5 minutes, a linear gradient of 0-40% solvent B (250 mM KH2PO4, 30% acetonitrile, pH 2.7) in the following 35 min, a stiff increase of 40-100% B in 3 min, and flushing with 100% B for 5 min. Collected SCX fractions were desalted with C18 (Waters) and subjected to selective phosphopeptide enrichment using ZrO2 (Glygen, 50 µm i.d. resin) under acidic conditions in the presence of 2,5-dihydroxy benzoic acid (52, 53). Phosphopeptides selectively bound on ZrO2 were eluted with 4% NH4OH. The ZrO2 eluate of enriched phosphopeptides and the flow-through of each SCX fraction were analyzed by

nanoLC-tandem mass spectrometry (MSMS).

2.5.5 Mass Spectroscopy and Analysis

NanoLC-MSMS experiments were performed on a hybrid type mass spectrometer (Thermo, LTQ-Orbitrap XL) coupled to a nanoLC system (Eksigent, 2D nanoLC). Samples were separated on a custom capillary column (150 mm x 75 μm, 3 μm Sepax HP-C18) using a 120 min linear aqueous gradient (9-90% acetonitrile, 0.01% formic acid) delivered at 250 nL/min. The eluent was introduced on-line to the LTQ- Orbitrap via an electrospray device (Advion, TriVersa NanoMate) in positive ion mode.

The LTQ-Orbitrap was operated in a data-dependent mode alternating a full MS scan (300-1700 m/z at 60,000 resolution power at 400 m/z) in the Orbitrap analyzer and collision-induced dissociation scans (CID-MSMS) for the 7 most abundant ions with signal intensity above 500 from the previous MS scan in LTQ. Recurring precursor ions were dynamically excluded for 30 sec by applying charge-state monitoring, ions with 1 or unassigned charge states were rejected to increase the fraction of ions producing useful fragmentation. Lock mass ([(Si(CH3)2O)6]1+, m/z = 445.120029) was used for internal calibration. Each sample was analyzed by two LC-MS experiments. Raw LC- MS data file sets were processed, database searched, and quantified using MaxQuant (ver 1.0.13.8) and the Mascot search engine together. Mascot database searches were performed against a composite database of forward and reverse sequences of verified yeast open reading frames from the Saccharomyces Genome Database. Variable modifications were allowed for oxidation (M) and phosphorylations (STY), as well as a fixed modification of carbamidomethylation (C). Peptide, protein, and phosphorylation site identifications were filtered at a false discover rate of 5%. The MaxQuant normalized H/L (heavy/light) ratios with significance

scores less than 0.05 were considered statistically significant.

2.5.6 RNA sequencing and analysis

Single colonies of respective strains (yCK186 and DSY005) were inoculated in YPD and grown overnight at 30 C. In the morning, the amount of cells corresponding to a total of 1.25 OD were harvested at 4000 rpm for 4 minutes and resuspended in 5ml SLAD+Ura bringing the final OD_{600} to 0.25 per ml. The cultures were grown for another 6 hours in SLAD+Ura. The cells were harvested, and RNA was isolated using an Invitrogen RiboPure, Yeast kit following the manufacturer's instructions. The amount of RNA was determined with Nanodrop and quality of RNA was assessed at the University of Michigan Sequencing Core with BioAnalyzer. The sequencing was done with an Illumina HiSeq 4000 Single End 51 Cycle. The bioinformatic analysis of differential expression at gene and isoform level were done using Deseq2 and Tuxedo suits.

2.5.7 Gene Ontology Term Analysis

The transcripts that were significantly increased and significantly decreased in both Deseq2 and Tuxedo suite analysis were analyzed for common biological processes using DAVID 6.8 [42] . The GO terms determined were summarized using REVIGO [43]

2.6 Tables and Figures

Figure 2.1 Ksp1 kinase activity regulates pseudohyphal growth.

A) Colony morphology pictures and quantification of pseudohyphal growth phenotype for colonies grown on low nitrogen SLAD plates for 5-7 days B) Zoomed in pictures of edges of colonies shown in A C) Single cell analysis of pseudohyphal growth of the cells at the edges of the colonies. p values are determined by a z-test. n for each strain is noted in parentheses in the bars. D) Invasive growth phenotypes for diploid strains. Surface cells are washed from the spotted culture to identify invasive growth. Invasive growth was quantified as the pixel intensity of washed cultures relative to the pixel intensity of the spotted culture prior to washing. Measurements indicate the mean and standard deviation of three replicates.

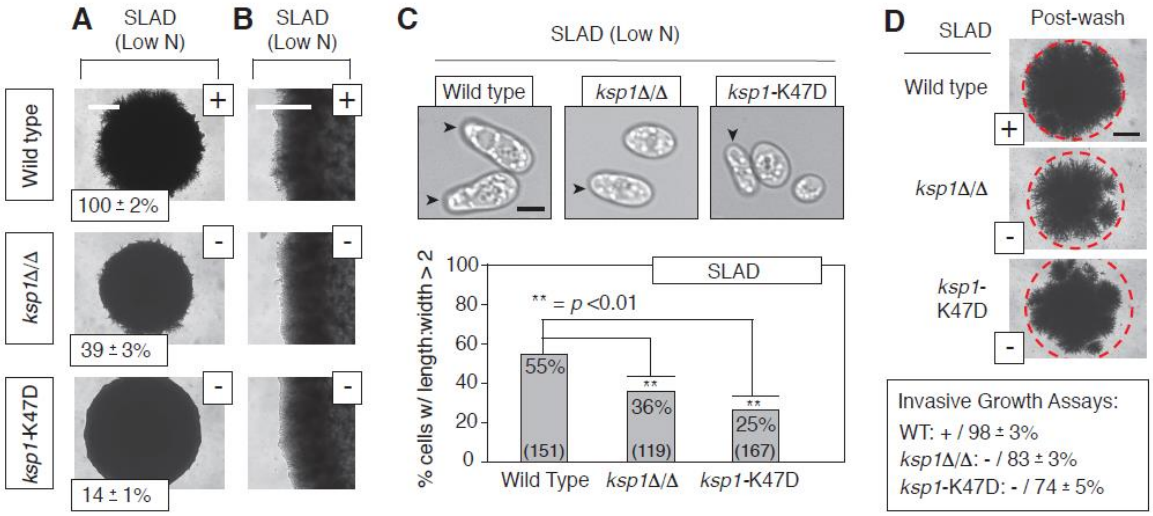

Figure 2.2 Quantitative phosphoproteomic analysis of Ksp1 signaling under filamentous growth inducing conditions by SILAC.

A) A diagram of the major steps in protein labeling and mass spectrometry-based identification of Ksp1 kinase-dependent phosphorylation. B) List of proteins that had at least one phosphosite differentially phosphorylated.

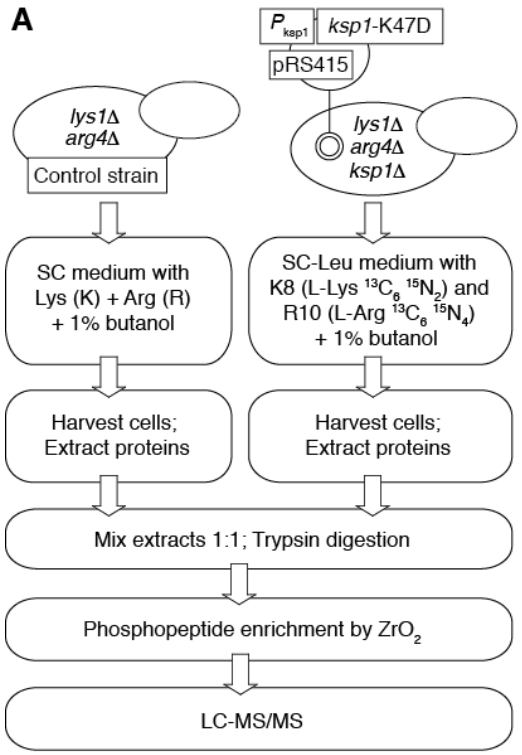

B

Hypo-phosphorylated in *ksp1*-K47D

Apm4	Dps1	Hom3	Maf1	Pdr16	Scp160	Tom70
Asr1	Duo1	Hos3	Mcm4	Pfk26	Sec65	Tpo4
Avt4	Fol2	Hsp12	Mdg1	Pik1	Seg1	Tsl1
Bap2	Fps1	Hsp30	Msc3	Pin4	Shm2	Ubp11
Ccc1	Fun12	Hsp42	Mtc4	Pma1	Sin3	Ugp1
Cdc19	Fun26	Hxk1	Npl3	Pxr1	Spt7	Uso1
Cdc60	Gat1	Igd1	Nth2	Rad53	Sse2	Vhs2
Cmk1	Gcd1	Iks1	Nvj1	Rie1	Ste20	Vid27
Cmk2	Gep3	Inp53	Ola1	Rli1	Tda1	Yck1
Ctr9	Gph1	Kel3	Osh3	Rod1	Tgl1	Ymr196w
Cub1	Gre2	Leu1	Pbi2	Rpa49	Tif4631	Ypt11
Dhh1	Hbt1	Lsp1	Pbp1	Rpc19	Tmc1	Yro2

Hyper-phosphorylated in *ksp1*-K47D

Ale1	Crp1	Gly1	Nha1	Rpl12b	Smi1	Tpo4
Aly2	Cue5	Gpd2	Pbp1	Rpp2b	Spa2	Ubp13
Avt1	Cus1	Hek2	Pdr12	Rps9a	Spc105	Ufd1
Bfr1	Cwc24	Iml2	Pdr5	Rps9b	Src1	Utp14
Bni5	Dcp2	Lhp1	Pwp1	Sec3	Ssa1	Utp30
Caf20	Def1	Lys20	Rcn2	Sec4	Ssn2	Vps41
Cho1	Dig1	Lys21	Rdi1	Sec7	Sub1	Xrn1
Chs5	Drn1	Mob1	Rfc1	Shs1	Sum1	Ycf1
Clc1	Fba1	Mpp10	Rho5	Sir2	Tpo3	Zeo1
Cmp2	Gin4					

Figure. 2.3 Potential Ksp1 targets are enriched in stress granule assembly proteins.
A) Gene Ontology term analysis using the Saccharomyces Genome Database. B) Gene Ontology term analysis using DAVID. C) The interrelationship network of Ksp1 and potential stress granule assembly proteins depicted using CytoScape.

A

GO ID:	GO Term:	*p*-Value:	FDR:	Expected FP:	Proteins Annotated to the GO Term:
34063	Stress granule assembly	6.2×10^{-4}	0	0	Dhh1, Pbp1, Ste20, Tif4631

B

DAVID Annotation Cluster	Enrichment Score: 2.7						
GO ID:	GO Term:	Annotated Proteins:	*p*-Value:	Fold Enrichment:	Bonferroni Correction:	Benjamini-Hochberg Procedure:	FDR:
Bio. Process 34063	Stress granule assembly	Dhh1, Pbp1, Ste20, Tif4631	1.4×10^{-4}	36	4.3×10^{-2}	4.3×10^{-2}	0.18
Cell. Comp. 10494	Cytoplasmic stress granule	Dhh1, Fun12, Leu1, Npl3, Pbp1, Tif4631, Ugp1	1.3×10^{-3}	5.6	0.13	4.4×10^{-2}	1.5
Mol. Function 3729	mRNA binding	Dhh1, Npl3, Pbp1, Pin4, Scp160, Ste20, Tif4631	5.8×10^{-2}	2.5	0.99	0.71	52

C

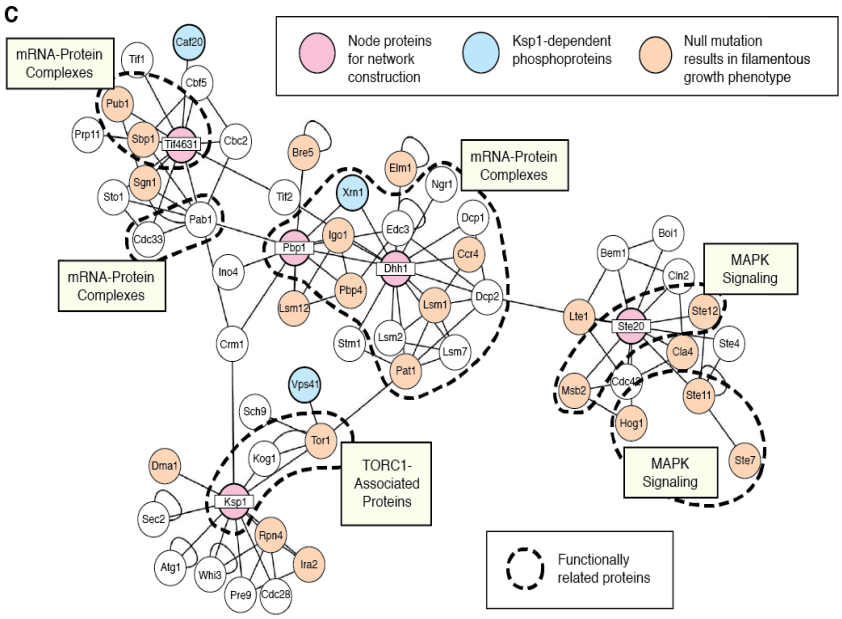

Figure 2.4 The Ksp1 dependent phosphorylation of stress granule markers regulate filamentous growth.

A) Colony morphology of stress granule marker protein mutants after 5-7 days on low nitrogen containing SLAD media. B) Invasive growth assay done by gentle washing of colonies. The percentages depict the percentage of the pixels of colonies after wash when compared to the area they occupied before wash. C) Activity of PKA pathway in stress granule protein markers as determined by a beta-galactosidase assay. The error bars represent standard deviation of 3 independent repeats.

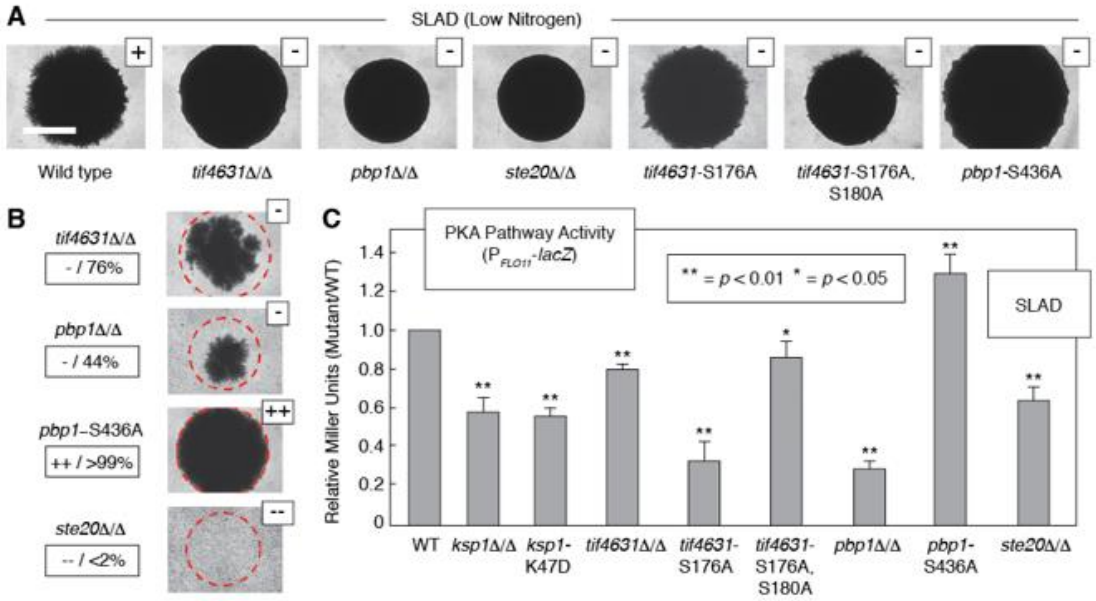

Figure 2.5 Ksp1 is required for wild type localization of stress granule marker proteins

The RNP component Pbp1p was visualized as a carboxy-terminal GFP fusion generated by integration of a GFP cassette at the 3'-end of *PBP1*. Cells were examined after seven days of incubation with shaking in liquid cultures of minimal medium with normal levels of ammonium sulfate. Stars indicate foci. Quantification of puncta is provided. The number of cells examined depicted inside the bars. P value is determined with a z-test. Scale bar, 3 μm. B) RNPs were visualized as foci using *PGK1* modified to contain 16 binding sites for U1A-mCherry in its 3'-UTR. mCherry-tagged RNA was analyzed after 7 days of growth in minimal medium with normal levels of ammonium sulfate. Stars indicate PGK1-mCherry puncta. Quantification of puncta is provided. p value is determined with a z-test.

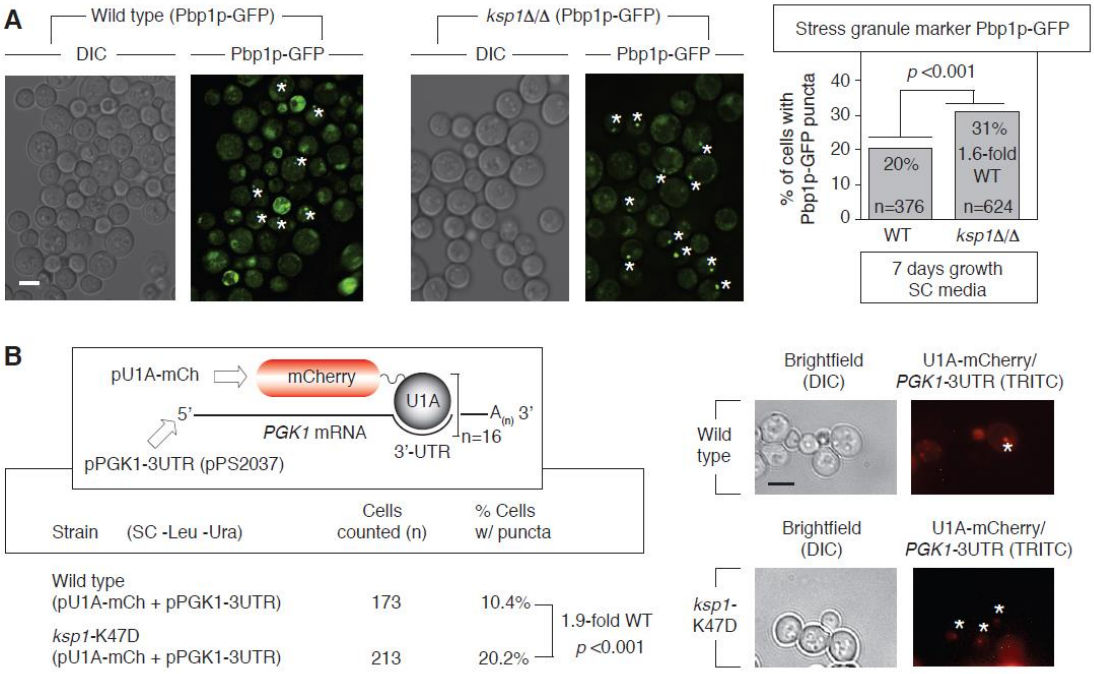

Figure 2.6 Ksp1 dependent phosphorylation sites of stress granule proteins are required for wild type stress granule localization.

A) The localization of Pbp1 and PGK1-mRNA in wild type and Ksp1 dependent phosphosite mutant and quantification of GFP puncta .Strains containined C-terminal GFP fused proteins as well as the PGK1 mRNA-U1A-mCherry system were grown in SC medium lacking uracil and leucine for 24 hours. The localization is detected by fluorescence microscopy. Quantification is done manually and blindly. Percentage of cells with puncta compared in both strains. p values are determined using a z-test. n for each strain is indicated in the graph. B) The localization of Stre20 and PGK1-mRNA in wild type and Ksp1 dependent phosphosite mutant and quantification of GFP puncta.Strains containined C-terminal GFP fused proteins as well as the PGK1 mRNA-U1A-mCherry system were grown in SC medium lacking uracil and leucine for 24 hours. The localization is detected by fluorescence microscopy. Quantification is done manually and blindly. Percentage of cells with puncta compared in both strains. p values are determined using a z-test. n for each strain is indicated in the graph.

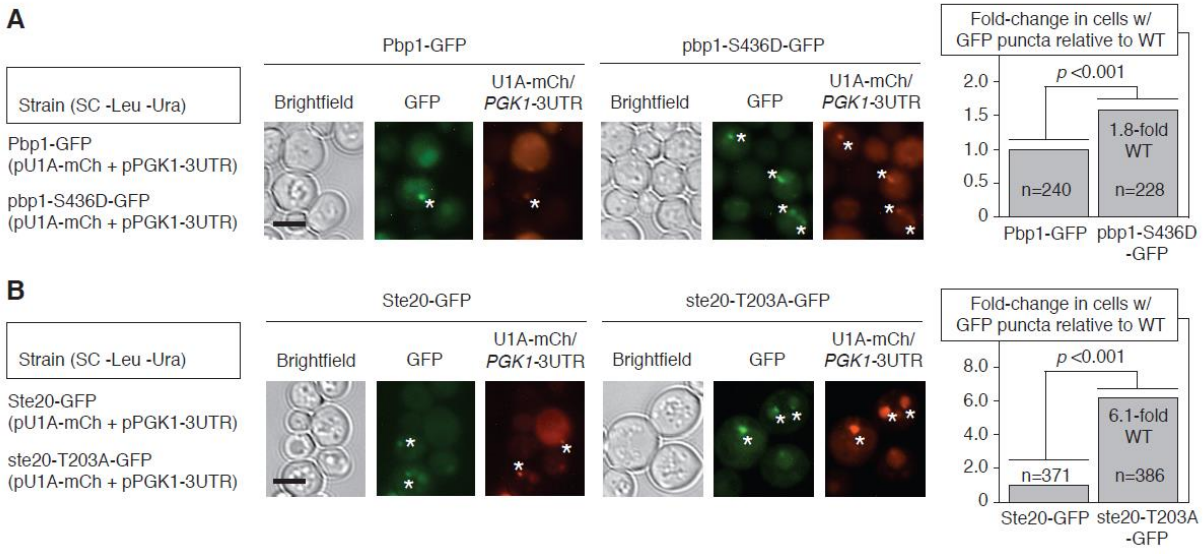

Figure 2.7 Ksp1 kinase activity regulates expression of transcripts related to a variety of cellular stress response under nitrogen stress.

A) Workflow of transcriptomic analysis **B)** Number of transcripts that are found to be significantly differentially expressed with DeSeq2 and Tuxedo suite analyses. **C)** Gene Ontology term analysis summary of genes that are downregulated in ksp1K47D mutant after 6 hours of low nitrogen stress as generated by REVIGO. The size of each rectangle is proportional to the enrichment of that GO term in the data set. **D)** Gene Ontology term analysis summary of genes that are upregulated in ksp1K47D mutant after 6 hours of low nitrogen stress as generated by REVIGO. The size of each rectangle is proportional to the enrichment of that GO term in the data set.**E)** Heat map showing the difference in levels of flocculation and pseudohyphal related transcripts in ksp1K47D mutant when compared to wild type **F)** Heat map showing the difference in levels of amino acid metabolism related transcripts in ksp1K47D mutant when compared to wild type **G)** Heat map showing the difference in levels of autophagy related transcripts in ksp1K47D mutant when compared to wild type **H)** Heat map showing the difference in levels of sporulation related transcripts in ksp1K47D mutant when compared to wild type

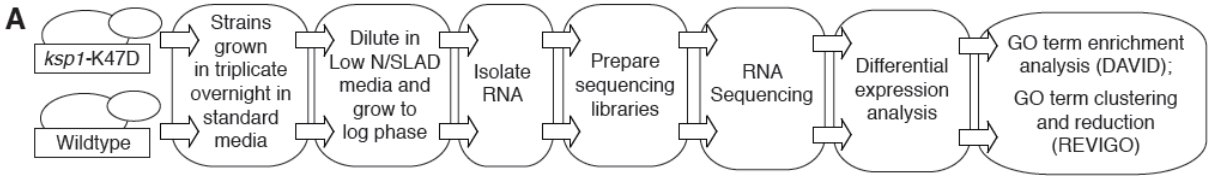

B

Analysis method	Comparison	Total count	Count of differentially expressed genes
deseq2	ksp1-KD_v_WT	6499	972
tuxedo_	ksp1-KD_v_WT	7036	1142

C

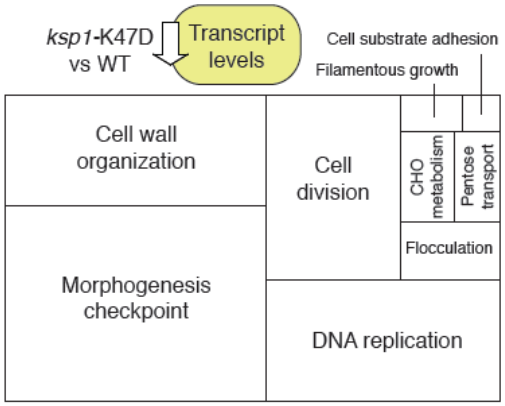

D

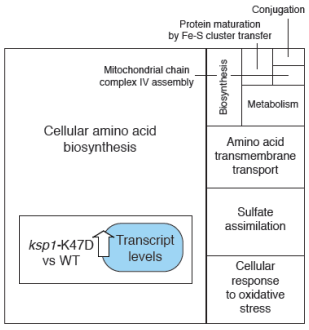

E

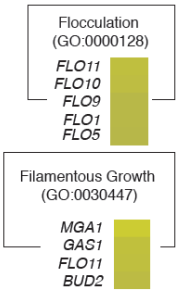

F

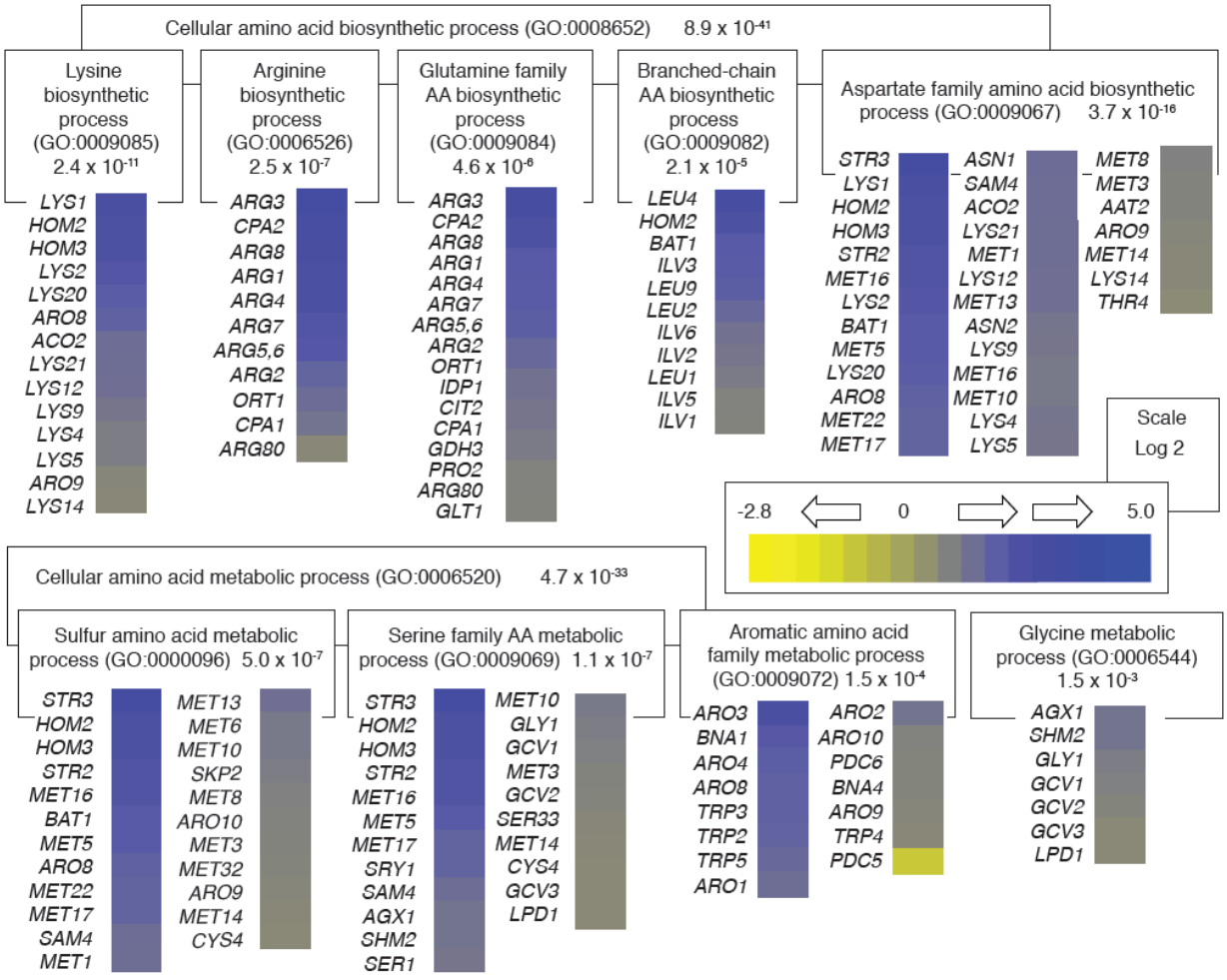
Cellular amino acid biosynthetic process (GO:0008652) 8.9 x 10-41
Lysine biosynthetic process (GO:0009085) 2.4 x 10-11
LYS1 HOM2 HOM3 LYS2 LYS20 ARO8 ACO2 LYS21 LYS12 LYS9 LYS4 LYS5 ARO9 LYS14
Arginine biosynthetic process (GO:0006526) 2.5 x 10-7
ARG3 CPA2 ARG8 ARG1 ARG4 ARG7 ARG5,6 ARG2 ORT1 CPA1 ARG80
Glutamine family AA biosynthetic process (GO:0009084) 4.6 x 10-6
ARG3 CPA2 ARG8 ARG1 ARG4 ARG7 ARG5,6 ARG2 ORT1 IDP1 CIT2 CPA1 GDH3 PRO2 ARG80 GLT1
Branched-chain AA biosynthetic process (GO:0009082) 2.1 x 10-5
LEU4 HOM2 BAT1 ILV3 LEU9 LEU2 ILV6 ILV2 LEU1 ILV5 ILV1
Aspartate family amino acid biosynthetic process (GO:0009067) 3.7 x 10-16
STR3 LYS1 HOM2 HOM3 STR2 MET16 LYS2 BAT1 MET5 LYS20 ARO8 MET22 MET17
ASN1 SAM4 ACO2 LYS21 MET1 LYS12 MET13 ASN2 LYS9 MET16 MET10 LYS4 LYS5
MET8 MET3 AAT2 ARO9 MET14 LYS14 THR4
Scale Log 2
-2.8 0 5.0
Cellular amino acid metabolic process (GO:0006520) 4.7 x 10-33
Sulfur amino acid metabolic process (GO:0000096) 5.0 x 10-7
STR3 HOM2 HOM3 STR2 MET16 BAT1 MET5 ARO8 MET22 MET17 SAM4 MET1
MET13 MET6 MET10 SKP2 MET8 ARO10 MET3 MET32 ARO9 MET14 CYS4
Serine family AA metabolic process (GO:0009069) 1.1 x 10-7
STR3 HOM2 HOM3 STR2 MET16 MET5 MET17 SRY1 SAM4 AGX1 SHM2 SER1
MET10 GLY1 GCV1 MET3 GCV2 SER33 MET14 CYS4 GCV3 LPD1
Aromatic amino acid family metabolic process (GO:0009072) 1.5 x 10-4
ARO3 BNA1 ARO4 ARO8 TRP3 TRP2 TRP5 ARO1
ARO2 ARO10 PDC6 BNA4 ARO9 TRP4 PDC5
Glycine metabolic process (GO:0006544) 1.5 x 10-3
AGX1 SHM2 GLY1 GCV1 GCV2 GCV3 LPD1

G **H**

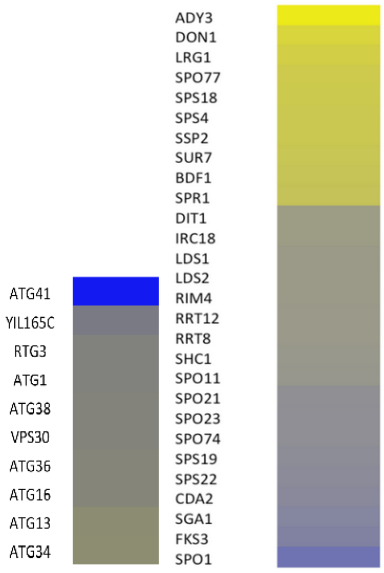
ATG41
YIL165C
RTG3
ATG1
ATG38
VPS30
ATG36
ATG16
ATG13
ATG34
ADY3
DON1
LRG1
SPO77
SPS18
SPS4
SSP2
SUR7
BDF1
SPR1
DIT1
IRC18
LDS1
LDS2
RIM4
RRT12
RRT8
SHC1
SPO11
SPO21
SPO23
SPO74
SPS19
SPS22
CDA2
SGA1
FKS3
SPO1

Table 2.1 List of strains used in this study.

Strain	Genotype	Source
yCK021	*ura3-52/ura3-52 leu2Δ0/LEU2 TRP1/trp1-1 MATa/MATα*	Johnson et al., 2014
yCK109	*ura3-52/ura3-52 leu2Δ0/LEU2 TRP1/trp1-1 MATa/MATα ksp1Δ::kanMX/ksp1Δ::kanMX*	This study
yCK186	*ura3-52/ura3-52 leu2Δ0/LEU2 TRP1/trp1-1 MATa/MATα ksp1*^{K47D}/ksp1^{K47D}	This study
yCK061	*ura3-52/ura3-52 leu2Δ0/LEU2 TRP1/trp1-1 MATa/MATα tif4631Δ::kanMX/tif4631Δ::kanMX*	This study
yCK190	*ura3-52/ura3-52 leu2Δ0/LEU2 TRP1/trp1-1 MATa/MATα tif4631*^{S176A}/tif4631^{S176A}	This study
DSY035	*ura3-52/ura3-52 leu2Δ0/LEU2 TRP1/trp1-1 MATa/MATα tif4631*^{S176,180A}/tif4631^{S176,180A}	This study
yCK059	*ura3-52/ura3-52 leu2Δ0/LEU2 TRP1/trp1-1 MATa/MATα pbp1Δ::kanMX/pbp1Δ::kanMX*	This study
DSY178	*ura3-52/ura3-52 leu2Δ0/LEU2 TRP1/trp1-1 MATa/MATα pbp1*^{S436A}/pbp1^{S436A}	This study
yCK083	*ura3-52/ura3-52 leu2Δ0/LEU2 TRP1/trp1-1 MATa/MATα ste20Δ::kanMX*/ste20Δ*::kanMX*	This study
DSY052	*his3Δ1 leu2Δ0 met15Δ0 ura3Δ0 PBP1-GFP-HIS3MX6 MATa*	GFP collection
DSY241	*his3Δ1 leu2Δ0 met15Δ0 ura3Δ0 pbp1S436D-GFP::HisMX MATa*	This study
DSY226	*his3Δ1 leu2Δ0 lys2D0 ura3Δ0 Ste20-GFP::His3MX6 MATα*	GFP collection
DSY240	*his3Δ1 leu2Δ0 lys2D0 ura3Δ0 ste20T203A-GFP::His3MX6 MATα*	This study
DSY200	*ura3-52/ura3-52 trpΔ/TRP LEU/leu2Δ0+* p*FLO11 6/7*	This study
DSY202	*ura3-52/ura3-52 trpΔ/TRP LEU/leu2Δ0 Δksp1::KanMX6/Δksp1::KanMX6+pFLO11 6/7*	This study
DSY204	*ura3-52/ura3-52 trpΔ/TRP LEU/leu2Δ0 ksp1K47D/ksp1K47D+pFLO11 6/7*	This study
DSY208	*ura3-52/ura3-52 trpΔ/TRP LEU/leu2Δ0 Δtif4631::KanMX6/Δtif4631::KanMX6 +pFLO11 6/7*	This study
DSY210	*ura3-52/ura3-52 trpΔ/TRP LEU/leu2Δ0 tif4631S176A/tif4631S176A+pFLO11 6/7*	This study
DSY214	*ura3-52/ura3-52 trpΔ/TRP LEU/leu2Δ0 tif4631S176,180A/tif4631S176,180A+pFLO11 6/7*	This study
DSY216	*ura3-52/ura3-52 trpΔ/TRP LEU/leu2Δ0 Δpbp1::KanMX6/Δpbp1::KanMX6 +pFLO11 6/7*	This study
DSY218	*ura3-52/ura3-52 trpΔ/TRP LEU/leu2Δ0 pbp1S436A/pbp1S436A+pFLO11 6/7*	This study
DSY220	*ura3-52/ura3-52 trpΔ/TRP LEU/leu2Δ0 Δste20::KanMX6/Δste20::KanMX6 +pFLO11 6/7*	This study
DSY225	*his3Δ1 leu2Δ0 met15Δ0 ura3Δ0 LYS2 PBP1-GFP-HIS3MX6* +pPS2037 + pDS7	This study
DSY226	*his3Δ1 leu2Δ0 lys2D0 ura3Δ0 Ste20-GFP::His3MX6* +pPS2037 + pDS7	This study
DSY228	*his3Δ1 leu2Δ0 lys2D0 ura3Δ0 ksp1Δ::KanMX* + Pbp1-GFP::KanMX6+pPS2037 + pDS7	This study
DSY185	*his3Δ1 leu2Δ0 lys2D0 ura3Δ0 ksp1K47D+* pPS2037 + pDS7	This study
DSY240	*his3Δ1 leu2Δ0 lys2D0 ura3Δ0 ste20T203A-GFP::His3MX6* +pPS2037 + pDS7	This study
DSY242	*his3Δ1 leu2Δ0 met15Δ0 ura3Δ0 LYS2 pbp1S436D-GFP::HisMX* +pPS2037 + pDS7	This study

Table 2.2 List of plasmids used in this study.

Short name	Description	Source
pRS406	*URA3*, *Cen,* AMP	
pLG669-Z FLO11 6/7	*URA3*, 2 µ, AMP, p*FLO11*::LacZ-6/7	
pPS2037	*URA3,* 2µ, AMP, PGK1-U1A-PGK1 3' UTR	
pDS7	*LEU*, 2 µ, AMP, U1A-mCherry	This study
	pFA6a-GFP(S65T)-HisMX6	
	pFA6a-KanMX	
	pKSP1-ksp1^{K47D}	This study
	pPKSP1-KSP1	This study

Table 2.3 List of summary of Gene Ontology terms enriched in the set of transcripts whose expression is decreased in kinase dead ksp1 mutant under low nitrogen conditions.

term_ID	description	frequencyInDb	log10pvalue	uniquueness	dispensability	representative
GO:0000128	flocculation	0.13%	-4.1337	0.902	0	flocculation
GO:0005975	carbohydrate metabolic process	4.50%	-3.4685	0.91	0	carbohydrate metabolism
GO:0031589	cell-substrate adhesion	0.13%	-1.0262	0.97	0	cell-substrate adhesion
GO:0071555	cell wall organization	3.30%	-7.1555	0.827	0	cell wall organization
GO:0007020	microtubule nucleation	0.27%	-3.8697	0.695	0.159	cell wall organization
GO:0010696	positive regulation of spindle pole body separation	0.11%	-2.4738	0.626	0.626	cell wall organization
GO:0071970	fungal-type cell wall (1->3)-beta-D-glucan biosynthetic process	0.08%	-1.6771	0.725	0.58	cell wall organization
GO:0031122	cytoplasmic microtubule organization	0.13%	-1.3826	0.724	0.639	cell wall organization
GO:0031106	septin ring organization	0.46%	-1.8628	0.769	0.549	cell wall organization
GO:0030472	mitotic spindle organization in nucleus	0.16%	-1.8628	0.635	0.649	cell wall organization
GO:0051301	cell division	4.50%	-6.7595	0.847	0.031	cell division
GO:0007049	cell cycle	11.59%	-9.8928	0.834	0.181	cell division
GO:0030435	sporulation resulting in formation of a cellular spore	2.49%	-1.0453	0.833	0.14	cell division
GO:0015750	pentose transport	0.06%	-1.8849	0.829	0.064	pentose transport
GO:1901684	arsenate ion transmembrane transport	0.03%	-1.0262	0.944	0.162	pentose transport
GO:0044879	morphogenesis checkpoint	0.06%	-3.3686	0.708	0.09	morphogenesis checkpoint
GO:0000278	mitotic cell cycle	6.12%	-1.5656	0.709	0.623	morphogenesis checkpoint
GO:0000433	negative regulation of transcription from RNA polymerase II promoter by glucose	0.15%	-1.0928	0.717	0.536	morphogenesis checkpoint

GO:0055072	iron ion homeostasis	0.87%	-1.3131	0.896	0.207	morphogenesis checkpoint
GO:0070301	cellular response to hydrogen peroxide	0.22%	-1.1761	0.869	0.319	morphogenesis checkpoint
GO:0006974	cellular response to DNA damage stimulus	5.15%	-2.6908	0.841	0.477	morphogenesis checkpoint
GO:0016310	phosphorylation	6.00%	-1.0645	0.831	0.609	morphogenesis checkpoint
GO:0000083	regulation of transcription involved in G1/S transition of mitotic cell cycle	0.42%	-2.0237	0.61	0.606	morphogenesis checkpoint
GO:0016584	nucleosome positioning	0.16%	-1.0193	0.792	0.502	morphogenesis checkpoint
GO:0000079	regulation of cyclin-dependent protein serine/threonine kinase activity	0.43%	-3.2226	0.641	0.476	morphogenesis checkpoint
GO:0035556	intracellular signal transduction	3.47%	-1.5748	0.744	0.2	morphogenesis checkpoint
GO:0007064	mitotic sister chromatid cohesion	0.58%	-1.9388	0.642	0.645	morphogenesis checkpoint
GO:0007067	mitotic nuclear division	3.60%	-3.2976	0.633	0.497	morphogenesis checkpoint
GO:0046777	protein autophosphorylation	0.36%	-1.2169	0.82	0.58	morphogenesis checkpoint
GO:0006468	protein phosphorylation	3.58%	-1.5608	0.788	0.603	morphogenesis checkpoint
GO:0008361	regulation of cell size	0.16%	-1.2232	0.805	0.423	morphogenesis checkpoint
GO:0006355	regulation of transcription, DNA-templated	10.78%	-3.214	0.672	0.561	morphogenesis checkpoint
GO:0000086	G2/M transition of mitotic cell cycle	0.60%	-1.7817	0.737	0.666	morphogenesis checkpoint
GO:0030466	chromatin silencing at silent mating-type cassette	0.79%	-1.9409	0.63	0.358	morphogenesis checkpoint
GO:0006260	DNA replication	2.36%	-2.9336	0.749	0.094	DNA replication
GO:0006298	mismatch repair	0.37%	-1.5219	0.74	0.491	DNA replication
GO:0019655	glycolytic fermentation to ethanol	0.11%	-1.8849	0.725	0.371	DNA replication
GO:2000531	regulation of fatty acid biosynthetic process by regulation of transcription from RNA polymerase II promoter	0.06%	-1.0262	0.723	0.48	DNA replication

GO:0009263	deoxyribonucleotide biosynthetic process	0.15%	-1.5149	0.72	0.473	DNA replication
GO:0006273	lagging strand elongation	0.28%	-1.0193	0.772	0.601	DNA replication
GO:0006279	premeiotic DNA replication	0.12%	-1.2715	0.65	0.438	DNA replication
GO:0006281	DNA repair	4.47%	-1.3808	0.681	0.669	DNA replication
GO:0009298	GDP-mannose biosynthetic process	0.05%	-2.1719	0.828	0.153	DNA replication
GO:0006473	protein acetylation	1.02%	-1.0262	0.851	0.131	DNA replication
GO:0045740	positive regulation of DNA replication	0.16%	-1.0262	0.73	0.557	DNA replication
GO:0009186	deoxyribonucleoside diphosphate metabolic process	0.02%	-1.0262	0.782	0.628	DNA replication
GO:0035753	maintenance of DNA trinucleotide repeats	0.16%	-1.0193	0.701	0.451	DNA replication
GO:2001020	regulation of response to DNA damage stimulus	0.33%	-1.0262	0.802	0.497	DNA replication
GO:0030447	filamentous growth	1.96%	-1.6549	0.896	0.096	filamentous growth

Table 2.4 List of summary of Gene Ontology terms enriched in the set of transcripts whose expression is increased in kinase dead ksp1 mutant under low nitrogen conditions.

term_ID	description	frequencyInDb	log10pvalue	uniqueness	dispensability	representative	
GO:0008152	metabolic process	56.47%	-5.7747	0.988	0	metabolism	
GO:0008652	cellular amino acid biosynthetic process	1.97%	-44.7773	0.364	0	cellular amino acid biosynthesis	
GO:0006546	glycine catabolic process	0.06%	-2.6096	0.464	0.547	cellular amino acid biosynthesis	
GO:0006067	ethanol metabolic process	0.27%	-1.7542	0.599	0.369	cellular amino acid biosynthesis	
GO:0009082	branched-chain amino acid biosynthetic process	0.24%	-6.8539	0.414	0.689	cellular amino acid biosynthesis	
GO:0006531	aspartate metabolic process	0.08%	-1.6696	0.462	0.694	cellular amino acid biosynthesis	
GO:0006526	arginine biosynthetic process	0.18%	-7.8996	0.418	0.67	cellular amino acid biosynthesis	
GO:0009102	biotin biosynthetic process	0.09%	-1.9685	0.416	0.627	cellular amino acid biosynthesis	
GO:0000050	urea cycle	0.03%	-3.1308	0.662	0.334	cellular amino acid biosynthesis	
GO:0006164	purine nucleotide biosynthetic process	0.99%	-1.7908	0.55	0.471	cellular amino acid biosynthesis	
GO:0009423	chorismate biosynthetic process	0.06%	-2.6096	0.478	0.605	cellular amino acid biosynthesis	
GO:0006116	NADH oxidation	0.15%	-1.3045	0.593	0.568	cellular amino acid biosynthesis	
GO:0006592	ornithine biosynthetic process	0.06%	-2.6096	0.463	0.605	cellular amino acid biosynthesis	
GO:0006730	one-carbon metabolic process	0.27%	-2.4996	0.614	0.369	cellular amino acid biosynthesis	
GO:0006103	2-oxoglutarate metabolic process	0.11%	-1.9685	0.522	0.683	cellular amino acid biosynthesis	
GO:0008615	pyridoxine biosynthetic process	0.09%	-1.047	0.538	0.69	cellular amino acid biosynthesis	
GO:0000105	histidine biosynthetic process	0.15%	-2.108	0.446	0.658	cellular amino acid biosynthesis	
GO:0006097	glyoxylate cycle	0.15%	-3.068	0.516	0.484	cellular amino acid biosynthesis	
GO:00192	lactate biosynthetic process	0.03%	-2.2406	0.486	0.57	cellular amino	

49						acid biosynthesis
GO:0006099	tricarboxylic acid cycle	0.46%	-5.2976	0.489	0.543	cellular amino acid biosynthesis
GO:0006090	pyruvate metabolic process	0.81%	-2.2958	0.463	0.642	cellular amino acid biosynthesis
GO:0006635	fatty acid beta-oxidation	0.28%	-2.2958	0.478	0.617	cellular amino acid biosynthesis
GO:0055114	oxidation-reduction process	7.12%	-21.9031	0.64	0.357	cellular amino acid biosynthesis
GO:0009073	aromatic amino acid family biosynthetic process	0.22%	-4.7077	0.419	0.685	cellular amino acid biosynthesis
GO:0030435	sporulation resulting in formation of a cellular spore	2.49%	-2.4735	0.816	0.125	cellular amino acid biosynthesis
GO:0033617	mitochondrial respiratory chain complex IV assembly	0.33%	-1.4283	0.931	0.021	mitochondrial respiratory chain complex IV assembly
GO:0034599	cellular response to oxidative stress	1.78%	-6.1746	0.899	0.026	cellular response to oxidative stress
GO:0006979	response to oxidative stress	1.96%	-1.9006	0.938	0.462	cellular response to oxidative stress
GO:0006855	drug transmembrane transport	0.21%	-1.1126	0.781	0.446	cellular response to oxidative stress
GO:0098869	cellular oxidant detoxification	0.55%	-4.8013	0.909	0.493	cellular response to oxidative stress
GO:0031669	cellular response to nutrient levels	2.05%	-1.1978	0.911	0.381	cellular response to oxidative stress
GO:0000746	conjugation	1.88%	-1.1978	0.925	0.026	conjugation
GO:0000103	sulfate assimilation	0.15%	-5.4597	0.808	0.057	sulfate assimilation
GO:0070814	hydrogen sulfide biosynthetic process	0.09%	-4.5622	0.747	0.553	sulfate assimilation
GO:0019379	sulfate assimilation, phosphoadenylyl sulfate reduction by phosphoadenylyl-sulfate reductase (thioredoxin)	0.05%	-1.6696	0.655	0.526	sulfate assimilation
GO:0016226	iron-sulfur cluster assembly	0.36%	-3.3261	0.708	0.617	sulfate assimilation
GO:0097428	protein maturation by iron-sulfur cluster transfer	0.12%	-1.5787	0.902	0.06	protein maturation by iron-sulfur cluster transfer
GO:0007039	protein catabolic process in the vacuole	0.18%	-1.0114	0.867	0.175	protein maturation by iron-sulfur cluster transfer

GO:0003333	amino acid transmembrane transport	0.61%	-2.1595	0.74	0.075	amino acid transmembrane transport	
GO:0055085	transmembrane transport	7.02%	-6.8041	0.892	0.381	amino acid transmembrane transport	
GO:0006820	anion transport	2.90%	-1.7542	0.854	0.607	amino acid transmembrane transport	
GO:0006839	mitochondrial transport	1.97%	-1.7542	0.901	0.278	amino acid transmembrane transport	
GO:1902358	sulfate transmembrane transport	0.09%	-1.1978	0.781	0.696	amino acid transmembrane transport	
GO:0009058	biosynthetic process	32.15%	-3.7235	0.88	0.098	biosynthesis	
GO:0006807	nitrogen compound metabolic process	38.44%	-2.4558	0.879	0.238	biosynthesis	

2.7 References

1. Cullen, P. J. & Sprague, G. F. The Regulation of Filamentous Growth in Yeast. *Genetics* **190**, 23–49 (2012).
2. Mitchell, A. P. Dimorphism and virulence in Candida albicans. *Curr. Opin. Microbiol.* **1**, 687–692 (1998).
3. Lo, H.-J. *et al.* Nonfilamentous C. albicans Mutants Are Avirulent. *Cell* **90**, 939–949 (1997).
4. Jin, R., Dobry, C. J., McCown, P. J. & Kumar, A. Large-Scale Analysis of Yeast Filamentous Growth by Systematic Gene Disruption and Overexpression. *Mol. Biol. Cell* **19**, 284–296 (2008).
5. Ryan, O. *et al.* Global Gene Deletion Analysis Exploring Yeast Filamentous Growth. *Science (80-.).* **337**, 1353–1356 (2012).
6. Fleischmann, M., Stagljar, I. & Aebi, M. Allele-specific suppression of a Saccharomyces cerevisiae prp20 mutation by overexpression of a nuclear serine/threonine protein kinase. *Mol. Gen. Genet.* **250**, 614–25 (1996).
7. Umekawa, M. & Klionsky, D. J. Ksp1 kinase regulates autophagy via the target of rapamycin complex 1 (TORC1) pathway. *J. Biol. Chem.* **287**, 16300–10 (2012).
8. Bharucha, N. *et al.* Analysis of the yeast kinome reveals a network of regulated protein localization during filamentous growth. *Mol. Biol. Cell* **19**, 2708–17 (2008).
9. Soulard, A. *et al.* The Rapamycin-sensitive Phosphoproteome Reveals That TOR Controls Protein Kinase A Toward Some But Not All Substrates. *Mol. Biol. Cell* **21**, 3475–3486 (2010).
10. Borneman, A. R. *et al.* Target hub proteins serve as master regulators of development in

yeast. *Genes Dev.* **20**, 435–48 (2006).

11. Gimeno, C. J. & Fink, G. R. Induction of pseudohyphal growth by overexpression of PHD1, a Saccharomyces cerevisiae gene related to transcriptional regulators of fungal development. *Mol. Cell. Biol.* **14**, 2100–12 (1994).
12. Gavrias, V., Andrianopoulos, A., Gimeno, C. J. & Timberlake, W. E. Saccharomyces cerevisiae TEC1 is required for pseudohyphal growth. *Mol. Microbiol.* **19**, 1255–63 (1996).
13. Pothoulakis, G. & Ellis, T. Synthetic gene regulation for independent external induction of the Saccharomyces cerevisiae pseudohyphal growth phenotype. *Commun. Biol.* **1**, 7 (2018).
14. Love, M. I., Huber, W. & Anders, S. Moderated estimation of fold change and dispersion for RNA-seq data with DESeq2. *Genome Biol.* **15**, 550 (2014).
15. Trapnell, C. *et al.* Differential gene and transcript expression analysis of RNA-seq experiments with TopHat and Cufflinks. *Nat. Protoc.* **7**, 562–578 (2012).
16. Giannattasio, M. & Branzei, D. S-phase checkpoint regulations that preserve replication and chromosome integrity upon dNTP depletion. *Cell. Mol. Life Sci.* **74**, 2361–2380 (2017).
17. Ewald, J. C. How yeast coordinates metabolism, growth and division. *Curr. Opin. Microbiol.* **45**, 1–7 (2018).
18. Lo, W. S. & Dranginis, A. M. The cell surface flocculin Flo11 is required for pseudohyphae formation and invasion by Saccharomyces cerevisiae. *Mol. Biol. Cell* **9**, 161–71 (1998).
19. Ong, S.-E. *et al.* Stable isotope labeling by amino acids in cell culture, SILAC, as a simple

and accurate approach to expression proteomics. *Mol. Cell. Proteomics* **1**, 376–86 (2002).

20. Protter, D. S. W. & Parker, R. Principles and Properties of Stress Granules. *Trends Cell Biol.* **26**, 668–679 (2016).

21. Shively, C. A. *et al.* Large-Scale Analysis of Kinase Signaling in Yeast Pseudohyphal Development Identifies Regulation of Ribonucleoprotein Granules. *PLOS Genet.* **11**, e1005564 (2015).

22. Smoot, M. E., Ono, K., Ruscheinski, J., Wang, P.-L. & Ideker, T. Cytoscape 2.8: new features for data integration and network visualization. *Bioinformatics* **27**, 431–432 (2011).

23. Ryan, O. *et al.* Global Gene Deletion Analysis Exploring Yeast Filamentous Growth. *Science (80-.).* **337**, 1353–1356

24. Cullen, P. J. & Sprague, G. F. Glucose depletion causes haploid invasive growth in yeast. *Proc. Natl. Acad. Sci. U. S. A.* **97**, 13619–24 (2000).

25. Sweeney, F. D. *et al.* Saccharomyces cerevisiae Rad9 Acts as a Mec1 Adaptor to Allow Rad53 Activation. *Curr. Biol.* **15**, 1364–1375 (2005).

26. Lao, J. P. *et al.* The Yeast DNA Damage Checkpoint Kinase Rad53 Targets the Exoribonuclease, Xrn1. *G3: Genes|Genomes|Genetics* **8**, g3.200767.2018 (2018).

27. Wen, X. & Klionsky, D. J. An overview of macroautophagy in yeast. *J. Mol. Biol.* **428**, 1681–99 (2016).

28. Yao, Z., Delorme-Axford, E., Backues, S. K. & Klionsky, D. J. Atg41/Icy2 regulates autophagosome formation. *Autophagy* **11**, 2288–99 (2015).

29. Delorme-Axford, E. & Klionsky, D. J. Transcriptional and post-transcriptional regulation

of autophagy in the yeast Saccharomyces cerevisiae. *J. Biol. Chem.* **293**, 5396–5403 (2018).

30. Wheeler, J. R., Matheny, T., Jain, S., Abrisch, R. & Parker, R. Distinct stages in stress granule assembly and disassembly. *Elife* **5**, (2016).

31. Jain, S. *et al.* ATPase-Modulated Stress Granules Contain a Diverse Proteome and Substructure. *Cell* **164**, 487–498 (2016).

32. Alberti, S., Halfmann, R., King, O., Kapila, A. & Lindquist, S. A Systematic Survey Identifies Prions and Illuminates Sequence Features of Prionogenic Proteins. *Cell* **137**, 146–158 (2009).

33. Treeck, B. Van *et al.* RNA self-assembly contributes to stress granule formation and defining the stress granule transcriptome. *Proc. Natl. Acad. Sci.* **115**, 2734–2739 (2018).

34. Mitchell, S. F., Jain, S., She, M. & Parker, R. Global analysis of yeast mRNPs. *Nat. Struct. Mol. Biol.* **20**, 127–33 (2013).

35. Wang, J. T. *et al.* Regulation of RNA granule dynamics by phosphorylation of serine-rich, intrinsically disordered proteins in C. elegans. *Elife* **3**, (2014).

36. Reineke, L. C. *et al.* Casein Kinase 2 Is Linked to Stress Granule Dynamics through Phosphorylation of the Stress Granule Nucleating Protein G3BP1. *Mol. Cell. Biol.* **37**, (2017).

37. Yoon, J.-H., Choi, E.-J. & Parker, R. Dcp2 phosphorylation by Ste20 modulates stress granule assembly and mRNA decay in Saccharomyces cerevisiae. *J. Cell Biol.* **189**, 813–27 (2010).

38. Wippich, F. *et al.* Dual specificity kinase DYRK3 couples stress granule condensation/dissolution to mTORC1 signaling. *Cell* **152**, 791–805 (2013).

39. Boeynaems, S. *et al.* Protein Phase Separation: A New Phase in Cell Biology. *Trends Cell Biol.* **28**, 420–435 (2018).

40. Holehouse, A. S. & Pappu, R. V. Functional Implications of Intracellular Phase Transitions. *Biochemistry* **57**, 2415–2423 (2018).

41. Simpson, C. E. & Ashe, M. P. Adaptation to stress in yeast: to translate or not? *Biochem. Soc. Trans.* **40**, 794–9 (2012).

42. Huang, D. W., Sherman, B. T. & Lempicki, R. A. Systematic and integrative analysis of large gene lists using DAVID bioinformatics resources. *Nat. Protoc.* **4**, 44–57 (2009).

43. Supek, F., Bošnjak, M., Škunca, N. & Šmuc, T. REVIGO Summarizes and Visualizes Long Lists of Gene Ontology Terms. *PLoS One* **6**, e21800 (2011).

CHAPTER 3

Inositol Polyphosphates Regulate and Predict Yeast Pseudohyphal Growth Phenotypes

3.1 Abstract

Pseudohyphal growth is a nutrient-regulated program in which budding yeast form multicellular filaments of elongated and connected cells. Filamentous growth is required for virulence in pathogenic fungi and provides an informative model of stress-responsive signaling. Filametous growth can be regulated by cellular signaling, transcriptional control as well as small metabolites such as alcohol. The genetics and regulatory networks that modulate pseudohyphal growth have been studied extensively, but little is known regarding the changes in metabolites that enable pseudohyphal filament formation. Inositol signaling molecules are an important class of metabolite messengers encompassing highly phosphorylated and diffusible inositol polyphosphates (IPs). We report here that the IP biosynthesis pathway is required for normal pseudohyphal growth. Under nitrogen-limiting conditions that induce filamentation, IPs exhibited characteristic profiles. When we profiled the IP content of cells using HPLC, we were able to distinguish two different IP_7 pyrophosphate isoforms, namely 1PP-IP_5 and 5PP-IP_5. Some mutants of IP biosynthesis pathway kinases and phosphatases exhibited hyper-filamentous growth. Those mutants that exhibited hyper-filamentous growth had elevated levels of 5PP-IP_5 relative to 1PP-IP_5 and IP_8. Overexpression of *KCS1*, which promotes formation of inositol pyrophosphates, was

sufficient to drive pseudohyphal filamentation on medium with normal nitrogen levels. We found that the kinases Snf1p (AMPK), Kss1p, and Fus3p (MAPKs), required for wild-type pseudohyphal growth, are also required for wild-type IP levels. Deletion analyses of the corresponding kinase genes indicated elevated IP_3 levels and an absence of exaggerated 5PP-IP_5 peaks in trace profiles from *snf1*Δ/Δ and *kss1*Δ/Δ mutants exhibiting decreased pseudohyphal filamentation. Elevated 5PP-IP_5 levels were present in the hyperfilamentous *fus3* deletion mutant. We also showed that IP profile of *Candida albicans* is altered under filamentation inducing conditions and several IP metabolism genes cause aberrant filamentation phenotypes when deleted. Collectively, the data identify the presence of elevated 5PP-IP_5 levels relative to other inositol pyrophosphates as an *in vivo* marker of hyper-filamentous growth, while providing initial evidence for the regulation of IP signaling by pseudohyphal growth kinases.

3.2 Introduction

Although much still remains to be understood regarding the changes in cellular properties, signaling pathways, and proteins underlying the pseudohyphal growth transition, even less is known with respect to the changes in metabolites associated with filamentation. Short-chain alcohols, such as 1-butanol, can induce pseudohyphal growth, and these alcohols are now recognized as part of a quorum-sensing mechanism in *S. cerevisiae* [1,2] Yeast cells secrete alcohol, such that corresponding alcohol levels roughly gauge cell density and population [1]. Tetrahydrofolate (vitamin B9) also induces pseudohyphal growth through uncharacterized mechanisms that impact *FLO11* expression levels [3]. The phytohormone indole-3-acetic acid is produced in yeasts and is known to induce pseudohyphal filamentation [4]; its mechanism of action is unclear.

Our studies of pseudohyphal growth signaling pathways led us to consider the role of another metabolite, inositol polyphosphate, in the yeast pseudohyphal growth transition. Using quantitative phosphoproteomics to profile changes in protein phosphorylation dependent upon a set of eight kinases required for wild-type pseudohyphal growth (Ste20p, Ste11p, Ste7p, Kss1p, Fus3p, Tpk2p, Snf1p, and Elm1p), we observed differences in the phosphorylation state of several kinases in the InsP biosynthetic pathway [5]. InsPs are a ubiquitous class of second messengers with an increasingly recognized role in a diverse array of cellular processes.

Soluble InsPs are derived from membrane localized phosphatidylinositol 4,5-bisphosphate (PIP_2) through the action of phospholipase C [6], which cleaves $InsP_3$ from PIP_2. The inositol polyphosphate $InsP_3$ is a 6-carbon cyclic alcohol with phosphate groups at the carbon-1, carbon-4, and carbon-5 positions. A variety of InsP species with additional phosphate groups are derived from $InsP_3$ through a sequentially acting set of InsP kinases and phosphatases [reviewed in [7]]. Arg82p, the *Saccharomyces cerevisiae* ortholog of human IMPK, generates $InsP_5$ from $InsP_3$ through reactions that sequentially add phosphate groups to the carbon-6 and then carbon-3 positions of $InsP_3$ [8,9]. The InsP kinase Ipk1p can convert $InsP_5$ to $InsP_6$ (York et al. 1999). Both $InsP_5$ and $InsP_6$ can be pyrophosphorylated, acquiring two phosphate groups at a single carbon position. In *S. cerevisiae*, the kinases Kcs1p and Vip1p are capable of pyrophosphorylating InsPs [10]. Pyrophosphorylated isoforms of $InsP_7$ and $InsP_8$, as well as the kinases catalyzing the respective reactions, are summarized in Figure 3.1. InsP phosphorylation is balanced by dephosphorylation through the phosphatases Siw14p, Ddp1p, and Vip1p, with the latter exhibiting both kinase and phosphatase activity[11–13]. The actions of these kinases and phosphatases generate dynamic changes in the cellular abundance and availability of different InsP isoforms, making them strong candidates to act as signal transducers in response to environmental perturbations.

InsPs are known to act as secondary messengers for cellular signal transduction. Perhaps most famously, $InsP_3$ binds to calcium channel receptors, regulating intracellular calcium release; however, this regulatory effect is not observed in *S. cerevisiae*, being restricted to higher eukaryotes [14]. InsPs and inositol pyrophosphates have been shown to regulate a broad range of processes, including phosphate sensing, insulin secretion, viral particle release, glycolysis, ribosome synthesis, telomere length, cellular energy dynamics, dynein-driven transport, prion propagation, and amino acid signaling [15–24]. Although it has been suggested that $InsP_3$ is the only true second messenger among the InsP species [25], there is no doubt that inositol pyrophosphates are important for cellular signaling, particularly since they contain high-energy phosphate bonds [26,27]. Two mechanisms have been proposed for the actions of pyrophosphates in cell signaling. First, inositol pyrophosphates may bind to proteins allosterically, changing their conformation, localization, and activity [28]. Secondly, InsPs may regulate signaling through the transfer of a phosphate group to previously phosphorylated serine residues, generating pyrophosphorylated proteins [29,30] (Bhandari et al. 2007; Saiardi 2016). In the pathogenic fungus *Cryptococcus neoformans*, $InsP_7$ was found to be crucial for metabolic adaptation to host environment and virulence [31]. Asp1p, an ortholog of Vip1p in *S. pombe*, regulates polarized growth and the dimorphic switch [32]. Hence, InsPs can regulate physiological responses to various environmental stimuli in yeast.

Building on our observation that InsP pathway kinases are differentially phosphorylated in pseudohyphal growth kinase mutants, this work from our laboratory indicates that InsP signaling regulates pseudohyphal growth [33].

3.3 Results

3.3.1 IP Profiles Under Pseudohyphal Growth Conditions Are Distinct and Distinguish IP7 Isoforms

Previous studies from our lab showed that kinases that regulate pseudohyphal growth regulate phosphorylation of kinases in the IP biosynthesis pathway. When we monitored pseduohyphal growth in the deletion mutants of said kinases, we saw aberrant pseudohyphal filamentation phenotypes. This led us to ask whether the IP content of yeast is important for pseudodyphal growth. To identify the relative levels of IP species during pseudohyphal growth, we used the approach of Azevedo and Saiardi [34] in which yeast strains are cultured in media with radiolabeled *myo*-inositol; labeled inositol is taken up by yeast and subsequently metabolized into downstream IPs and inositol pyrophosphates. IP levels were monitored by this method in wild-type filamentous yeast (Σ1278b) grown in normal media and under pseudohyphal growth-inducing conditions in low-nitrogen media with reduced ammonium sulfate. Notable characteristics were evident in the profiles under conditions of low nitrogen (Figure 3.2A). In particular, two peaks corresponding to IP_7 isoforms were present, whereas only one IP_7 peak has classically been reported in strains grown in media with normal levels of ammonium sulfate. In addition, the peak corresponding to IP_5 was absent under low-nitrogen conditions, and an increased and broad trace corresponding to IP_3 was observed. This broad IP_3 trace presumably indicates IP_3 or IP_4 isoforms that we were not able to detect with our standard deletion strains. To consider if the changes were specific to pseudohyphal growth or represented a more general response to nitrogen limitation, we determined the IP profile for a non-filamentous strain (BY4743) on identical low-nitrogen growth media (Fig. 3.2A). The IP traces exhibited a number of similarities, but in the non-filamentous strain, IP_5 levels did not drop as substantially, and the peaks corresponding to PP-IP_4 and IP_8 were elevated relative to those observed from the filamentous strain on low-nitrogen media.

With two IP_7 isoforms detected in wild type under conditions of low nitrogen availability, we clarified the identity of each isoform peak by profiling IP levels in homozygous diploid mutants deleted singly for the inositol pyrophosphate kinases *VIP1* and *KCS1* (Fig. 3.2B). Deletion of *VIP1* under low-nitrogen conditions resulted in a striking increase in the second IP_7 isoform peak, presumably corresponding to Kcs1p-produced 5PP-IP_5. Deletion of *KCS1* resulted in decreased IP_7 isoforms. The peak corresponding to the second IP_7 isoform that was elevated in *vip1*Δ/Δ was lost in traces of *kcs1*Δ/Δ; the peak corresponding to the first IP_7 isoform was decreased but still evident in the trace from *kcs1*Δ/Δ, and hence is most likely Vip1p-produced 1PP-IP_5. Analysis of *kcs1*Δ/Δ also identified elevated levels of PP-IP_4 and two profile peaks that were not observed in other IP kinase pathway mutants that we could not conclusively identify from alignment with our standards. As indicated in Figure 1, the *vip1*Δ/Δ mutant that accumulates 5PP-IP_5 exhibited exaggerated pseudohyphal filamentation, while the *kcs1*Δ/Δ mutant that lacks elevated levels of 5PP-IP_5 was hypofilamentous. Collectively, these data are consistent with the second IP_7 isoform peak corresponding to 5PP-IP_5 and suggest that the relative levels of pyrophosphorylated IP_7 isoforms correlate with pseudohyphal growth phenotypes.

3.3.2 The Kinase Domain of Vip1p Suppresses Pseudohyphal Growth

IP levels are established through the actions of both kinases and phosphatases; phosphatases in the IP biosynthesis pathway (Siw14p, Ddp1p, and Vip1p) are indicated in Figure 3A. Vip1p exhibits both IP kinase and phosphatase activity. Vip1p contains an amino-terminal RimK/ATP-grasp domain responsible for phosphorylating the 1 position of IP_6 and a C-terminal phosphatase-like domain that acts to dephosphorylate molecules produced by Vip1p itself [11]. To determine if the elevated filamentation in *vip1*Δ/Δ resulted from loss of its kinase activity or

phosphatase activity, we constructed chromosomal point mutations encoding kinase-defective (*vip1*-D487A) or phosphatase-defective (*vip1*-H548A) forms of Vip1p, in which the indicated conserved catalytically important residue was mutated to alanine. Haploid *vip1*-D487A and diploid *vip1*-D487A/D487A strains showed increased invasive growth and surface-spread filamentation, respectively (Fig. 3.3B and 3.3C). The *vip1*-H548A strains exhibited wild-type filamentous growth. IP profiles of *vip1*-D487A/D487A indicated an increase in 5PP-IP_5 levels, closely resembling the levels observed in a *vip1*Δ/Δ mutant (Fig. 3.3D). The *vip1*-H548A/H548A mutant exhibited a very similar profile to that of a wild-type strain under conditions of low nitrogen, other than the substantial increase in IP_8 levels observed in the mutant. Neither point mutant replicated the large increase in IP_3 levels detected in *vip1*Δ/Δ. From these results, we conclude that the kinase domain of Vip1p, but not its phosphatase-like domain, inhibits pseudohyphal growth.

To consider the molecular basis of the pseudohyphal growth phenotypes in the *vip1* mutants, we assessed mRNA levels of the flocculence gene *FLO11*. The *FLO11* gene encodes a GPI-anchored cell surface flocculin, often used as a molecular marker of pseudohyphal growth. Deletion of *FLO11* yields a pseudohyphal growth defect under conditions of low nitrogen, and its complex promoter has been long studied as an important regulatory point in the pseudohyphal response. Transcription of *FLO11* is controlled through MAPK signaling (positively through Kss1p and negatively through Fus3p), the PKA pathway, and the Snf1p signaling system. We observed a strong increase in *FLO11* mRNA levels in the hyperfilamentous *vip1*-D487A mutant relative to wild-type under conditions of low nitrogen, but less marked changes in *FLO11* mRNA levels in the phosphatase-defective *vip1*-H548A/H548A strain (Table 3.3).

3.3.3 Loss of the IP Phosphatase Siw14 Results in Elevated 5PP-IP$_5$ Levels and Hyper-Filamentous Growth

Phenotypic analysis of the homozygous diploid *siw14Δ/Δ* deletion mutant indicated exaggerated surface-spread filamentation relative to wild type. The *ddp1Δ/Δ* mutant was wild-type with respect to pseudohyphal growth (Fig. 4.4A). IP profiling of both strains under conditions of nitrogen limitation identified elevated levels of 5PP-IP5 in siw14Δ/Δ and increased levels of 1PP-IP5 in *ddp1Δ/Δ* (Fig. 4.4B). In both mutants, the reservoir of IP6 was depressed, accounting partially for increases in the respective IP7 isoforms. The scale in Figure 4B has been adjusted to indicate the change in IP6 levels. These results highlight the strong correlation between elevated 5PP-IP5 levels and hyperactive pseudohyphal growth. To further consider the effect of perturbing levels of the 1PP-IP5 isoform of IP7, we generated a homozygous diploid strain of yeast containing a phosphatase-defective allele of VIP1 and a deletion of DDP1. As Ddp1p and Vip1p are both capable of removing the β-phosphate group from position one of PP-IPs, we expected this mutant to produce highly elevated levels of 1PP-IP5. IP profiling of the vip1-H548A/H548A *ddp1Δ/Δ* double mutant under conditions of nitrogen limitation identified elevated levels of 1PP-IP5 relative to wild type, but comparable to those observed in ddp1Δ/Δ. The double mutant exhibited wild-type levels of pseudohyphal growth, similar to the phenotype of *ddp1Δ/Δ* (Fig.4. 4A).

3.3.4 Inositol Pyrophosphate Kinase Overexpression Driving Elevated 5PP-IP$_5$ Levels Results in Elevated Pseudohyphal Growth

Our results thus far indicate that IP signaling is required for pseudohyphal growth and that IP profiles, particularly with respect to the levels of 5PP-IP$_5$ and other inositol pyrophosphates,

change in correlation with the degree of pseudohyphal growth. To establish these points more strongly, we sought to further perturb IP signaling towards the production of specific IP species for analysis of pseudohyphal growth. Because of the charged phosphate groups decorating the *myo*-inositol backbone, IPs cannot be exogenously added for efficient uptake in yeast. Consequently, we utilized gene overexpression and deletion to impact IP signaling.

To overexpress *KCS1* and *VIP1*, we cloned each gene into a high copy vector such that the coding sequence was expressed under transcriptional control of the constitutive *ADH2* promoter. The overexpression of *KCS1* and *VIP1* were verified using qRT-PCR (Table 3.4). Relative to wild type, *KCS1* overexpression under conditions of nitrogen limitation resulted in elevated levels of IP_3, 5PP-IP_5, and IP_8, with decreased levels of 1PP-IP_5 (Fig. 3.5A). *VIP1* overexpression resulted in a similar profile, except that levels of 5PP-IP_5 were present at approximately one-third the value observed in the *KCS1* overexpression mutant. Analysis of pseudohyphal growth phenotypes in the mutants indicated elevated surface-spread filamentation in the *KCS1* overexpression mutant under conditions of nitrogen limitation, while the *VIP1* overexpression strain exhibited decreased filamentation relative to wild type (Fig. 3.5A). Deletion of *SIW14*, *IPK1*, and *VIP1* in a strain carrying the pSGP47-*KCS1* plasmid overexpressing *KCS1* resulted in hyper-filamentous growth, matching the background *KCS1* overexpression mutant (Fig. 3.5B). Deletion of *SIW14* and *IPK1*, however, did alter that phenotype, resulting in exaggerated pseudohyphal filamentation relative to wild type (Fig. 3.5B). In contrast to the background *VIP1* overexpression strain carrying the pSGP47-*VIP1* construct, IP profiling of *siw14*Δ/Δ with pSGP47-*VIP1* grown in low-nitrogen media indicated strongly elevated levels of 5PP-IP_5 (Fig. 3.5B). Elevated levels of 5PP-IP_5 were also evident in the *siw14*Δ/Δ homozygous diploid strain, consistent with the hyper-filamentous phenotype of both mutants.

FLO11 mRNA levels were elevated in the hyperfilamentous *siw14*Δ/Δ strains, with particularly high levels evident in *siw14*Δ/Δ backgrounds carrying either pSGP47-*KCS1* or pSGP47-*VIP1* (Table 3.3)

3.3.5 Inositol Polyphosphate Profiles of *Candida albicans* Under Normal and Filamentation Inducing Conditions Hints at Conservation of the Link Between Inositol Polyphosphate Metabolism and Filamentous Growth

Pseudohyphal growth is a good model for filamentation in pathogenic fungi. After establishing the fact that inositol polyphosphate metabolism regulates pseudohyphal growth, this regulation is conserved in other fungi. First, we have analyzed the IP profiles of C. albicans under non-filamentous and filamentous conditions. The non-filamented C. albicans was grown in rich media at 30 C while it filamented in 10% serum supplemented media at 37C. Using a similar protocol to the one we used to extract IPs from S. cerevisiae, we were able to extract IPs from C. albicans as evidenced by IP profiles fitting IP profiles of similar species. Under both conditions the dominant IP species was IP_6 as expected. While we observed IP_7 peak in both conditions, the peak for IP_7 for the filamenting Candida came later than the IP_7 peak of the at non-filamenting conditions. This is in accordance with the peak for the filamentation inducing conditions belonging to 5PP-IP_5 while the peak of yeast form belonging to 1PP-IP_5. We have observed a broader IP_3 peak for yeast grown in filamentation inducing conditions than those grown in normal conditions. This is in accordance with the IP_3 peak we have seen for S. cerevisiae under pseudohyphal growth inducing conditions. The decrease in the IP_5 peak in the filamentation inducing conditions also resembles that of S. cerevisiae.

Next, we wanted to find out whether inositol polyphosphate metabolism regulates

filamentation in *C. albicans.* For that, we constructed heterozygous deletion mutants of inositol polyphosphate metabolism gene homologs in *C. albicans*. *AFL1* is the Candida homolog of S. cerevisiae *VIP1* which causes hyperfilamentation when deleted. The *afl1Δ/AFL1* mutant showed a hyperfilamentous phenotype even under the non-filamentous conditions. Interestingly, it did not grow when the medium is supplemented is with 10% serum and the temperature is switched to 37 C which are the conditions for wild type *C. albicans* filamentation. *C. albicans KCS1* deletion had a similar effect. It hyperfilamented under non-filamenting conditions for wild type. *Kcs1Δ/KCS1* mutants were extremely slow growers in filamentation inducing conditions and showed no signs of filamentation. The *ARG82* homolog *IPK2* deletion caused hypofilamentation under filamentation inducing conditions. These results imply that there is conservation of the relationship between inositol polyphosphate metabolism and filamentous growth, at least to some degree, between *S. cerevisiae* and *C. albicans*.

3.4 Discussion

IP signaling has been studied for over two decades, but its functional significance has not been fully elucidated. Owing partially to the labor involved, IPs have not been profiled over a broadly representative spectrum of growth conditions. Here, we used the genetic workhorse *Saccharomyces cerevisiae* to profile IP levels under conditions of nitrogen limitation in a filamentous background, and our results indicate a new role for IP signaling in the pseudohyphal growth response. Perturbation of the IP biosynthesis pathway altered pseudohyphal growth, and *in vivo* measurement of IP levels in these mutants identified characteristic profiles, particularly with respect to the inositol pyrophosphates, that were predictive of pseudohyphal growth states.

Mutation of genes encoding IP kinases and phosphatases enabled pseudohyphal growth in the absence of nitrogen limitation. Although not shown in the results section of this thesis, this project also showed that IP profiles are substantially altered in mutants deleted of *SNF1, KSS1,* and *FUS3,* suggesting that these well studied kinase regulators of pseudohyphal growth contribute to the establishment and/or maintenance of wild-type IP levels under conditions of nitrogen limitation.

Considered collectively, the data suggest the ratio of the IP_7 isoforms and IP_8 is indicative of the pseudohyphal growth state. Elevated levels of 5PP-IP_5 relative to the levels of 1PP-IP_5 and IP_8 were evident in strains that showed exaggerated pseudohyphal growth. This pattern held consistent under conditions of nitrogen limitation in homozygous diploid *vip1*Δ/Δ, *vip1*-D487A/D487A, *siw14*Δ/Δ, *KCS1* overexpression, and *fus3*Δ/Δ strains. Further, in low-nitrogen media, overexpression of *VIP1* in a strain deleted of *SIW14* resulted in elevated levels of 5PP-IP_5 and hyperfilamentation. In these six hyperfilamentous mutants, the mean ratio of 5PP-IP_5 to 1PP-IP_5 was 5.9 with a standard deviation of 1.5; in contrast, the hypofilamentous *kcs1*Δ/Δ, *VIP1* overexpression, *snf1*Δ/Δ, and *kss1*Δ/Δ mutants along with the non-filamentous BY4743 strain exhibited a mean 5PP-IP_5 to 1PP-IP_5 ratio of 0.68 with a standard deviation of 0.12. By an independent samples T-test, this difference between hyperfilamentous and hypofilamentous strains is significant ($p<0.001$). It is interesting that wild-type pseudohyphal growth did not indicate highly elevated levels of 5PP-IP_5 relative to 1PP-IP_5 and IP_8, but instead was characterized by decreased IP_5 and elevated IP_7 isoforms, with 1PP-IP_5 showing the greater increase. It should also be noted that exaggerated levels of PP-IP_4 and 1,5$(PP)_2$-IP_3 in *ipk1*Δ/Δ promote pseudohyphal growth, although the effects may be observed only upon removal of the higher energy IP_7 and IP_8 pyrophosphates, as we did not observe consistent changes in PP-IP_4 and 1,5$(PP)_2$-IP_3 levels over the mutants we analyzed. Additional IP profiling in a larger mutant set will likely be necessary to

refine the characteristic IP signatures, but the data are consistent with the notion that IP profiles are a predictive indicator of pseudohyphal growth state.

These results highlight the importance of inositol pyrophosphates, and particularly IP_7 isoforms, in the pseudohyphal growth response. It is notable that two peaks corresponding to the IP_7 isoforms 5PP-IP_5 and 1PP-IP_5 are present in profiles of strains grown in low-nitrogen media. Previous analyses of IP profiles in yeast by HPLC-based fractionation have presented a single peak corresponding to IP_7: however, these studies were not undertaken using nitrogen-limiting growth media, nor using the 15-minute extended separation gradient we employed here. In fact, our IP profiles of the wild-type Σ1278b strain under normal growth conditions do indicate a single IP_7 peak. This single peak had previously been identified from analyses of non-filamentous yeast as 5PP-IP_5 [34–36]; however, our fractionation profiles indicate that this peak corresponds to 1PP-IP_5. Several lines of evidence support this conclusion. First, IP profiles of *kcs1*Δ/Δ grown on low-nitrogen media identify a small peak aligning with the one observed in profiles of a wild-type strain under normal growth conditions. This peak most likely corresponds to Vip1p-produced 1PP-IP_5, as Vip1p is capable of pyrophosphorylating IP_6 in a strain deleted of *KCS1*. Second, profiles of *vip1*Δ/Δ indicate a very large peak aligning with the later IP_7 isoform fraction, which, by similar logic, likely represents Kcs1p-produced 5PP-IP_5. Further, an identical peak is observed in profiles of *siw14*Δ/Δ in which 5PP-IP_5 accumulates, as this isomer cannot be dephosphorylated in the absence of *SIW14* [12]. Thus, the data indicate that we can efficiently separate IP_7 isomers in yeast under low nitrogen conditions through an extended gradient, with 1PP-IP_5 fractionating just ahead of 5PP-IP_5.

Beyond its relevance to yeast pseudohyphal growth, this study is also informative in considering the role of IPs in the cellular response to nitrogen limitation. Filamentous and non-

filamentous strains grown in media with reduced ammonium sulfate exhibit many similar changes in IP levels, including elevated levels of pyrophosphorylated IP_7 isoforms as discussed above. These data suggest that the transition to conditions of decreased nitrogen availability necessitates the increased accumulation of both IP_7 isoforms, making them detectable by labeling and fractionation protocols. It is additionally interesting that overexpression of *KCS1* in normal media results in IP fractionation peaks corresponding to 5PP-IP_5 and 1PP-IP_5, mimicking the profile observed in strains grown under conditions of low nitrogen with associated filamentation. Thus, IP levels can be manipulated to uncouple pseudohyphal growth from nitrogen limitation, and, further, inositol pyrophosphate abundance may be an intracellular signal of nitrogen conditions, functioning as part of the cellular response in yeast to manage nitrogen limitation.

IP profiles in this study as well as previous phosphoproteomic data are consistent with a role for AMPK and MAPK signaling in regulating IP levels under conditions of nitrogen limitation, and the results here provide the first evidence that AMPK and MAPK signaling is required for wild-type levels of IPs. Interestingly, inositol polyphosphate multikinase has previously been demonstrated to be capable of binding AMPK [37]. These signaling modules are established regulators of cellular responses to nutrient levels, and functions for Snf1p, Kss1p, and Fus3p in controlling IP levels would provide an important point of crosstalk between classic cell signaling pathways and metabolic second messengers. In sum, this work further establishes the foundation for additional studies of the regulation and downstream effectors of IP signaling in cellular stress responses and pseudohyphal growth.

3.5 Materials and Methods

3.5.1 Strains, plasmids, and media

S. cerevisiae strains were cultured on YPD (1% yeast extract, 2% peptone, 2% glucose) or minimal media (0.67% yeast nitrogen base (YNB) without amino acids, 2% glucose, and 0.2% of the appropriate amino acid drop-out mix). Nitrogen starvation and pseudohyphal growth phenotypic assays were conducted in synthetic low ammonium dextrose (SLAD) medium (0.17% YNB without amino acids and without ammonium sulfate, 2% glucose, 50 μM ammonium sulfate and supplemented with appropriate amino acids if necessary). Inositol polyphosphate profiles were conducted by first growing cells in minimal medium-inositol (0.17% YNB without inositol, 2 % glucose, 0.5% ammonium sulfate and supplemented with appropriate amino acids) and when necessary further growth in SLAD-inositol (0.17% YNB without amino acids , ammonium sulfate and inositol, 2% glucose, 50 μM ammonium sulfate, and supplemented with amino acids as appropriate).

3.5.2 Expression analysis of *FLO11*, *KCS1*, and *VIP1*

Single colonies were inoculated in 4 ml appropriate medium (YPD or SC-Ura). Overnight cultures were diluted 1:1000 in 5 ml YPD or SC-URA and let grow for 16–20 hours. The cells were harvested at 3000*g* for 5 minutes and washed twice with water. If no nitrogen stress was utilized, the cells were either stored at -80°C or subjected to RNA extraction right away. If nitrogen stress was utilized, the cells were resuspended in 5 ml SLAD medium and incubated at 30°C for 8 hours. After incubation, the cells were harvested and washed twice with water. The cells were either stored at -80°C or subjected to RNA extraction right away. RNA extraction was done using the RiboPure-Yeast kit (Invitrogen) according to manufacturer's directions. The amount of RNA isolated was determined using a NanoDrop spectrophotometer/ fluorometer. For each sample, 1 μg of RNA was converted to cDNA using the Radiant cDNA Synthesis Kit, 1-Step. The resulting

cDNA was diluted 1:100 and 2 µl of the diluted cDNA was used as a template for qPCR. qPCR mixes were prepared using the Radiant Green Hi-ROX qPCR kit and run with an Applied Biosystems StepOne Plus qPCR machine. The relative amounts of *FLO11*, *KCS1*, and *VIP1* expression were calculated using the double delta Ct method with *ACT1* as the reference gene.

Primers used for qRT-PCR are as follows:

ACT1-qPCR-F: CTGCCGGTATTGACCAAACT;

ACT1-qPCR-R: CGGTGATTTCCTTTTGCATT;

FLO11-qPCR-FWD3: GTTGTTTCGCCAGCGGAGTT;

FLO11-qPCR-RVS3: CTACCACCCCTGTCCGACG;

KCS1-qPCR-FWD3: GCAATAATGGCGGGTCCGTG;

KCS1-qPCR-RVS3: TGCGCCACGTGTTTATTGGG;

VIP1-qPCR-FWD1: AGAGCTCTTTTTGGGGCCGA;

VIP1-qPCR-RVS1: GTGGGGGAGCTTCCTTACCC.

3.5.3 HPLC analysis of inositol polyphosphates

HPLC analysis of inositol polyphosphate levels was conducted as previously described with some modifications [34]. In brief, cultures are grown overnight at 30°C with shaking at 250 rpm until fully saturated in rich media. 5 µl of saturated culture is added to 5 ml of SC-inositol supplemented with 25 µl of *myo*[1,2-^{3}H]inositol 1 mCi/ml 30 Ci/mmol (American Radiolabeled Chemicals cat. no. ART02611MC) and allowed to grow overnight at 30°C with shaking at 250 rpm until reaching an OD_{600} of 0.9. At this point, cells are either harvested and frozen at -80°C until further use or harvested and washed with H_2O and resuspended in 5 ml of SLAD-inositol and grown for 8 hours at 30°C at 250rpm. These cultures are then harvested and frozen at -80°C until

further use. Inositol polyphosphates are extracted by resuspending the pellet in 300 µl of 1M perchloric acid with 3mM EDTA and bead beating at 4°C for five minutes. Samples are spun down and the resulting supernatant is saved and allowed to neutralize with the addition of 1 M potassium carbonate and 3 mM EDTA until a pH of 6.0-8.0 is reached and allowed to sit on ice for two hours. The sample is again centrifuged, and the clear supernatant is run on the HPLC (Hewlett Packard Series 1100) connected to a Partisphere 5 µm SAX cartridge column 125 x 4.6 mm (HiCHROM cat. no. 4621-0505). Inositol polyphosphates are eluted from the column with a gradient from mixing buffer A (1 mM EDTA) and buffer B (1.3 M $(NH_4)_2HPO_4$, 1 mM EDTA, pH to 3.8 with H_3PO_4). The gradient used is as follows: 0-5 min, 0% buffer B; 5-10 min, 0-10% buffer B; 10-90 min, 10-100% Buffer B; 90-100 min, 100% Buffer B; 100-101 min, 0% buffer B; 101-110 min 0% buffer B. The gradient is run at a flow rate of 1 ml/min and one 1ml fractions are collected every minute for the first 90 minutes. Fractions are mixed with 4 ml of Ultima-Flo AP liquid scintillation cocktail (Perkin-Elmer cat. no. 6013599) and counted using a scintillation counter.

For the inositol polyphosphate analysis of Candida albicans, wild type *Candida albicans* carrying a plasmid for Uracil synthesis were grown in SC-Ura at 30 C for 24 hours for non-filamentous conditions. For filamentation induction, the same strain was grown in Sc-Ura supplemented with 10% FCS and the cells were grown for 24 hours at 37 C. The filamentation was verified at the cellular level with microscopy. The inositol polyphosphate extraction and analysis were performed as described above.

3.5.4 Generation of *Candida albicans* mutants and filamentation analysis

Candida albicans strains used in this study were derived from the BWP17 genetic background (*ura3::imm434/ura3::imm434 iro1/iro1::imm434 his1::hisG/his1::hisG arg4/arg4*)

supplemented with the plasmid pMB7 containing hisG-URA3-hisG cassette. The heterozygote mutants were generated independently by allele replacement using a *HIS1* cassette that was amplified from the plasmid pSN52. The list of the plasmids used for amplification can be found at Table 3.2. To induce hyphal formation, 4 ul of overnight grown strains were spotted onto standard SC-Ura or SC-His-Ura plates supplemented with 10% fetal calf serum (FCS) and grown for 5-7 days at 37 C. The control plates without the FCS supplement were incubated at 30 C for the same amount of time. The pictures of the colonies were taken by a stereomicroscope.

3.6 Figures and Tables

Figure 3.1 Inositol polyphosphate pathway in *Saccharomyces cerevisiae.*
The known inositol polyphosphate and inositol pyrophosphate molecules and their phosphorylation/ dephosphorylation pathway are depicted below with the respective kinases and phosphatases. (Figure reprinted from Mutlu & Kumar, 2019)

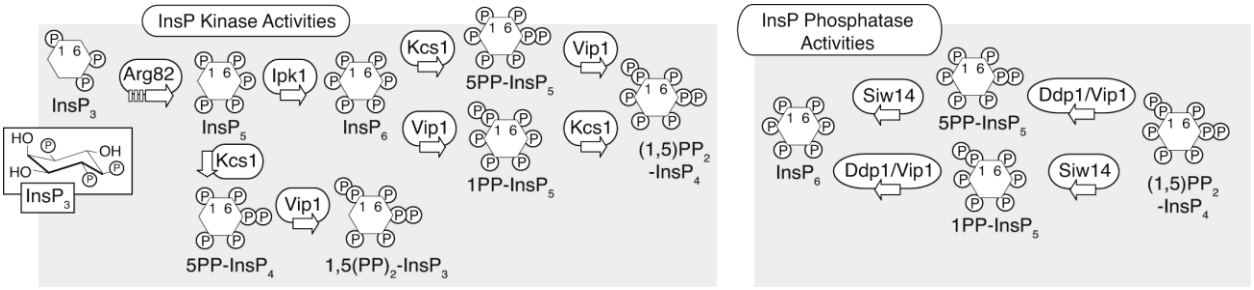

Figure 3.2 Analysis of InsP levels in yeast pseudohyphal growth.

A representative profile is shown from at least two independent biological replicates for each strain and growth condition tested**. A**) InsP profiles are altered under conditions that induce pseudohyphal filamentation (growth in low-nitrogen SLAD media for eight hours), with distinguishable $InsP_7$ isoforms. InsP profiles are shown for a diploid wild-type filamentous strain grown under standard conditions (Σ1278b), a wild-type filamentous strain grown in low-nitrogen media for eight hours (Σ1278b SLAD), and a non-filamentous wild-type strain grown in low-nitrogen media for eight hours (BY4743 SLAD). **(B)** Representative InsP profiles of homozygous diploid *vip1*Δ/Δ and *kcs1*Δ/Δ mutants grown in low-nitrogen media compared to wild type. Profile regions corresponding to $InsP_7$ and $InsP_8$ are enlarged in the inset box. Each trace indicates counts per min (CPM) as a percentage of total CPM, with background subtracted. Elution fractions are indicated on the X-axis. The mean ratio of 5PP-IP_5 to 1PP-IP_5 is listed with standard deviation for each strain.

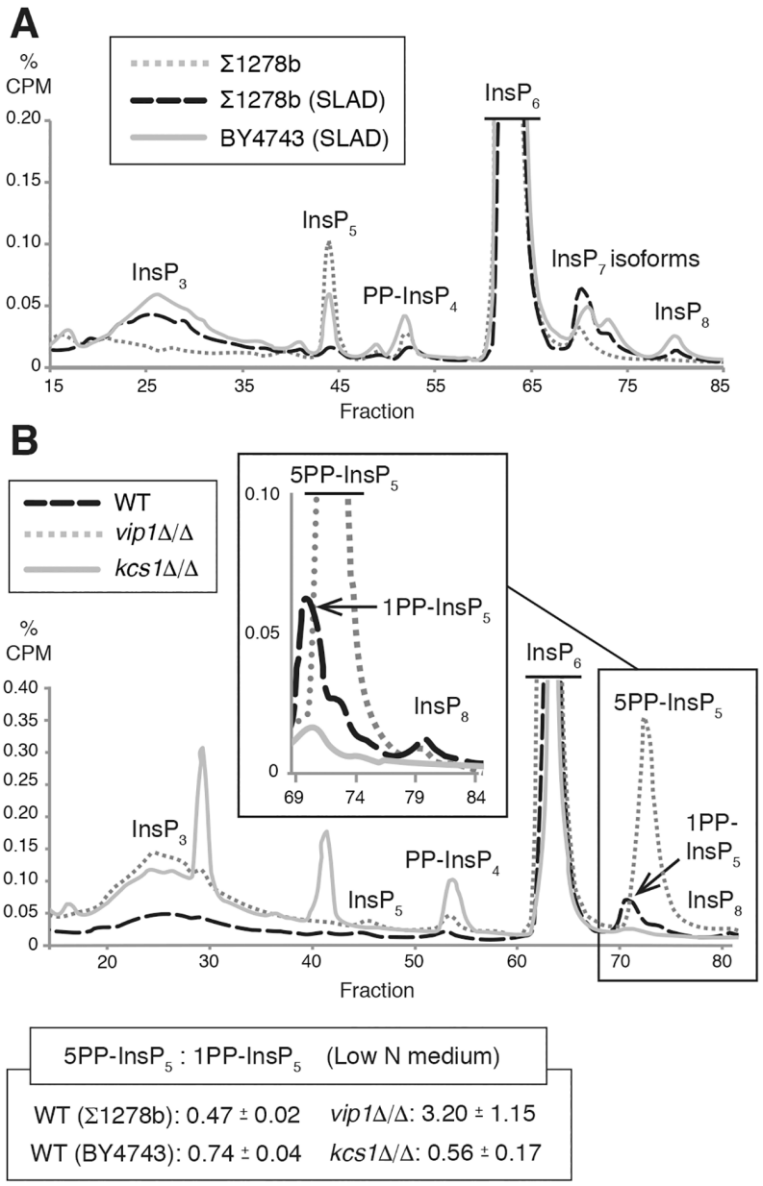

5PP-$InsP_5$: 1PP-$InsP_5$ (Low N medium)	
WT (Σ1278b): 0.47 ± 0.02	*vip1*Δ/Δ: 3.20 ± 1.15
WT (BY4743): 0.74 ± 0.04	*kcs1*Δ/Δ: 0.56 ± 0.17

Figure 3.3 Mutation of the Vip1p kinase domain results in exaggerated pseudohyphal growth..
A) Diagram indicating phosphatases affecting inositol pyrophosphates. Vip1p phosphatase activity acts redundantly with Ddp1p. **(B)** Haploid invasive growth phenotypes are shown for strains containing a kinase-defective *vip1* allele (D487A) and phosphatase-defective *vip1* allele (H548A), respectively. For comparison, haploid wild type and *vip1*Δ mutants are included. Assays were performed and quantified as described previously. Mean values with standard deviation for three replicates are provided. Scale bar, 2 mm. **(C)** Surface pseudohyphal filamentation is shown for the indicated homozygous diploid strains grown on low-nitrogen SLAD medium. Mean values with standard deviation for three replicates are provided. Scale bar, 500 μm. **(D)** Representative InsP profiles of kinase-defective and phosphatase-defective *vip1* mutants grown in low-nitrogen minimal media for eight hours. Diploid wild type and *vip1*Δ/Δ strains grown under identical conditions are shown for comparison. Plots of $InsP_7$ isoforms and $InsP_8$ are enlarged in the boxed inset.

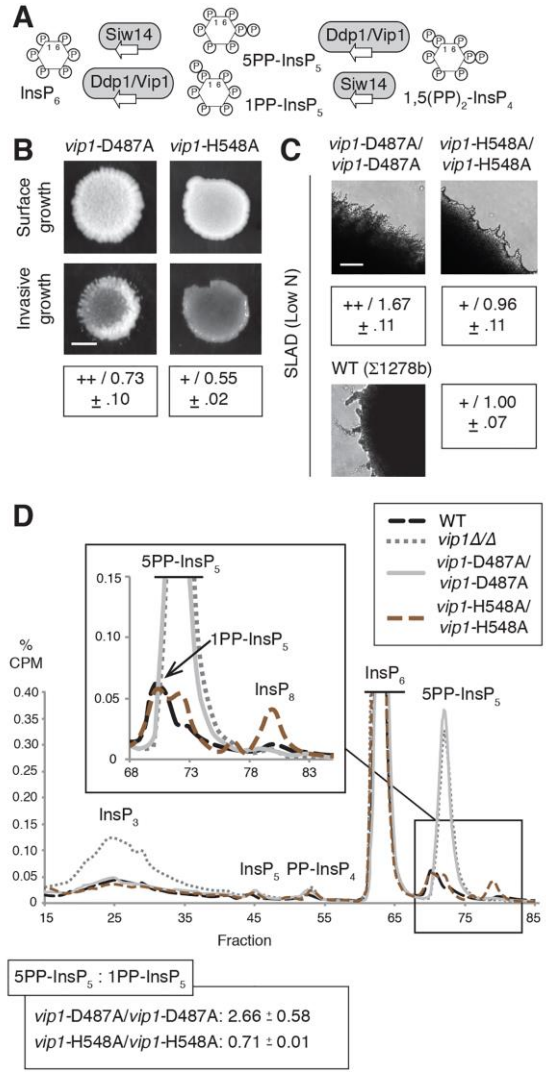

Figure 3.4 Deletion of the *SIW14* phosphatase gene results in exaggerated pseudohyphal growth.
A)Surface pseudohyphal filamentation phenotypes of homozygous diploid strains with the indicated InsP phosphatase mutations. Strains were grown on low-nitrogen SLAD medium. Exaggerated pseudohyphal growth in the *siw14*Δ/Δ mutant is indicated with a "++"; wild-type pseudohypha growth levels are indicated with a "+". Pseudohyphal growth assays were performed and quantified as described; mean values with standard deviation for three replicates are indicated. Scale bar, 500 μm.
(B) Representative InsP profiles of mutated InsP phosphatase strains grown in low-nitrogen minimal media for eight hours. The proportional CPM counts are shown to 1% in order to indicate the changes in IP_6 levels. The InsP trace for a wild-type control strain is shown below the plot. Ratios of $5PP\text{-}InsP_5$:$1PP\text{-}InsP_5$ are indicated as mean with standard deviation.

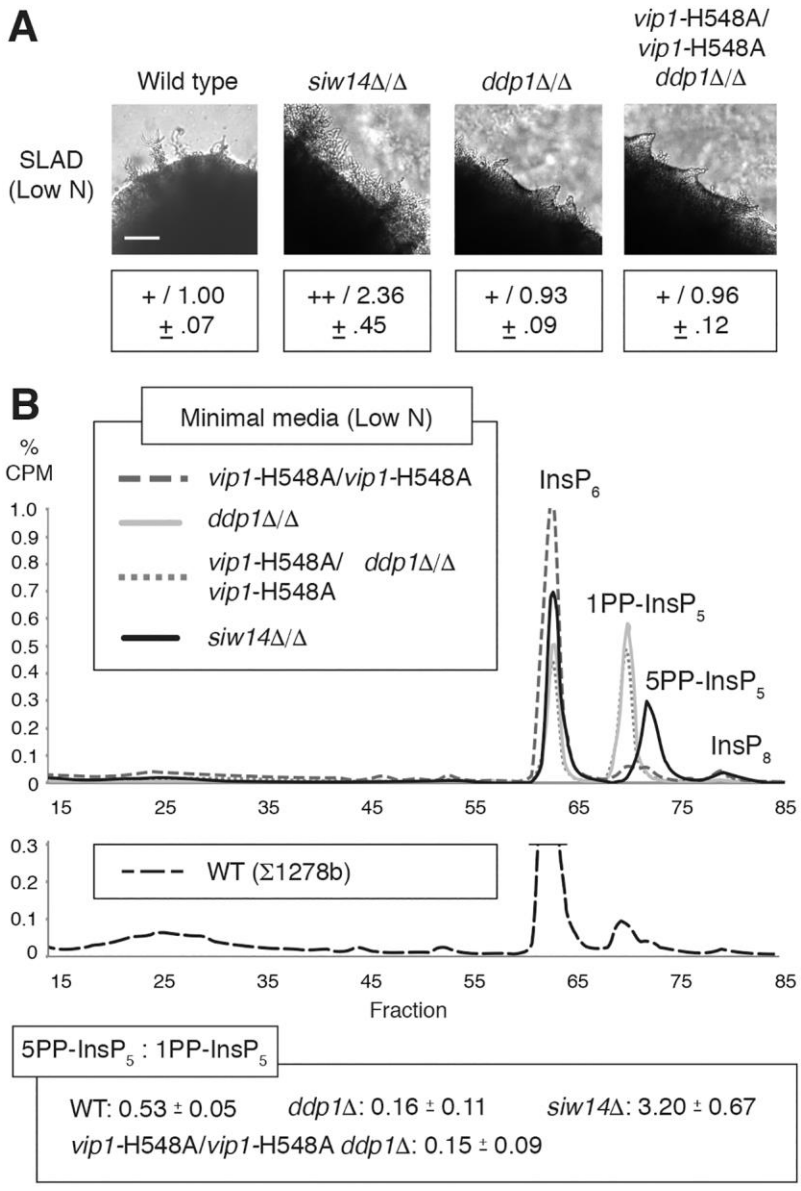

Figure 3.5 Overexpression mutants with elevated levels of 5PP-InsP$_5$ relative to other inositol pyrophosphates exhibit exaggerated pseudohyphal growth.
(A) Representative InsP profiles of strains overexpressing *VIP1* and *KCS1* grown for eight hours in low-nitrogen minimal media. The ratio of InsP$_7$ isoforms is indicate as mean values with standard deviations shown. **(B)** Representative InsP profile of *VIP1* overexpression in a *siw14*Δ/Δ background strain grown in low nitrogen media; a representative InsP profile for *siw14*Δ/Δ is included also. The InsP trace of the wild-type strain for this analysis is shown in panel A; all strains were grown under identical conditions. Pseudohyphal growth phenotypes are provided for the indicated mutants. Filamentation was quantified as described in Materials and Methods; mean values with standard deviation are indicated. Scale bars, 500 μm.

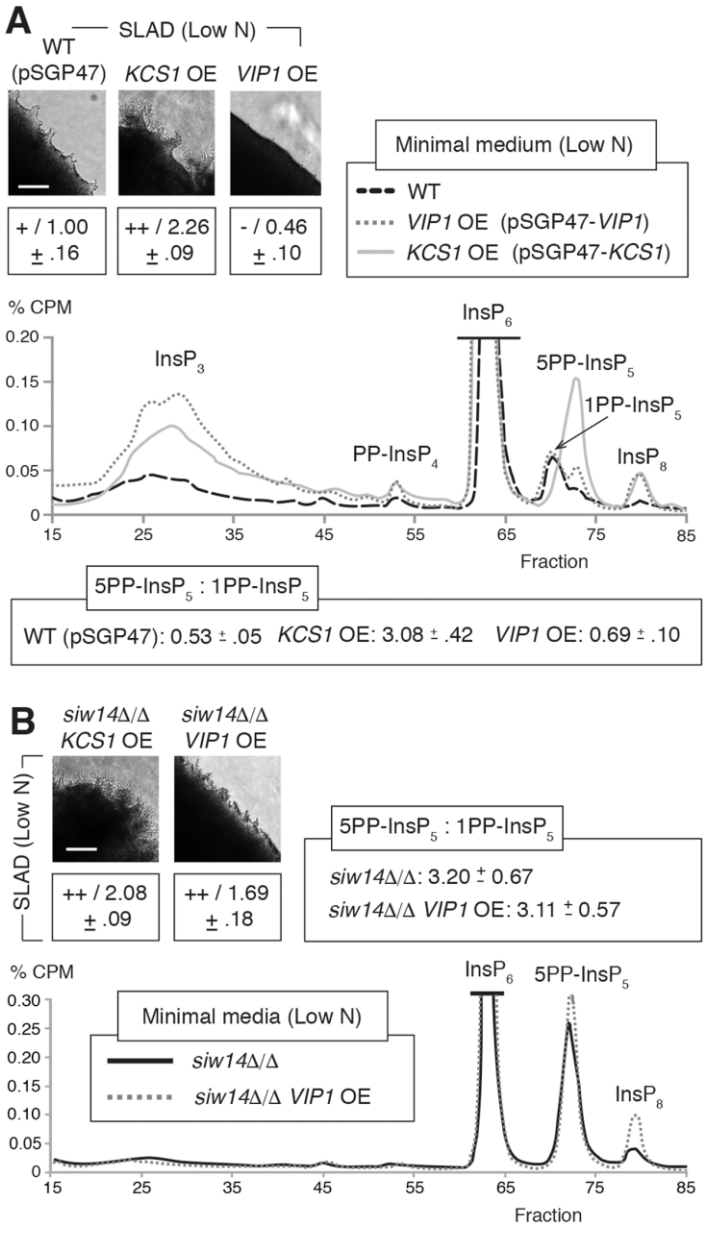

Figure 3.6 Inositol polyphosphate metabolism regulates filamentation in *Candida albicans*
A) Representative inositol polyphosphate profiles of wild-type *Candida albicans* under normal and filamentation inducing conditions. Normal growth was achieved by incubation in Sc-Ura at 30 C. Filamentation was achieved by incubation in Sc-Ura supplemented with 10% fecal calf serum at 37 C. For both conditions, the strain was grown for 24 hours before labeling and inositol polyphosphate extraction. B) Filamentous growth phenotypes of inositol polyphosphate metabolism mutants as depicted by colony morphology

A.

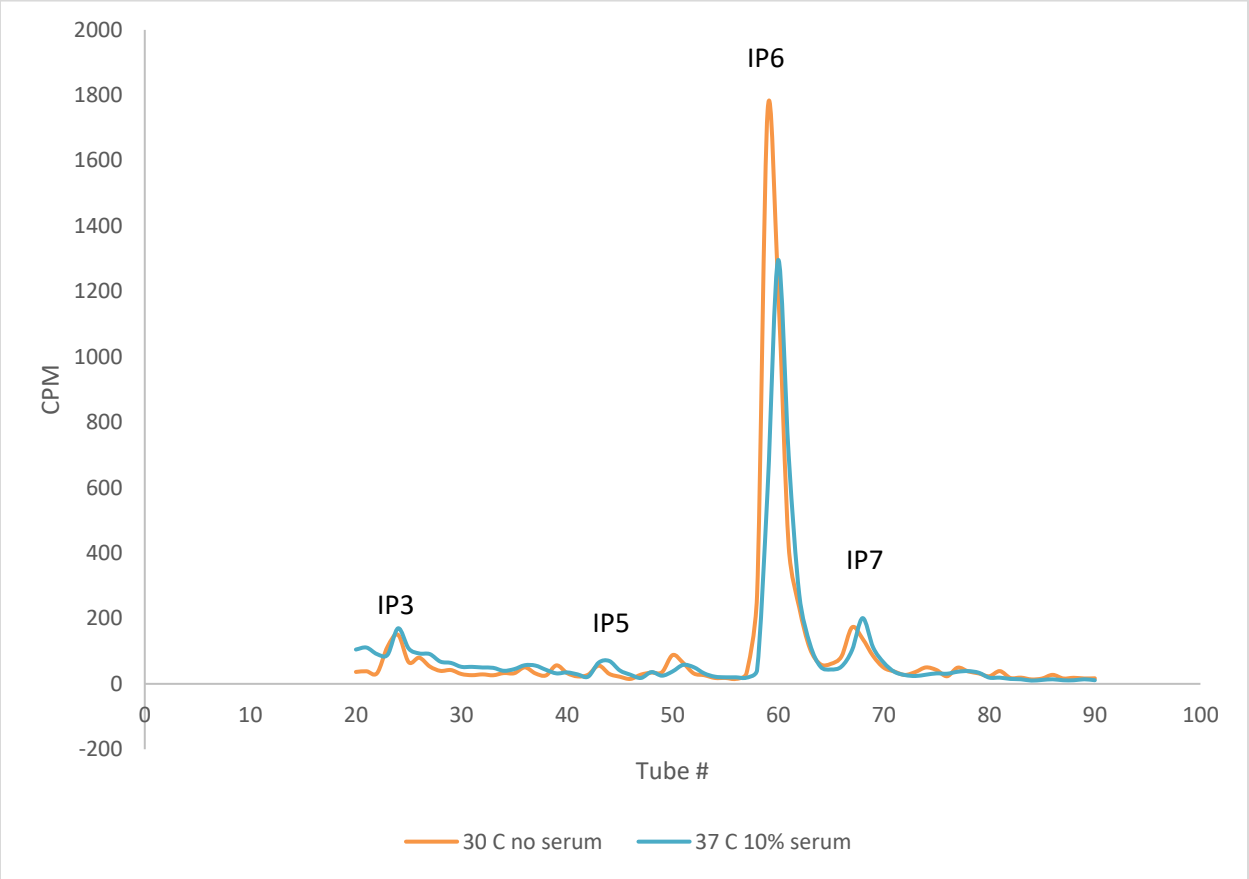
2000
1800
1600
1400
1200
1000
800
600
400
200
0
-200
CPM
IP6
IP7
IP3
IP5
0
10
20
30
40
50
60
70
80
90
100
Tube #
30 C no serum
37 C 10% serum

B.

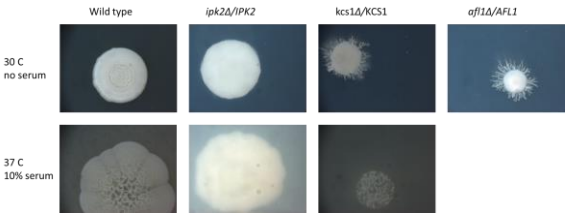
Wild type
ipk2Δ/IPK2
kcs1Δ/KCS1
afl1Δ/AFL1
30 C
no serum
37 C
10% serum

Table 3.1 List of strains used in this study.

Strain	Genotype	Source
Y825	*ura3-52 leu2Δ0 MAT***a**	M. Snyder (Stanford, CA)
HLY337	*ura3-52 trp1-1 MAT*α	G. Fink (MIT, MA)
Y825xHLY337	*ura3-52/ura3-52 leu2Δ0 trp1-1 MATa/α*	
BY4743	*MATa/α his3Δ1/his3Δ1 leu2Δ0/leu2Δ0 LYS2/lys2Δ0 met15Δ0/MET15 ura3Δ0/ura3Δ0*	This study
yKN12	*arg82Δ::KanMX6 ura3-52 leu2Δ0 MAT***a**	This study
yKN13	*arg82Δ::KanMX6 ura3-52 trp1-1 MAT*α	This study
yKN14	*arg82Δ::KanMX6/arg82Δ::KanMX6 ura3-52/ura3-52 leu2Δ0 trp1-1 MATa/α*	This study
yKN15	*ipk1Δ::KanMX6 ura3-52 leu2Δ0 MAT***a**	This study
yKN16	*ipk1Δ::KanMX6 ura3-52 trp1-1 MAT*α	This study
yKN17	*ipk1Δ::KanMX6/ ipk1Δ::KanMX6 ura3-52/ura3-52 leu2Δ0 trp1-1 MATa/α*	This study
yKN18	*vip1Δ::KanMX6 ura3-52 leu2Δ0 MAT***a**	This study
yKN19	*vip1Δ::KanMX6 ura3-52 trp1-1 MAT*α	This study
yKN20	*vip1Δ::KanMX6/vip1Δ::KanMX6 ura3-52/ura3-52 leu2Δ0 trp1-1 MATa/α*	This study
yKN21	*kcs1Δ::KanMX6 ura3-52 leu2Δ0 MAT***a**	This study
yKN22	*kcs1Δ::KanMX6 ura3-52 trp1-1 MAT*α	This study
yKN23	*kcs1Δ::KanMX6/kcs1Δ::KanMX6 ura3-52/ura3-52 leu2Δ0 trp1-1 MATa/α*	This study
yKN24	*ddp1Δ::KanMX6 ura3-52 leu2Δ0 MAT***a**	This study
yKN25	*ddp1Δ::KanMX6 ura3-52 trp1-1 MAT*α	This study
yKN26	*ddp1Δ::KanMX6/ddp1Δ::KanMX6 ura3-52/ura3-52 leu2Δ0 trp1-1 MATa/α*	This study
yKN27	*siw14Δ::KanMX6 ura3-52 leu2Δ0 MAT***a**	This study
yKN28	*siw14Δ::KanMX6 ura3-52 trp1-1 MAT*α	This study

yKN29	*siw14Δ::KanMX6/siw14Δ::KanMX6 ura3-52/ura3-52 leu2Δ0 trp1-1 MATa/α*	This study
yKN30	*ura3-52/ura3-52 leu2Δ0 trp1-1 MATa/α* + pSGP47-*KCS1*	This study
yKN31	*ura3-52/ura3-52 leu2Δ0 trp1-1 MATa/α* + pSGP47-*VIP1*	This study
yKN32	*fus3Δ::HphMX4/fus3Δ::KanMX6 ura3-52/ura3-52 leu2Δ0 trp1-1 MATa/α*	This study
yKN33	*kss1Δ::HphMX4/kss1Δ::KanMX6 ura3-52/ura3-52 leu2Δ0 trp1-1 MATa/α*	This study
yKN34	*snf1Δ::KanMX6 vip1Δ::HphMX4 ura3-52 leu2Δ0 MAT***a**	This study
yKN35	*snf1Δ::KanMX6 vip1Δ::HphMX4 ura3-52 trp1-1 MATα*	This study
yKN36	*snf1Δ::KanMX6/ snf1Δ::KanMX6 vip1Δ::HphMX4/ vip1Δ::HphMX4 ura3-52/ura3-52 leu2Δ0 trp1-1 MATa/α*	This study
yKN37	*snf1Δ::KanMX6/snf1Δ::KanMX6 ura3-52/ura3-52 leu2Δ0 trp1-1 MATa/α* + pSGP47-*VIP1*	This study
yKN38	*snf1Δ::KanMX6/snf1Δ::KanMX6 ura3-52/ura3-52 leu2Δ0 trp1-1 MATa/α* + pSGP47-*KCS1*	This study
yKN39	*ipk1Δ::KanMX6/ ipk1Δ::KanMX6 ura3-52/ura3-52 leu2Δ0 trp1-1 MATa/α* + pSGP47-*KCS1*	This study
yKN40	*ipk1Δ::KanMX6/ ipk1Δ::KanMX6 ura3-52/ura3-52 leu2Δ0 trp1-1 MATa/α* + pSGP47-*VIP1*	This study
yKN41	*vip1Δ::KanMX6/vip1Δ::KanMX6 ura3-52/ura3-52 leu2Δ0 trp1-1 MATa/α* + pSGP47-*KCS1*	This study
yKN42	*kcs1Δ::KanMX6/kcs1Δ::KanMX6 ura3-52/ura3-52 leu2Δ0 trp1-1 MATa/α* + pSGP47-*VIP1*	This study
yKN43	*siw14Δ::KanMX6/siw14Δ::KanMX6 ura3-52/ura3-52 leu2Δ0 trp1-1 MATa/α* + pSGP47-*KCS1*	This study
yKN44	*siw14Δ::KanMX6/siw14Δ::KanMX6 ura3-52/ura3-52 leu2Δ0 trp1-1 MATa/α* + pSGP47-*VIP1*	This study
yCS1	*snf1Δ::KanMX6 ura3-52 leu2Δ0 MAT***a**	This study
yCS2	*snf1Δ::KanMX6 ura3-52 trp1-1 MATα*	This study
yCS3	*snf1Δ::KanMX6/snf1Δ::KanMX6 ura3-52/ura3-52 leu2Δ0 trp1-1 MATa/α*	This study

Table 3.2 List of plasmids used in this study.

Strain	Genotype	Source
pSGP47	*URA*, high copy, Amp^r	DNASU Plasmid Repository (Tempe, AZ)
pSGP47-*KCS1*	P_{ADH2}-*KCS1 URA*, high copy, Amp^r	This Study
pSGP47-*VIP1*	P_{ADH2}-*VIP1 URA*, high copy, Amp^r	This Study

Table 3.3 *FLO11* mRNA levels in InsP phosphatase mutants

Strain[a]	*FLO11* mRNA levels: WT[b]	Pseudohyphal growth phenotype[c]
Wild type	1.00 ± 0.09	WT (+) / 1.00 ± 0.04
*vip1*Δ/Δ	3.08 ± 2.00	++ / 1.62 ± 0.04
vip1-D487A/D487A	9.15 ± 2.94	++ / 1.67 ± 0.11
vip1-H548A/H548A	2.32 ± 1.03	+ / 0.96 ± 0.11
*ddp1*Δ/Δ	1.37 ±0.27	+ / 0.93 ± 0.09
*siw14*Δ/Δ	2.14 ± 0.53	++ / 2.36 ± 0.45
*siw14*Δ/Δ *KCS1* OE	5.62 ± 1.77	++ / 2.08 ± 0.09
*siw14*Δ/Δ *VIP1* OE	5.93 ± 0.53	++ / 1.69 ± 0.18

[a]All indicated strains are diploid and are derived from the Σ1278b genetic background.

[b]*FLO11* mRNA levels are presented for the mutants relative to levels measured in the wild-type strain under conditions of low nitrogen. Data are presented as mean with standard deviation indicated.

[c]Pseudohyphal growth is presented as the ratio of the circumference of a colony of the indicated mutant strain to the circumference of the wild-type strain colony under conditions of low nitrogen.

Table 3.4 mRNA levels of over-expressed *KCS1* and *VIP1* in high-copy vectors with the *ADH2* promoter.

Strain	Growth condition	Gene	mRNA levels[a]
Wild type	YPD (Normal N)	*KCS1*	0.73 ± 0.40
KCS1 OE (pSGP47-*KCS1*)	SC –Ura (Normal N)	*KCS1*	17.3 ± 7.6
	SLAD (Low N)	*KCS1*	526 ± 114
Wild type	YPD (Normal N)	*VIP1*	1.40 ± 0.09
VIP1 OE (pSGP47-*VIP1*)	SC –Ura (Normal N)	*VIP1*	37.5 ± 18.8
	SLAD (Low N)	*VIP1*	587 ± 174

[a]Quantified as fold-change relative to levels in WT strain grown in SLAD

3.7 References

1. Chen, H. & Fink, G. R. Feedback control of morphogenesis in fungi by aromatic alcohols. *Genes Dev.* **20**, 1150–61 (2006).
2. Lorenz, M. C., Cutler, N. S. & Heitman, J. Characterization of Alcohol-induced Filamentous Growth in *Saccharomyces cerevisiae*. *Mol. Biol. Cell* **11**, 183–199 (2000).
3. Güldener, U. *et al.* Characterization of the Saccharomyces cerevisiae Fol1 protein: starvation for C1 carrier induces pseudohyphal growth. *Mol. Biol. Cell* **15**, 3811–28 (2004).
4. Prusty, R., Grisafi, P. & Fink, G. R. The plant hormone indoleacetic acid induces invasive growth in Saccharomyces cerevisiae. *Proc. Natl. Acad. Sci. U. S. A.* **101**, 4153–7 (2004).
5. Shively, C. A. *et al.* Large-Scale Analysis of Kinase Signaling in Yeast Pseudohyphal Development Identifies Regulation of Ribonucleoprotein Granules. *PLOS Genet.* **11**, e1005564 (2015).
6. Flick, J. S. & Thorner, J. Genetic and biochemical characterization of a phosphatidylinositol-specific phospholipase C in Saccharomyces cerevisiae. *Mol. Cell. Biol.* **13**, 5861–76 (1993).
7. Monserrate, J. P. & York, J. D. Inositol phosphate synthesis and the nuclear processes they affect. *Curr. Opin. Cell Biol.* **22**, 365–73 (2010).
8. Hatch, A. J. & York, J. D. SnapShot: Inositol Phosphates. *Cell* **143**, 1030-1030.e1 (2010).
9. Saiardi, A., Erdjument-Bromage, H., Snowman, A. M., Tempst, P. & Snyder, S. H. Synthesis of diphosphoinositol pentakisphosphate by a newly identified family of higher inositol polyphosphate kinases. *Curr. Biol.* **9**, 1323–1326 (1999).
10. Mulugu, S. *et al.* A conserved family of enzymes that phosphorylate inositol

hexakisphosphate. *Science* **316**, 106–9 (2007).

11. Pöhlmann, J. *et al.* The Vip1 Inositol Polyphosphate Kinase Family Regulates Polarized Growth and Modulates the Microtubule Cytoskeleton in Fungi. *PLoS Genet.* **10**, e1004586 (2014).
12. Steidle, E. A. *et al.* A Novel Inositol Pyrophosphate Phosphatase in Saccharomyces cerevisiae: Siw14 PROTEIN SELECTIVELY CLEAVES THE β-PHOSPHATE FROM 5-DIPHOSPHOINOSITOL PENTAKISPHOSPHATE (5PP-IP5). *J. Biol. Chem.* **291**, 6772–83 (2016).
13. Wundenberg, T., Grabinski, N., Lin, H. & Mayr, G. W. Discovery of InsP6-kinases as InsP6-dephosphorylating enzymes provides a new mechanism of cytosolic InsP6 degradation driven by the cellular ATP/ADP ratio. *Biochem. J.* **462**, 173–84 (2014).
14. Michell, R. H., Kirk, C. J., Jones, L. M., Downes, C. P. & Creba, J. A. The stimulation of inositol lipid metabolism that accompanies calcium mobilization in stimulated cells: defined characteristics and unanswered questions. *Philos. Trans. R. Soc. Lond. B. Biol. Sci.* **296**, 123–38 (1981).
15. Azevedo, C., Burton, A., Ruiz-Mateos, E., Marsh, M. & Saiardi, A. Inositol pyrophosphate mediated pyrophosphorylation of AP3B1 regulates HIV-1 Gag release. *Proc. Natl. Acad. Sci. U. S. A.* **106**, 21161–6 (2009).
16. Chakraborty, A. *et al.* Inositol pyrophosphates inhibit Akt signaling, thereby regulating insulin sensitivity and weight gain. *Cell* **143**, 897–910 (2010).
17. Chanduri, M. *et al.* Inositol hexakisphosphate kinase 1 (IP6K1) activity is required for cytoplasmic dynein-driven transport. *Biochem. J.* **473**, 3031–47 (2016).
18. Kim, S. *et al.* Cell Metabolism Amino Acid Signaling to mTOR Mediated by Inositol

Polyphosphate Multikinase. (2011). doi:10.1016/j.cmet.2011.01.007

19. Lee, Y.-S., Mulugu, S., York, J. D. & O'Shea, E. K. Regulation of a Cyclin-CDK-CDK Inhibitor Complex by Inositol Pyrophosphates. *Science (80-.).* **316**, 109–112 (2007).

20. Saiardi, A., Resnick, A. C., Snowman, A. M., Wendland, B. & Snyder, S. H. Inositol pyrophosphates regulate cell death and telomere length through phosphoinositide 3-kinase-related protein kinases. *Proc. Natl. Acad. Sci. U. S. A.* **102**, 1911–4 (2005).

21. Szijgyarto, Z., Garedew, A., Azevedo, C. & Saiardi, A. Influence of inositol pyrophosphates on cellular energy dynamics. *Science* **334**, 802–5 (2011).

22. Thota, S. G., Unnikannan, C. P., Thampatty, S. R., Manorama, R. & Bhandari, R. Inositol pyrophosphates regulate RNA polymerase I-mediated rRNA transcription in Saccharomyces cerevisiae. *Biochem. J.* **466**, 105–14 (2015).

23. Wickner, R. B., Kelly, A. C., Bezsonov, E. E. & Edskes, H. K. [PSI+] prion propagation is controlled by inositol polyphosphates. *Proc. Natl. Acad. Sci. U. S. A.* **114**, E8402–E8410 (2017).

24. Wild, R. *et al.* Control of eukaryotic phosphate homeostasis by inositol polyphosphate sensor domains. *Science* **352**, 986–90 (2016).

25. Shears, S. B. *et al.* Defining signal transduction by inositol phosphates. *Subcell. Biochem.* **59**, 389–412 (2012).

26. Bennett, M., Onnebo, S. M. N., Azevedo, C. & Saiardi, A. Inositol pyrophosphates: metabolism and signaling. *Cell. Mol. Life Sci.* **63**, 552–64 (2006).

27. Chakraborty, A., Kim, S. & Snyder, S. H. Inositol pyrophosphates as mammalian cell signals. *Sci. Signal.* **4**, re1 (2011).

28. Wu, M., Chong, L. S., Perlman, D. H., Resnick, A. C. & Fiedler, D. Inositol

polyphosphates intersect with signaling and metabolic networks via two distinct mechanisms. *Proc. Natl. Acad. Sci. U. S. A.* **113**, E6757–E6765 (2016).

29. Bhandari, R. *et al.* Protein pyrophosphorylation by inositol pyrophosphates is a posttranslational event. *Proc. Natl. Acad. Sci. U. S. A.* **104**, 15305–10 (2007).

30. Saiardi, A. Protein pyrophosphorylation: moving forward. *Biochem. J.* **473**, 3765–3768 (2016).

31. Lev, S. *et al.* Fungal Inositol Pyrophosphate IP7 Is Crucial for Metabolic Adaptation to the Host Environment and Pathogenicity. *MBio* **6**, e00531-15 (2015).

32. Pöhlmann, J. & Fleig, U. Asp1, a conserved 1/3 inositol polyphosphate kinase, regulates the dimorphic switch in Schizosaccharomyces pombe. *Mol. Cell. Biol.* **30**, 4535–47 (2010).

33. Norman, K. L. *et al.* Inositol polyphosphates regulate and predict yeast pseudohyphal growth phenotypes. *PLOS Genet.* **14**, e1007493 (2018).

34. Azevedo, C. & Saiardi, A. Extraction and analysis of soluble inositol polyphosphates from yeast. *Nat. Protoc.* **1**, 2416–2422 (2006).

35. Saiardi, A., Caffrey, J. J., Snyder, S. H. & Shears, S. B. The inositol hexakisphosphate kinase family. Catalytic flexibility and function in yeast vacuole biogenesis. *J. Biol. Chem.* **275**, 24686–92 (2000).

36. York, J. D., Odom, A. R., Murphy, R., Ives, E. B. & Wente, S. R. A phospholipase C-dependent inositol polyphosphate kinase pathway required for efficient messenger RNA export. *Science* **285**, 96–100 (1999).

37. Bang, S. *et al.* AMP-activated protein kinase is physiologically regulated by inositol polyphosphate multikinase. *Proc. Natl. Acad. Sci. U. S. A.* **109**, 616–20 (2012).

CHAPTER 4

Future Directions

4.1 Introduction

The future directions presented here are ideas and hypotheses based on work done in Chapters 2 and 3 and literature. Although I won't have enough time to even cause a dent in any of those experiments in this chapter, I will hopefully have enough time to revise the paper based on Chapter 2 before I leave the Kumar lab.

The data we gathered so far for the signaling network implicates a wide variety of cellular processes that are affected by Ksp1 transcriptionally or post-translationally. Among those, stress granule formation seems to be regulated by Ksp1 and many stress granule proteins regulate pseudohyphal growth in a Ksp1 phosphorylation dependent way. However, it is also very possible that this is only part of the pathway and there are other redundant/non-redundant pathways regulating pseudohyphal growth and stress granules that are waiting to be identified.

Moreover, our study puts Ksp1 in a central role as a signaling protein for a wide range of cellular processes. There are many avenues for researching the role of Ksp1 in different aspects of cell biology including but not limited to translation, nutrient sensitive TOR and PKA signaling, trehalose and aminoacid metabolism, DNA repair, autophagy and regulation of cell size.

While the work that has been discussed in Chapter 4 is the first report of inositol

polyphosphate content of the cell and the ability to filament, there still is more mechanistic questions that are waiting to be answered especially with regards to how inositol polyphosphate metabolism pathway relates to other pathways regulating pseudohyphal growth.

Below I discuss any hypotheses and additional experiments that can be employed to answer open questions about the role of Ksp1 in cellular processes, the relationship between pseudohyphal growth and mRNP granules and inositol polyphosphate metabolism.

4.2 Ksp1

4.2.1 Finding direct targets of Ksp1

Our mass spectroscopy analysis revealed more than 100 potential substrates for Ksp1. We do not still know if any of those proteins whose phosphorylation depends on the kinase activity of Ksp1 is a direct target of Ksp1 with one exception, eIF4G. *In vitro* kinase assays are good assays for understanding if Ksp1 can directly phosphorylate any target.

Our initial hypothesis was that the scaffolding translation factor Tif4631 is a direct target of Ksp1 since it is both a core stress granule protein and a translation initiation factor. Purifying Tif4631 and Ksp1 were problematic since both are quite big proteins. I eventually purified GST tagged Tif4631 and 9myc tagged Ksp1 kinase domain from *E. coli*. However, while this work was going on in our lab, another group showed that Ksp1 phosphorylate Tif4631 under glucose deprivation conditions [1]. Hence, as of now, the only known target of Ksp1 is Tif4631.

4.2.2 Ksp1 and mRNA localization and translation

Ksp1p is one of the two kinases that have been found to bind RNA in a CLIP-Seq study [2]

. Since our data points to a role of *KSP1* in the regulation of mRNP granules, I hypothesize that Ksp1p brings specific RNAs to mRNP granules. To test this hypothesis, one can first crosslink Ksp1p and mRNAs using UV under normal and stress granule inducing conditions. For immunoprecipitation the cell extracts with crosslinked protein and mRNAs using the anti-Ksp1 antibody our lab has developed against untagged Ksp1p can be used. Then, RNA sequencing can be used to determine which RNAs are bound to Ksp1p in normal and stress granule inducing conditions.

The other kinase that has been found to bind RNA in the same study is Ste20p. In our studies with *KSP1* we show that *KSP1* regulates phosphorylation and localization of Ste20p under stress. It is also possible that Ksp1p regulates RNA content of mRNP granules through Ste20p. Then, finding out the RNAs that bind to Ste20 under normal conditions and stress following the same experimental plan outlined in the previous paragraph would be helpful to test this hypothesis.

Ksp1p directly phosphorylates the scaffolding protein of translation initiation complex, eIF4G. eIF4G is a component of cap binding eIF4F complex. Another component of eIF4F complex is the cap binding protein eIF4E. The interaction between eIF4G and eIF4E is central to regulation of translation initiation. This interaction is regulated by small proteins that bind to eIF4E. [3] Human eIF4E binding protein 4E-BP has a well-established role in regulating translation in cancer [4]. Yeast has two eIF4E binding proteins identified so far. Caf20p and Eap1p bind to eIF4E and inhibit its interaction with eIF4G [5,6]. All eIF4E binding proteins share the eIF4E binding motif YXXXXLϕ [7]. Through bioinformatics analysis we have found three sites throughout Ksp1p for eIF4E binding. It's possible that eIF4E interacts with Ksp1. We have tried yeast two hybrid and immunoprecipitation to test this hypothesis. To our dismay, neither of these techniques worked good enough to give a definite answer to the question whether Ksp1 and eIF4E interacts. More

troubleshooting of these techniques and/or employing a different technique such as a biocomplementation assay would be helpful to understand if/when Ksp1 interacts with eIF4E.

Since Ksp1 phosphorylates an important component of translation initiation machinery we wondered whether this phosphorylation might be important for translation. A ribosome profiling assay done in collaboration with Elizabeth Tran's lab at Purdue University revealed that there is not a significant difference in general translation between wild type cells and deletion and kinase inactive mutants of *KSP1* under rich media conditions (data not shown). Since nutritional stress causes a huge reduction in translation, we were not able to do a ribosome profiling analysis under stress conditions. Hence, we cannot eliminate the possibility that phosphorylation of eIF4G by KSP1 might affect translation under nitrogen stress.

Another possibility is that this phosphorylation of eIF4G might regulate translation of specific transcripts. In filamentous strains, invasive growth genes are translated via a cap-independent mechanism and this translation depends on eIF4G [8]. In order to understand whether phosphorylation of eIF4G by Ksp1p might regulate translation of invasive growth genes I have checked the induction of the protein that had been shown to be the most responsive to deletion of eIF4G in both wild type and kinase inactive Ksp1 mutants. While expression of this protein, YMR181c, has been induced in both strains after nitrogen depletion, I was not able to see any difference between the levels of this protein in wild type and non-phosphorylable eIF4G mutant after several hours of nitrogen depletion as evidenced by a western blot (data not shown). However, other invasive growth genes can still be tested to see if the increase in their protein levels after nitrogen depletion depends on phosphorylation of eIF4G by Ksp1p. Moreover, trying to assess translation by a western blot do not account for differences in mRNA levels. It tells us the protein levels rather than translation efficiency. An in vitro translation assay would be a more

accurate way of understanding whether phosphorylation of eIF4G by Ksp1p plays a role in cap independent translation of invasive growth genes. Another experimental approach to understand if phosphorylation of eIF4G by Ksp1 might affect translation of specific transcripts is doing a ribosome footprinting analysis [9]. This analysis would tell us which transcripts are getting translated.

4.2.3 Ksp1 and TOR and AMPK signaling

As evidenced by both high throughput and low throughput studies Ksp1p associates with TORC1. TORC1 localizes to stress granules under heat shock [10] and Kog1p, a subunit of TORC1, has been shown to localize to distinct cytoplasmic foci when glucose is depleted from the medium[11,12]. However, those Kog1p foci did not colocalize with known stress granule markers. Since we showed that the kinase activity of Ksp1p regulates stress granules, we wondered whether kinase activity of Ksp1p regulates localization of TORC1, too. Our analysis of localization of Kog1 showed an increase in Kog1-GFP foci in cytoplasm in kinase deficient cells after 24 hours of growth in rich medium. In accordance with previous studies, these foci did not colocalize with stress granules Pab1 and Pub1 (data not shown).

Previous studies have shown that the yeast AMPK, Snf1p, regulates the localization of Kog1p to cytoplasmic foci. Deletion of *SNF1* causes a decrease in Kog1p foci under stress. Since Ksp1p kinase activity causes an increase in Kog1p foci, it's possible that Snf1p and Ksp1p acts on the same pathway or parallel pathways to regulate TORC1 localization. To test this hypothesis, a *snf1Δ* mutant in the ksp1K47D background could be created. If this mutant loses its phenotype of increased Kog1 foci under stress, then we can say that Snf1 acts upstream of Ksp1 in the regulation of localization of TORC1.

TORC1 associated proteins have been shown to regulate pseudohyphal growth[13]. To understand whether Snf1p might be important for Ksp1p dependent regulation of pseudohyphal growth I have tested whether overexpression of Snf1p can reverse the loss of pseudohyphal growth in *KSP1* mutants. When transformed with plasmids that make the cells constitutively overexpress *SNF1*, both *ksp1Δ* and ksp1K47D mutant cells showed similar levels of pseudohyphal growth to a wild type (data not shown). This result suggests that AMPK might regulate pseudohyphal through a TORC1-associated protein. However, this effect might just be due to the effect of *SNF1* overexpression being more dominant than a *KSP1* mutation on pseudohyphal growth. More experiments are needed to verify the relationship between *KSP1* and *SNF1* in terms pseudohyphal growth.

4.2.4 Ksp1 and PKA signaling

PKA phosphorylates Ksp1p in a rapamycin dependent manner[14]. We have created a nonphosphorylable mutant of Ksp1p by changing the Serine827 of Ksp1p to alanine. Interestingly, this mutation resulted in significantly smaller cells when compared to wild type (data not shown). While this made any analysis of GFP foci in these mutants very difficult, within itself this is a very interesting phenotype. PKA regulates cell size by phosphorylating another RNA binding protein, Whi3 [15]. It would be interesting to see if PKA dependent phosphorylation of Ksp1 is another pathway PKA regulates cell size or if Ksp1 is in the same pathway as PKA and Whi3.

Our mass spectrometry analysis of potential Ksp1 targets revealed four trehalose metabolism proteins as potential targets of Ksp1. Interestingly, among those Nth1 and Nth2 are known targets of PKA [16]. Moreover, the Ksp1 dependent phosphorylation sites we found for these two proteins are known sites of PKA phosphorylation and has been shown to be directly

phosphorylated by PKA *in vitro*. This raises the question whether Ksp1 might be regulating the phosphorylation of these proteins via PKA. Moreover, by regulating phosphorylation of trehalose metabolism proteins, Ksp1 might regulate trehalose metabolism. To investigate this possibility, I have measured trehalose levels in wild type and *ksp1Δ* and *ksp1K47D* mutants in the stationary phase when trehalose accumulates. I did not see any difference in trehalose levels between wild type and Ksp1 mutants. However, the trehalose metabolism proteins that are potential targets of Ksp1 are mainly work on degradation of trehalose. Hence, measuring the trehalose levels during recovery from stress might give us more informative data about potential involvement of Ksp1 in trehalose metabolism.

4.3. Inositol Polyphosphate Metabolism and Filamentous Growth

Our study on the effect of inositol polyphosphate metabolism on filamentation shows a clear relationship between the inositol polyphosphate content of a cell, the kinases/phosphatases of inositol polyphosphate metabolism and pseudohyphal growth in *S. cerevisiae*. The inositol polyphosphate analysis of filamenting and non-filamenting *C. albicans* shows inositol polyphosphate content of this pathogenic fungus also changes during filamentation and inositol polyphosphate kinase deletions cause aberrant filamentation phenotypes. It would be interesting to see if inositol polyphosphate content change occurs in inositol polyphosphate metabolism gene mutants as expected. Moreover, a more comprehensive analysis of filamentation in inositol polyphosphate metabolism mutants by generating double mutants of the heterozygous mutants we have already analyzed as well as analyzing mutants of other proteins on the pathway would be useful to understand the relationship between inositol polyphosphates and filamentation in *C. albicans.*

4.4. Summary

This thesis outlines new and intriguing relationships between pseudohyphal growth and mRNP granules, and between filamentous growth and inositol polyphosphate metabolism. I have summarized some ideas for experiments that would help understanding the mechanism of how these interactions work and how they might be related to filamentation in pathogenic fungi. Hopefully, these experiments will help us understand how cells survive under different stresses and how different stress responses are coordinated.

4.5 References

1. Chang, Y. & Huh, W.-K. Ksp1-dependent phosphorylation of eIF4G modulates post-transcriptional regulation of specific mRNAs under glucose deprivation conditions. *Nucleic Acids Res.* **46**, 3047–3060 (2018).

2. Mitchell, S. F., Jain, S., She, M. & Parker, R. Global analysis of yeast mRNPs. *Nat. Struct. Mol. Biol.* **20**, 127–33 (2013).

3. Hinnebusch, A. G. & Lorsch, J. R. The mechanism of eukaryotic translation initiation: new insights and challenges. *Cold Spring Harb. Perspect. Biol.* **4**, a011544 (2012).

4. Mamane, Y., Petroulakis, E., LeBacquer, O. & Sonenberg, N. mTOR, translation initiation and cancer. *Oncogene* **25**, 6416–6422 (2006).

5. Cosentino, G. P. *et al.* Eap1p, a novel eukaryotic translation initiation factor 4E-associated protein in Saccharomyces cerevisiae. *Mol. Cell. Biol.* **20**, 4604–13 (2000).

6. Altmann, M., Schmitz, N., Berset, C. & Trachsel, H. A novel inhibitor of cap-dependent translation initiation in yeast: p20 competes with eIF4G for binding to eIF4E. *EMBO J.* **16**, 1114–1121 (1997).

7. Kamenska, A., Simpson, C. & Standart, N. eIF4E-binding proteins: new factors, new locations, new roles. *Biochem. Soc. Trans.* **42**, 1238–1245 (2014).

8. Gilbert, W. V., Zhou, K., Butler, T. K. & Doudna, J. A. Cap-Independent Translation Is Required for Starvation-Induced Differentiation in Yeast. *Science (80-.).* **317**, 1224–1227 (2007).

9. Ingolia, N. T. Ribosome profiling: new views of translation, from single codons to genome scale. *Nat. Rev. Genet.* **15**, 205–13 (2014).

10. Takahara, T. & Maeda, T. Transient Sequestration of TORC1 into Stress Granules during Heat Stress. *Mol. Cell* **47**, 242–252 (2012).

11. Hughes Hallett, J. E., Luo, X. & Capaldi, A. P. Snf1/AMPK promotes the formation of Kog1/Raptor-bodies to increase the activation threshold of TORC1 in budding yeast. *Elife* **4**, (2015).

12. Sullivan, A., Wallace, R. L., Wellington, R., Luo, X. & Capaldi, A. P. Multilayered regulation of TORC1-body formation in budding yeast. *Mol. Biol. Cell* **30**, 400–410 (2019).

13. Laxman, S. & Tu, B. P. Multiple TORC1-Associated Proteins Regulate Nitrogen Starvation-Dependent Cellular Differentiation in Saccharomyces cerevisiae. *PLoS One* **6**, e26081 (2011).

14. Soulard, A. *et al.* The Rapamycin-sensitive Phosphoproteome Reveals That TOR Controls Protein Kinase A Toward Some But Not All Substrates. *Mol. Biol. Cell* **21**, 3475–3486 (2010).

15. Mizunuma, M. *et al.* Ras/cAMP-dependent Protein Kinase (PKA) Regulates Multiple Aspects of Cellular Events by Phosphorylating the Whi3 Cell Cycle Regulator in

Budding Yeast. *J. Biol. Chem.* **288**, 10558–10566 (2013).

16. Schepers, W., Van Zeebroeck, G., Pinkse, M., Verhaert, P. & Thevelein, J. M. In vivo phosphorylation of Ser21 and Ser83 during nutrient-induced activation of the yeast protein kinase A (PKA) target trehalase. *J. Biol. Chem.* **287**, 44130–42 (2012).

APPENDIX

Construction of an overexpression library in the filamentous yeast background

A.1. Introduction

Candida albicans is the most common human opportunistic fungus pathogen. It might cause life-threatening infections in immunocompromised people. The pathogenesis of *C. albicans* depends on its interaction with its host cell. Recently, NLRP3-inflammasome-mediated-caspase 1 activation has been identified as the mechanism how the macrophages respond to *C. albicans*. While there is a relationship between Candida filamentation and its ability to provoke immune response, some Candida strains that capable of filamentation cannot evoke the immune response. Interestingly, to a lesser degree than *C. albicans*, filamentous strains of *S. cerevisiae* also cause activation of NRPL3 inflammasome. We have constructed the library described in this Appendix to be used for a screen to identify *S. cerevisiae* genes that modulate NLRP3 inflammasome activation.

A.2. Materials and Methods

Yeast genomic tiling library was purchased from Dharmacon. This library is a systematic collection of *S. cerevisiae* genome in a 2-micron vector with LEU marker. The library contains single plasmid transformed into *E. coli* at 96 well format. The plasmids each contain a piece of a *S. cerevisiae* chromosome. The library covers about 95% of the genome in 1588 plasmids. Weisolated all the plasmids from the collection and retransformed them into the filamentous

Y825 strain in Σ1287b background.

A.2.1. Generating a Copy of the Collection

1. Add 1740 ul LB+Kanamycin to the 96-well plate.

2. Copy each plate by transferring bacteria using a 96 well pin.

3. Grow overnight at 37 C.

4.Spin at 1800 rpm for 5 min. Check pellet and tip off media.

5. Fill Hdyra with 45% glycerol (70 ul).

6. Empty into the new plate.

7. Fill Hydra with 280 ul sterile water.

8. Empty into the plate with bacterial cells. Vortex to resuspend.

9. Fill Hydra with 280 ul cell suspension

10. Dispense into the new plate.

11. Use the wash function to mix.

12. Seal the plate and store at -80 C.

13. Use the copy of the collection for downstream purposes.

A.2.2. Miniprep from *E. coli*

1. Grow bacteria at 37 C overnight.

2. Spin the uniplates at 2000 rpm for 7 minutes.

3. Check bacterial pellet. Discard medium.

4. Fill Hydra with 400 ul Solution II.

5. Dispense 100 ul to all filters.

6. Fill Hydra with 110 ul Sol I.

7. Dispense into uniplate containing bacteria. Vortex gently to resuspend.

8. Fill with 100 ul cell suspension from uniplate.

9. Dispense into filterplate containing 100 ul Sol II

10. Use wash function to mix.

11.Fill with 100 ul Sol III

12. Dispense into filter containing cell lysate.

13. Wash to mix.

14. Put filterplate at -20C for more than 10 minutes.

15. After 10 minutes, warm filter to room temperature. Filter the DNA with vacuum manifold into a deepwell.

16. Fill Hydra with 460 ul 100% Ethanol

17. Dispense 690 ul per well in 3 installments of 230 ul into the deepweel.

18. Put caps on and invert to mix twice.

19. Chill at -20 C for at least 5 minutes.

20. Spin at 3100 rpm for 25 minutes.

21. Check pellet and discard supernatant.

22. Fill Hydra with 460 ul 80% ethanol.

23. Dispense 230 ul into each well in the deepwell.

24. Carefully decant ethanol and air-dry DNA pellets.

25. Fill Hydra with 480 ul TE.

26. Dispense 60 ul into deepwell containing DNA.

27. Spin briefly. Cap and put at 37 C for at least 30 mins to resuspend. Before storing, cap deepwells with foil. Store at -20 C.

A.2.3 Yeast Cell Preparation

1. Grow 50 ml culture in YPD overnight.

2. Add 40 ml YPD and grow for 2-3 hours more.

3. Spin down 100 ul of the culture in an Eppendorf tube and check the pellet size. It should be approximately 5 ul. If greater, use less culture for following steps.

4. Spin down cells at 2000 rpm for 4 minutes. Resuspend in sterile water then spin down again.

5. Mix 72 ml water, 9 ml 10X TE pH 7.5 and 9 ml 1M LiAc

6. Resuspend yeast in LiAc/TE and put back in flask which was rinsed with sterile water. Shake at 30 C for 30 minutes.

7. Add 600 ul beta-mercaptoethanol. Shake at 30 C for 30 minutes.

8. Add 1.7 ml of 10 mg/ml carrier DNA. Cells are ready to use.

A.2.4. Yeast transformation

1. Spin down DNA at 1400 rpm for 2 minutes.

2. Fill Hydra with 400 ul of yeast cells from tray.

3. Dispense 100 ul into deepwells with digest.

4. Cap deepwells. Incubate at 30 C for 30 minutes on side.

5. Fill Hydra with 250 ul PEG mixture. Vortex yeast box to resuspend cells.

6. Dispense 250 ul into deepwell with yeast.

7. Use the wash function to mix cells and PEG.

8. Incubate deepwells at 30 C for 15-30 minutes on side.

9. Heat shock at 45 C for 15 minutes.

10. Pellet cells at 3000 rpm for 15 minutes at least. Tip PEG off quickly and carefully.

Wipe PEG off top of box. Put caps on. Resuspend by vortexing.

11. Fill Hydra with 580 ul 2X Sc-Leu

12. Empty onto cell pellet.

13. Put caps on. Vortex. Put on wheel. Grow for 4 days.

14. After 4th day, spin down cells at 2000 rpm for 5 minutes.

15. Resuspend cells with new media.

16. Grow on wheel one more day.

A.2.5 Checking the quality of plates

The quality of plates was checked with two approaches. First, a 96-pin handle is used to transfer yeast from the 96 well to plates and growth for each yeast is checked after 3 days incubation at 30 C. Second, random wells from the library were checked for the presence of the plasmid by a yeast miniprep.

A.2.6 Storage of library

I precipitated and washed the yeast cells with sterile water, precipitated and resuspended in a small amount (100 ul) of sterile water. I mixed 60 ul of those cells with 30 ul of 45% glycerol (final concentration 15%) in the 96 well plates and froze immediately.

A.2.7. Solutions

All the amounts are for making 500 ml of solutions.

A.2.7.1. Solution I

475 ml sterile water

12.5 ml 2M Tris pH 7.5

10 ml 0.5 M EDTA

1 ml 10 mg/ml RNAse

A.2.7.2 Solution II

440 ml water

10 ml 10M NaOH

50 ml 10% SDS

A.2.7.3 Solution III

300 ml 5M KAc

142 ml water

57.5 ml glacial acetic acid

A.2.7.4 TE (for DNA)

500 ml water

2.5 ml 2M Tris pH 7.5

1 ml 0.5 M EDTA

A.2.7.5 10X TE (for yeast and for 250 ml)

233 ml water

12.5 ml 2M Tris

55 ml 0.5M EDTA

A.2.7.6 PEG mixture

400 ml 50% PEG

50 ml 1X TE pH 7.5

50 ml 1M LiAc pH 7.5

A.3. Results

A copy of the library was sent to Damian Krysan's lab at the University of Rochester. There, it was used for screening *Saccharomyces* factors that trigger pyroptosis in macrophages. Table A.1. is a list of the plasmids that caused an aberrant phenotype when compared to wildtype in triggering pyroptosis.

A.4. References

1. Wellington M, Koselny K, Sutterwala FS, Krysan DJ (2014) Candida albicans Triggers NLRP3-Mediated Pyroptosis in Macrophages. *Eukaryot Cell* 13(2):329–340.

2. Jones, G. M. *et al*. (2008) A systematic library for comprehensive overexpression screens in Saccharomyces cerevisiae. *Nature Methods* **5**, 239–241

A.5 Tables

Table A.1. Plasmids with aberrant pyroptosis phenotypes.

Probable gene of interest	CLONE	PLATE	ROW	COL	CHR	BEGIN	END															
FLO1	YGPM33d10	A001	h	3	I	200307	210928	YAR047C	FLO1	YAR053W												
SED1	YGPM19p01	A003	d	9	IV	593740	604855	[TPS2]	PPH3	RAD55	SED1	SHU2	PET100	TFB5	[VPS41]*							
SPI1	YGPM18f12	A005	a	8	V	464928	475865	YER147C-A	[SPT15]	YER148W-A	PEA2	SPI1	tV(AAC)E2	UBP3	YER152C	YER152W-A	PET122	[OXA1]*				
MSB2	YGPM30a21	A006	d	10	VII	514310	527841	[YGR012W]&	[SNU71]	MSB2	YGR015C	YGR016W	YGR017W	YGR018C	UGA1	VMA7	[YGRl21W]*					
SIM1	YGPM8c03	A008	f	6	IX	122000	134498	[STH1]&	KGD1	AYR1	SIM1	POG1	QDR2	[QDR1]*								
TIR3	YGPM23l22	A008	a	10	IX	332118	343606	[PDR11]*	YIL012W	TIR3	DOT5	EST3	tD(GUC)J2	FAA3	URM1	[NAS2]&						
FLO11/MUC	YGPM13d18	A008	f	10	IX	383388	395016	[YIR016W]&	MET28	[YIR017W-A]	YAP5	YIR018C-A	MUC1	[YIR020C]	[YIR020W-A]*							
FLO11/MUC	YGPM2b16	A008	g	10	IX	388334	400147	MUC1	YIR020C	YIR020W-A	YIR020C-B	MRS1	YIR021W-A	SEC11	[DAL81]*							
YPS6	YGPM17n13	A008	d	11	IX	426401	438768	YPS6	YIR040C	YIR041W	YIR042C	YIR043C	YIR044C									
MNN5	YGPM20c11	A008	e	12	X	78443	90387	[SWE1]*	MNN5	YJL185C	GON7	MNN11	YJL182C	YJL181W	ATP12	PFD1	[ATG27]					
KRE9	YGPM10f13	A008	f	12	X	85372	98662	[YJL182C]	[YJL181W]	ATP12	PFD1	ATG27	RPL17B	SWI3	YJL175W	KRE9	KFA3	[CPS1]*				
KRE9	YGPM15f08	A008	g	12	X	90390	102974	[RPL17B]	SWI3	YJL175W	KRE9	KFA3	CPS1	YJL171C	ASG7	YJL169W	[SET2]&					
YNL190W	YGPM26g16	A013	a	11	XIV	275487	286609	[YNL193W]&	CHS1	YNL191W	YNL190W	SRP1	[KAR1]*									
EGT2	YGPM4p15	A013	g	6	XIV	13694	31196	[SNZ2]&	THI12	AAD14	RPD3	PEX6	MDJ2	EGT2	YNL326C	[FIG4]&	YNL324W]*					
TIR2	YGPM28l06	A014	h	12	XV	340508	350655	SLG1	YOR008C-A	YOR008W-B	TIR4	TIR2	[AUS1]*									
TIR2	YGPM25n08	A015	a	1	XV	346936	358181	[TIR2]*	AUS1	tI(AGU)O2	YOR011W-A	YOR012W	YOR013W	[RTS1]*								
SMP3	YGPM23l05	A015	a	5	XV	604547	614100	[ELG1]*	PNO1	YOR146W	MDM32	SPP2	SMP3	MRPL23	[RPB2]&							
SMP3	YGPM3h22	A015	b	5	XV	607431	619138	[MDM32]&	SPP2	SMP3	MRPL23	RPB2	YOR152C									
LIP5	YGPM2f24	A015	a	7	XV	708501	724146	[YOR192C-B]	[YOR192C-A]	tM(CAU)O1	PEX27	TOA1	SLK19	LIP5	MCA1	BFR1	YOR199W	YOR200W	PET56	HIS3	YOR203W	[DED1]*
FIT2 and FIT	YGPM4j12	A015	e	12	XV	1059218	1072431	[FIT2]	FIT3	FRE5	YOR385W	PHR1	YOR387C	[FDH1]&								

Table A.2. The filamentous yeast genomic tiling library plate 18 and 19

The filamentous yeast genomic tiling library has the same plasmids at the same coordinates except for those that are listed here as Plate 18 and 19 of filamentous yeast genomic tiling library and two that did not grow when transformed. Those are the plasmids corresponding to Plate 3A2 and Plate 3H5. For the purposes of display only the first two genes in a plasmid in Plate 18 and 19 are listed here. The chromosome pieces can be compared to the original library to understand whether it spans more than two genes.

PLATE	ROW	COL	CHR	BEGIN	END		
18	a	1	II	657839	667422	[ATG12]&	PYC2
18	b	1	IV	188763	201053	[NOP14]*	RPN5
18	c	1	IV	626074	633890	RLI1	UBC13
18	d	1	IV	1422845	1433559	[VPS52]&	VPS72
18	e	1	IV	863637	874941	[EBS1]&	UME6
18	f	1	IV	884068	895786	[tI(UAU)D]	
18	g	1	VII	957815	970366	[PHO81]*	YHB1
18	h	1	XII	426238	436626	[PUT1]&	tD(GUC)L1
18	a	2	IV	16562	23618	[THI13]&	AAD4
18	b	2	IV	254387	265978	[IWR1]*	YDL114W-A
18	c	2	IV	753763	765770	[KGD2]*	YDR149C
18	d	2	IV	842673	855150	[HST4]&	NUP42
18	e	2	IV	923798	934426	[PCF11]*	IVY1
18	f	2	IV	944248	957464	[SNU56]*	BUD26
18	g	2	VII	1018858	1028975	[YGR263C]*	MES1
18	h	2	XII	654664	666189	tA(AGC)L	YLR257W
18	a	3	III	39845	48808	[YCL049C]*	SPS22
18	b	3	IV	377711	384466	[SIR2]*	[YDL041W]
18	c	3	IV	819111	829779	[CSN9]*	[YDR179W-A]

18	d	3	IV	904254	916978		[SPR28]*	YDR219C
18	e	3	IV	983652	994541		[YDR261W-B]&	YDR261C-D
18	f	3	IV	1004591	1013989		[MSW1]&	YDR269C
18	g	3	VII	1074075	1087006		[MAL11]*	YGR290W
18	h	3	XII	706013	714564		[YLR283W]&	ECI1
18	a	4	III	208477	222616		[YCR045C]*	[YCR045W-A]
18	b	4	IV	762543	772733		[NUM1]&	CTH1
18	c	4	IV	894642	903179		[ADR1]	[RAD9]&
18	d	4	IV	973340	983649		[HSP78]*	YAP6
18	e	4	IV	1442238	1449501		[PUF6]*	ITR1
18	f	4	IV	1064538	1076750		[CFT1]&	GPI11
18	g	4	IX	12084	22363		[VTH1]&	YIL172C
18	h	4	XII	384445	396518		[CLF1]*	YLR118C
18	a	5	IV	17141	26793		[THI13]&	AAD4
18	b	5	IV	323339	334823		[snR63]*	BRE1
18	c	5	IV	956512	967257		[VHS1]&	YDR248C
18	d	5	IV	1131268	1143490		[YDR332W]&	YDR333C
18	e	5	IV	869989	881388		[MSS4]&	YDR209C
18	f	5	IV	1161851	1172008		YDR344C	HXT3
18	g	5	IX	405002	415920		[YVH1]*	DAL1
18	h	5	XV	287614	298807		[TAT2]&	tY(GUA)O
18	a	6	IV	25083	38489		[LRG1]&	ADY3
18	b	6	IV	386014	396565		YDL036C	GPR1
18	c	6	IV	1073481	1082524		[HNT2]*	YDR306C
18	d	6	IV	1181604	1191485		[YDR352W]	TRR1
18	e	6	IV	930198	941297		[RTN1]*	LYS4
18	f	6	IV	1291762	1303307		[SIZ1]&	STE14
18	g	6	IX	21966	38088		YIL169C	YIL168W
18	h	6	XII	453268	467442		[RDN25-1]*	YLR154W-B
18	a	7	IV	37827	48808		[YDL233W]&	OST4
18	b	7	IV	772341	782966		[SAC3]&	SSY1
18	c	7	IV	838033	846247		[CCT6]&	[SLY1]
18	d	7	IV	1428879	1438275		[RIB3]*	PAC11
18	e	7	IV	987330	999741		YDR261C-D	YDR261C-C
18	f	7	V	580	12306		[YEL077C]*	[YEL077W-A]
18	g	7	X	688655	698997		[IML1]&	HOM6
18	h	7	XII	484994	497840		[YLR159W]	RDN5-5
18	a	8	III	294718	304877		tT(AGU)C	GIT1
18	b	8	IV	528750	545864		[ENA5]*	ENA2
18	c	8	IV	1120059	1130540		[YCG1]&	YDR326C
18	d	8	IV	853864	865655		[YDR198C]*	[YDR199W]
18	e	8	IV	1048274	1061296		[SSD1]*	DPL1
18	f	8	VI	135182	145047		[MSH4]*	tN(GUU)F

18	g	8	XI	4960	17954		[YKL222C]*	MCH2
18	h	8	XIII	517113	528904		[YMR124W]&	[STO1]
18	a	9	III	65504	76856		[RRP7]*	HIS4
18	b	9	IV	351810	364647		[YDL057W]&	MBP1
18	c	9	IV	1468947	1480666		[SMT3]	YDR510C-A
18	d	9	IV	915315	926867		[HTA1]	ADK1
18	e	9	IV	874944	886406		[YDR210W-B]&	YDR210C-D
18	f	9	VIII	251452	260501		[PTC7]&	NMD2
18	g	9	X	483700	496716		YJR030C	GEA1
18	h	9	XIV	334528	344825		[CBK1]&	YGP1
18	a	10	IV	63671	73977		[CDC13]*	DTD1
18	b	10	IV	296615	309387		[YDL089W]	ASM4
18	c	10	IV	897859	906499		[ADR1]&	RAD9
18	d	10	IV	978719	985335		[EXG2]*	tS(AGA)D2
18	e	10	IV	939528	949955		[SEC26]*	YDR239C
18	f	10	VII	755058	767439		[YGR131W]&	PHB1
18	g	10	XII	51429	59739		[FPS1]&	ATG10
18	h	10	XV	287614	298807		[TAT2]&	tY(GUA)O
18	a	11	IV	71569	81606		[GDH2]*	PRR2
18	b	11	IV	361965	374594		[PBP4]*	SLC1
18	c	11	IV	965208	973553		[CHL4]&	RMD5
18	d	11	IV	1317317	1326354		[SIP1]*	CAD1
18	e	11	IV	998253	1007266		[AKR1]*	PEX10
18	f	11	VII	952327	961498		PHB2	NAS6
18	g	11	XII	820116	830911		[RPL26A]&	[YLR345W]
18	h	11	XIV	667701	677553		[YNR020C]*	YNR021W
18	a	12	IV	133700	141924		[LYS20]&	INH1
18	b	12	IV	373283	384032		[FAD1]*	MTF2
18	c	12	IV	1172128	1184997		YPS7	tM(CAU)D
18	d	12	IV	1436362	1447299		[FMP36]&	RSM28
18	e	12	IV	1061030	1070587		[BFR2]&	PRO1
18	f	12	VII	1065549	1080937		YGR287C	MAL13
18	g	12	XII	187689	197029		[UBR2]*	SNF7
18	h	12	XIV	752127	762433		[YSN1]*	YNR066C
19	a	1	I	1152	17249		YAL068C	YAL067W-A
19	a	2	I	75816	87215		[RBG1]*	FUN12
19	a	3	I	139942	154249		[SSA1]*	YAL004W
19	a	4	I	209884	217559		[YAR060C]	
19	a	5	II	367543	386633		[YBR063C]*	[YBR064W]
19	a	6	II	432071	442516		[YBR094W]&	RXT2
19	a	7	I	7010	18908		SEO1	YAL066W
19	a	8	II	438679	450058		[VPS15]&	MMS4
19	a	9	I	28911	34029		GDH3	[YAL061W]*

19	a	10	I	67191	79897		[CLN3]*	CYC3
19	a	11	III	39845	48808		[YCL049C]*	SPS22
19	a	12	XV	1018044	1030244		[PRE10]*	PIP2
19	b	1	XV	1028359	1039847		[RPS12]*	MRS6
19	b	2	XVI	714225	723366		[YPR089W]&	YPR091C
19	b	3	XVI	718335	728913		[YPR091C]*	[YPR092W]